2020-04-22

Role of Cdk5rap2 in Cell Senescence and CENP-A-mediated Centromeric Chromatin Integrity

Wang, Xidi

UNIVERSITY OF CALGARY

Role of Cdk5rap2 in Cell Senescence and CENP-A-mediated Centromeric Chromatin Integrity

by

Xidi Wang

A THESIS

SUBMITTED TO THE FACULTY OF GRADUATE STUDIES

IN PARTIAL FULFILMENT OF THE REQUIREMENTS FOR THE

DEGREE OF DOCTOR OF PHILOSOPHY

GRADUATE PROGRAM IN MEDICAL SCIENCE

CALGARY, ALBERTA

APRIL, 2020

Abstract

Cyclin-dependent kinase 5 (Cdk5) regulatory subunit-associated protein 2 (Cdk5rap2, also known as MCPH3) is one of the genes mutant in primary microcephaly (MCPH), an autosomal recessive neurodevelopmental disorder characterized by small brain and cognitive deficit. In fact, Cdk5rap2 is most abundant at the luminal surface of the brain's ventricular zone, particularly in cells lining the ventricular wall where neural stem and progenitor cells reside. However, since Cdk5rap2 is also expressed in other tissues, it is not surprising that loss-of-function mutations in Cdk5rap2 are further associated with cochlear and retinal developmental defects as well as primordial dwarfism, a developmental disorder associated with small body size and other growth abnormalities. The molecular mechanisms by which Cdk5rap2 loss-of-function mutations cause these developmental disorders remain obscure. In this study, I show that loss of Cdk5rap2 induces cell senescence through activation of p53 and subsequent downregulation of the wild-type p53-induced phosphatase 1 (WIP1). Using BJ-5ta human foreskin fibroblast cells, I show that Cdk5rap2 loss causes increased (i) senescence-associated heterochromatin foci (SAHF), which colocalize with that SAHF marker, heterochromatin protein 1γ (HP1γ), (ii) SA-β-gal staining, (iii) p53 activation as measured by increased phosphorylation at Ser15, (iv) p16INK4a and p21CIP1, and (v) G0/G1 population, resulting in reduced cell proliferation. Interestingly, increased phosphorylation of p53 at Ser15 does not correlate with activation of the p53 Ser15 kinases, Ataxia Telangiectasia Mutated (ATM), checkpoint kinase 1 (Chk1) and checkpoint kinase 2 (Chk2), but correlates with decreased level of the p53 phosphatase, WIP1. Ectopic expression of WIP1 reverses the senescent phenotypes observed in cells depleted of Cdk5rap2,

indicating that cell senescence due to loss of Cdk5rap2 is linked to down-regulation of WIP1. Since the WIP1 promoter contains an NF-κB binding site and β-catenin-associated NF-κB affects the expression of NF-κB target genes, I tested whether loss of Cdk5rap2 that reduces WIP1 level influences β-catenin expression. Indeed, I found that loss of Cdk5rap2 significantly reduces nuclear β-catenin level. Because β-catenin phosphorylation by GSK3β results in its degradation through the ubiquitin-proteasome pathway, I further examined whether Cdk5rap2 interacts with GSK3β and affects GSK3β activity. My studies show that Cdk5rap2 interacts with GSK3β and such interaction causes increased GSK3β phosphorylation and subsequent decrease in GSK3β activity. Consistently, Cdk5rap2-depleted cells exhibit decreased GSK3β phosphorylation and increased GSK3β activity. Depletion of GSK3β increases β-catenin and WIP1 levels while depletion of β-catenin inhibits WIP1 expression. These findings suggest that GSK3β activation due to Cdk5rap2 loss causes β-catenin phosphorylation and degradation, and subsequent downregulation of WIP1. The potent GSK3β inhibitor, TWS119, which increases β-catenin level and upregulates WIP1 expression, recues cell senescence due to Cdk5rap2 loss. TWS119 together with the potent WIP1 inhibitor, GSK2830371, causes recurrence of senescence due to Cdk5rap2 loss, suggesting that GSK3β activity controls the β-catenin/WIP1-mediated senescence due to Cdk5rap2 loss. Promoter bashing analysis by transfecting a luciferase reporter vector carrying wt WIP1 promoter (pGL3-WIP1) into cells depleted of β-catenin or Cdk5rap2 reveal reduced luciferase activity compared to cells that are not depleted of β-catenin or Cdk5rap2. Conversely, transfection with NF-κB binding site-deleted WIP1 (pGL3-WIP1-ΔκB) show no difference in luciferase activity in β-catenin-or Cdk5rap2-depleted and non-depleted cells. Reduced luciferase activity in Cdk5rap2-depleted cells transfected with pGL3-WIP1 is reversed by TWS119, suggesting that β-catenin/WIP1-mediated senescence due to Cdk5rap2 loss is controlled by GSK3β through regulation of the WIP1 promoter via β-catenin. Potentially, cell senescence contributes to the developmental disorders associated with loss-of-function of Cdk5rap2.

In previous studies, loss of Cdk5rap2 or CENtromeric Protein A (CENP-A) was shown to trigger the occurrence of lagging chromosomes, leading me to investigate a possible link between these two proteins. I demonstrate that Cdk5rap2 loss causes reduced CENP-A expression while ectopic Cdk5rap2 expression in cells depleted of endogenous Cdk5rap2 restores CENP-A expression. In this regard, I found that Cdk5rap2 is a nuclear protein that acts as a positive transcriptional regulator of CENP-A. Cdk5rap2 interacts with the CENP-A promoter and upregulates CENP-A transcription. Loss of Cdk5rap2 particularly causes reduced centromeric CENP-A, which is known to induce kinetochore recruitment. I found that aside from manifesting lagging chromosomes, cells lacking Cdk5rap2, and thus CENP-A, show increased micronuclei and chromatin bridge formation, indicating that loss of Cdk5rap2 compromises centromeric chromatin integrity through downregulation of CENP-A.

Acknowledgements

First and foremost, I would like to express my sincere gratitude to my supervisor Dr. Ki-Young Lee for the opportunity to be part of his lab. His guidance, patience, supports and mentorship was invaluable in helping me achieve this feat. His friendly personality makes me comfortable to discuss my thoughts and opinions with him freely. The belief he placed in my immature scientific thinking, and the freedom to carry out the experiments unrelated to his lab's immediate interest, helped me learn a lot in these years. I couldn't have asked for more from a supervisor.

I also would like to thank my co-supervisor Dr. Xu Gao at Harbin Medical University. As a member of his lab, Dr. Gao's complete trust in me and great support made it easiere for me to study at University of Calgary. He gave me great freedom to dream in scientific research.

I also would like to extend my sincere appreciation and gratitude towards my supervisory committee members Drs. Karl Riabowol, Susan Lees-Miller, and Paul Mains for their extremely valuable suggestions and guidance for successful completion of my projects. I also would like to express my sincere thanks to Drs. Hude Quan and Michael Hendzel for taking time out from their busy schedule to serve as the internal and external examiners, respectively, for my Ph.D. thesis defense examination. I also thanks to Drs. Tara Beattie and Karl Riabowol and for providing human fibroblast cell lines and adenovirus vectors, respectively.

I would like to thank all the members of our laboratory (present and past): Susie, Kyle, Zach, Saranya, Vincent, Wejdan, Gyeongyeon, Guohong, Jung-Kwon, Patrick, and some of the members of the Dr. Gao laboratory in Harbin Medical University: Dayong, Ning, Yang, Lingyun, Zhaoxia, for your patience and understanding in teaching me laboratory techniques and for providing your samples which I have utilized for the completion of my thesis work. I appreciate all the Arnie Charbonneau Cancer Institute members who have helped me with reagents and kind suggestions.

I would like to thank the friendly staff of the DNA/RNA synthesis laboratory, Core DNA service facility and the flow cytometry facility of the University. You have all been extremely helpful!

I would like to thank Kiran, Aggie and Calvin for their timely assistance.

Finally, special thanks to my parents for their endless love, support and understanding. No matter what happens, you are always there for me. And a special thanks to my love, Zizhen Si who is of great support in sharing all my crazy thoughts, as well as delighting my daily life!

When I am down and, oh my soul, so weary

When troubles come and my heart burdened be

Then, I am still and wait here in the silence

Until you come and sit a while with me

You raise me up, so I can stand on mountains

You raise me up, to walk on stormy seas

I am strong when I am on your shoulders

You raise me up, to more than I can be

There is no life -no life without its hunger

Each restless heart beats so imperfectly

But when you come and I am filled with wonder

Sometimes, I think I glimpse eternity

You raise me up, so I can stand on mountains

You raise me up, to walk on stormy seas

I am strong when I am on your shoulders

You raise me up, to more than I can be

To my most merciful Lord who has carried me through all my ups and downs.

Table of Contents

List of Tables

List of Figures

List of Abbreviations

Symbol	Definition
Ad	Adenovirus
an	Hertwig's anemia
AMPK	Adenosine monophosphate-activated protein kinase
ANOVA	Analysis of Variance
APC	Adenomatous polyposis coli protein
APS	Ammonium persulfate
ARF	Alternative reading frame
ATM	Ataxia telangiectasia mutated
ATR	Ataxia telangiectasia and rad3-related protein
BCR	B cell receptor
bp	Basepair
BSA	Bovine serum albumin
BTRC	β-transducin repeat-containing protein E3 ubiquitin ligase
BubR1	Budding uninhibited by benzimidazole-related 1
CCN	Cellular communication network factor
Cdc20	Cell division cycle 20
CDK	Cyclin dependent kinase
Cdk5rap2	CDK5 regulatory subunit associated protein 2
cDNA	Complementary deoxyribonucleic acid
CENP	Centromere protein

CEP	Centrosome-associated protein
ChIP	Chromatin immunoprecipitation
ChK	Checkpoint kinase
CIP1	Cdk inhibitor protein 1
CM	Cnn motif
Cnn	Centrosomin
CREB	cAMP-responsive element-binding protein
CRP	C-reactive protein
Da	Dalton
DAPI	4’,6-diamidino-2-phenylindole
DDR	DNA damage response
DMEM	Dulbecco’s modified eagle medium
DNA-SCARS	Segments with Chromatin Alterations Reinforcing Senescence
Dvl	Dishevelled
EB1	End-binding protein 1
EDTA	Ethylenediaminetetraacetic Acid
EMEM	Eagle's minimal essential medium
ERK	Extracellular signal-regulated kinase
FBS	Fetal bovine serum
GAPDH	Glyceraldehyde 3-phosphate dehydrogenase
GSK3β	Glycogen synthase 3β
Gy	Gray

HEK293	Human embryonic kidney 293 cell line
HP1γ	Heterochromatin protein 1γ
IL	Interleukin
INK4a	Inhibitor of kinase 4a
IR	Ionizing radiation
kDa	Kilo Dalton
LEF	Lymphoid enhancer-binding factor
MAD2	Mitotic arrest deficient 2
MAPK	Mitogen-activated protein kinases
MCPH	Microcephaly
MEF	Mouse embryonic fibroblast
miRNA	microRNA
MMP	Mitochondrial membrane potential
MOMP	Mitochondrial outer membrane permeabilization
MOPD	Microcephalic osteodysplastic primordial dwarfism
mTOR	mechanistic target of rapamycin kinase
NEK2	NIMA related kinase 2
NF-κB	Nuclear factor kappa-B
NIH	National Institutes of Health
NP40	Nonidet P 40
PAGE	Polyacrylamide gel electrophoresis
PCM	Pericentriolar matrix

PCNT	Pericentrin
PCR	Polymerase chain reaction
Plk	Polo Like Kinase
PP	Protein phosphatase
PTEN	Phosphatase and tensin homolog
PUMA	p53 up-regulated modulator of apoptosis
Rb	Retinoblastoma transcriptional corepressor
RNA	Ribonucleic acid
ROS	Reactive oxygen species
rpm	revolutions per minute
RT-PCR	Reverse transcription polymerase chain reaction
SA-β-gal	Senescence-associated β-galactosidase
SAHF	Senescence-associated heterochromatin foci
SASP	Senescence-associated secretory phenotype
SD	Standard deviation
SDS	Sodium dodecyl sulfonate
siRNA	small interfering RNA
SMC	Structural maintenance of chromosome
TCF	T cell factor
TCR	T cell receptor
TEMED	N,N,N’,N’-Tetramethyl ethylenediamine
TGF	Transforming Growth Factor

TNF	Tumor necrosis factor
Wip1	Wild-type p53-induced phosphatase 1
Wnt	Wingless/Integrated
X-gal	5-bromo-4-chloro-3-indolyl β-D-galactopyranoside
β-gal	β-galactosidase
μL	microliter
μM	micromolar
℃	degree celcius

Chapter One: Introduction

1.1 Loss of Cdk5rap2 triggers cellular senescence via β-catenin-mediated downregulation of WIP1

1.1.1 Cell senescence

It was believed that cells from organisms had unlimited potential with little or no changes as long as they were supplied with nutrients and tissue extracts in vitro [1]. This concept was universally accepted at least in part. Alexis Carrel claimed to have cultivated fibroblasts from chicken hearts and to have kept the culture growing for 34 years [2]. But this observation was suspected due to error-prone cell culture in experimental procedure [3, 4].

In 1961, this theory was overturned by Leonard Hayflick and Paul Moorhead. They reported that fibroblasts derived from human embryo grown in culture have a limited replicative life span [3]. The primary cells always entered a state of cell cycle arrest but remaining viable and metabolically active after a fixed number of cell divisions [5]. This state of proliferation arrest that primary cells entered after their certain replicative life span was exhausted was called replicative senescence [6]. And the number of times that a normal cell will divide until undergo replicative senescence is defined as Hayflick limit [7]. This new theory of limits on cell replication objected to the most popular theories and was heavily debated. But subsequent studies by many independent research groups reported replicative senescence in many other normal primary diploid cells including endothelial cells, vascular smooth muscle cells, chondrocytes and keratinocytes [8-11]. These results disproved the immortality theory and established the Hayflick limit as a credible biological theory that has been repeated by other scientists.

Later, cell senescence was soon considered as a reason of the limited lifespan of the organisms and further deemed a hallmark of aging [12, 13]. Together with apoptosis, senescence is now known as a major evolutionarily conserved tumor suppressor mechanism that prevents division of old, mutant or damaged cells [14, 15]. More and more researches have brought our understandings of how cell senescence links to aging and cancer, and even tissue regeneration, and cell reprogramming [16-19].

1.1.1.1 Features and biomarkers of cellular senescence

Several significant changes happen in cell morphology, cell metabolism, cell secretion and gene regulation under senescent state, such as lager cell size, formation of senescence associated heterochromatin foci (SAHF), activation of cell survival signaling pathway against apoptosis and increasing secretion of various proinflammatory factors, metalloproteinases and growth factors [20-23]. These alterations have been well studied and are important to identify senescent cells both in vitro and in vivo. However, the complex nature of cell senescence and multiple pathways involved makes it difficult to represent the senescence activation. And senescent cells share several morphological and biochemical features with quiescent cells, which make difficulties to distinguish them [24]. Due to these complexities, no features or biomarkers are unique to senescent cells and no features or biomarkers are shared by all senescent cells. It depends on the type of cells or tissues being studied, the types of stress stimulation and the mechanism by which senescence is induced. Thus, study of senescence needs to test for several of these biomarkers.

1.1.1.1.1 Morphological changes

The most easily-detected phenotypic biomarker is enlarged and flat morphology of a senescent cell [25]. Senescent cells are often much larger than young and non-senescent cells. This alteration is found in the replicative senescence, Ras-induced oncogene-induced senescence (OIS) and some types of DNA damage-induced senescence [26-28]. However morphological change is not universal to all types of cell senescence. Some cells undergo senescence induced by p400 become more like spindle shaped [29, 30].

1.1.1.1.2 Irreversible cell cycle exit and growth arrest

Irreversible cell cycle arrest or withdrawal is the most important characteristic of cell senescence [31]. Two major signaling pathways, p53-p21^{CIP1} pathway and Rb-p16^{INK4a} pathway are activated and maintain senescent state [32, 33]. When DNA damage response (DDR) is activated due to telomere shortening or DNA damage, ATM and ATR can be activated to phosphorylation and activation of p53 [34, 35]. Activated p53 can enter the nucleus, play the role of transcription factors, and promote the expression of p21^{CIP1} [36]. High expression of p21^{CIP1} prevents cell cycle progression and blocks G1 phase [37]. Permanent cell cycle arrest or exit is usually mediated by p16^{INK4a} [38]. Except Rb, the expression of p16^{INK4a} is also controlled by BMI1 and p38/MAPK and ERK signaling pathways [39, 40]. The high expression of p16^{INK4a} inhibits the activity of CDK4 and CDK6, resulting in the low phosphorylation of Rb, which blocks the cell cycle transition to the S phase leading to cell cycle arrest [41, 42]. Therefore, p16^{INK4a} is also utilized as a molecular biomarker of cell senescence [43].

1.1.1.1.3 Formation of senescence associated heterochromatin foci (SAHF)

Cell nuclei in senescent cells display high density spots by DAPI staining while non-senescent cells have a more diffused nuclear staining. These high density DAPI-stained regions are known as senescence associated heterochromatin foci (SAHF) [44]. SAHF are characterized by the presence of several heterochromatin associated proteins including HP1γ [45]. H3K9 methylation whcih is associated with transcriptional repression is also commonly found in SAHF while activation marks such as H3K9 acetylation and H3K4 methylation are completely absent in SAHF regions [46]. Cells compromised with p16INK4a/Rb bypass cell senescence exhibit SAHF formation, suggesting that p16INK4a/Rb signaling pathway is important for SAHF formation and initiating a chromatin remodelling program that leads to permanent growth arrest [47, 48].

1.1.1.1.4 Increased senescence associated β-galactosidase activity

Another biomarker that is commonly and traditionally utilized to identify senescent cells is increased senescence associated β-galactosidase activity [49]. Young cells and non-senescent cells also have β-galactosidase, but at very low level that only can be detected under pH=4.0 [50]. Senescent cells display increased activity of this enzyme and can be detected even at pH=6.0 [51]. Although the reason of increased β-galactosidase activity is not known, this alteration is commonly found under senescent state [52].

1.1.1.1.5 Senescence-associated secretory phenotypes

Senescence-associated secretory phenotypes (SASP) are another characteristic of cell senescence [53, 54]. Cell senescence may be associated with "inflammation" through SASP, especially in chronic inflammation and proteolysis leading to tissue dysfunction, age-related diseases and even the body aging itself [55-57]. SASP is believed to appear in the early stage of cell senescence [58]. Senescent cell can secrete a variety of cytokines to affect the surrounding cells [59]. One study showed that senescent cells secrete as many as 103 cytokines using isotopic labeling (SILAC) and mass spectrometry [60]. These cytokines mainly include transforming growth factor β (TGFβ), interleukin 1 (IL-1), interleukin 6 (IL-6), interleukin 8 (IL-8), matrix metalloproteinases (MMPs), and epidermal growth factor (EGF), etc [16].

The cytokine components of SASP are different in the early and late stages of cell senescence. In the early stages, SASP was mainly composed of TGFβ family members [61]. When these cytokines are received by surrounding cells, they can also induce cellular senescence in these cells. In the late stage, due to the activation of Notch pathway, pro-aging SASP is promoted to pro-inflammatory SASP, and a large amount of IL-6 and IL-8 is produced [62]. This change will greatly change the cell microenvironment, thereby affecting the biological function of the cells. In tumors, SASP cytokines can scavenge large numbers of tumor cells by recruiting immune cells [63]. However, the pro-inflammatory microenvironment caused by pro-inflammatory SASP may also be beneficial to tumor proliferation, angiogenesis, tumor metastasis and inhibition of anti-tumor immunity [64]. Therefore, SASP can be tumor-inhibiting and tumor-promoting, short-term SASP may be beneficial, and chronic long-term SASP may be harmful. Another study found that exposure of keratinocytes in an in vivo skin graft model to senescent cells for a short period of time can promote skin tissue regeneration, but prolonged exposure can inhibits their proliferation [65]. This may indicate that SASP produced by senescent cells may initially activate resident stem cells under injury conditions requiring repair, but is self-limited in nature.

1.1.1.1.6 Alterations in gene expression and activation of tumor suppressor

Senescent cells are featured by global changes in gene expression patterns. Over-expressions of various CDK inhibitors, particularly $p16^{INK4a}$ and $p21^{Cip1}$ occur in senescent cells [66].

Proteins essential for cell cycle progression such as PCNA, Cyclin A and E2F transcriptional target genes are suppressed in senescent cells [67-69]. The level of Rb accumulates in senescent cells in the active form and represses proliferative genes expression, and also promotes SAHF formation [70]. Both transcriptional activity of p53 and the activating phosphorylation on Ser15 residue are known to increase in many types of senescence [71, 72].

1.1.1.1.7 DNA damage markers

Another frequently observation in senescent cells is DNA damage. Senescent cells harbor prominent γH2AX foci called DNA-SCARS (Segments with Chromatin Alterations Reinforcing Senescence) [73]. DNA-SCARS are found to co-localized with many DNA damage response (DDR) proteins, such as activated ATM, ATR, Chk1, Chk2 kinases, 53BP1 and MDC1 [74]. Telomere shortening also causes DNA-SCARS in replicative senescent cells [75, 76]. However, DNA-SCARS is not observed in all senescent cells. Loss of CENP-A induced cell senescence is an example of this exception. Fibroblast cells lack of CENP-A undergo cell senescence in p53 dependent manner without any DNA damage foci [77].

1.1.1.1.8 Cell senescence inhibits cell apoptosis

Senescent cells show changes in apoptotic regulatory signals, which are usually shown as resistance to programmed cell death [78]. A key determinant of cell fate determination of senescent and apoptotic cells is through the p53 stress response pathway [79]. Total p53 levels and post-translational modifications were observed to regulate the expression profiles of downstream target genes. When aging stress occurs, the accumulation of p53 is lower than that of apoptosis, which leads to the expression of p53 up-regulated modulator of apoptosis (PUMA) and PMAIP1 as well as higher levels of Bcl2 family proteins [80]. Bcl2, Bcl-xl (also known as Bcl-2l1) and Bcl-w (also known as Bcl-2l2) are highly expressed in senescent cells, thereby inhibiting mitochondrial outer membrane permeabilization (MOMP) and cell apoptosis [81]. Studies have shown that cells with p53 lacking of acetyl receptor residue K117 cannot undergo apoptosis, but still retain the ability to enter cell senescence by upregulation of p21^{CIP1} expression [82]. p21^{CIP1} itself can block apoptosis and may directly inhibit caspase 3 (CASP3) activity [83]. Conversely, apoptotic cells can silence the expression of p21^{CIP1} through p53-dependent DNA -methyltransferase 3A (DNMT3A), thus inhibiting the occurrence of cell senescence [84].

1.1.1.2 Major molecular mechanisms in cellular senescence

With increasing senescence inducing stress, cells can activate variety of pathways, many of which activate p53, and all in the activation of cell cyclin-dependent kinase (CDK) inhibitors p16^{INK4a}, p15, p21^{CIP1}, and p27 (Figure 1) [85].

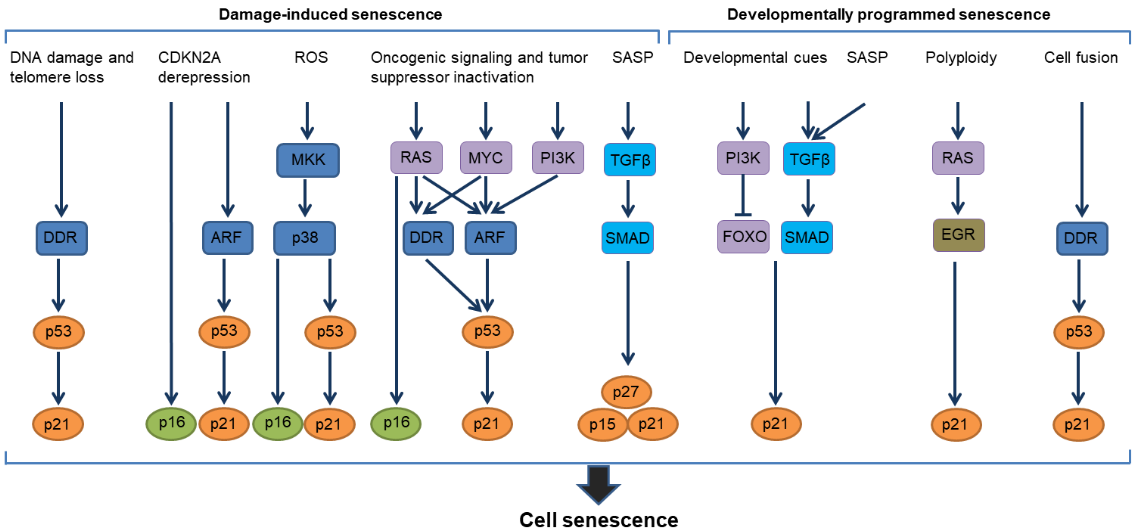

Figure 1. The major pathways of cell senescence.

Since there are so many factors that trigger cell senescence and different cell types, the mechanisms that ultimately lead to senescence can also vary according to cell types and stimuli [20].

1.1.1.2.1 Telomere shortening

A telomere is a region of repetitive nucleotide sequences at each end of a chromosome, which protects the end of the chromosome from deterioration or from fusion with neighboring chromosomes [86]. Telomeres are replenished by telomerase reverse transcriptase [87]. In eukaryotes, the telomere ends become shorter due to uncompleted replication at the end of the chromosome during chromosome replication in cell divisions [88]. It is now well established that telomere shortening is the major cause of replicative senescence [89]. And telomere is considered as the clock of life span [90]. Cells with longer telomeres live longer than those with short telomeres [91].

Progressive loss of telomeres through consecutive cell cycles ultimately leads to unprotected chromosomal ends that can result in activation of DNA damage response causing cell senescence [92]. In addition to replicative telomere shortening, telomeres are particularly sensitive to external DNA damage stress [93]. This is because the structure of telomeres is difficult to repair through DNA damage responses pathway. The main mediators of DNA damage response pathway are DNA damage kinases ATM, ATR, ChK1 and ChK2, which phosphorylate and activate several downstream effectors; especially p53 [94]. Phosphorylated p53 protein activates the expression of $p21^{CIP1}$, binds to and inhibits some Cdk-Cyclin complexes, and thus induces cell senescence.

Telomerase is a ribonucleoprotein that carries a short RNA molecule, and functions as a reverse transcriptase with the RNA molecule adds a species-dependent telomere repeat sequence to the 3' end of telomeres [95]. Telomerase is expressed at quite low levels in normal cells [96]. Thus the length of telomere is shortened in cell division leading to cell senescence. But in stem cells, Telomerase is highly expressed to elongate telomere length ensuring unlimited proliferation potential [97, 98]. Many types of cancer cells also harbor high levels of telomerase to maintain their telomere length [99]. Over-expression of telomerase in normal cells is sufficient to maintain telomere length and also extend cellular lifespan [100, 101]. These observations point to the critical roles of telomerase and telomere shortening in cell senescence.

Replicative senescence is also associated with the CDKN2A locus (also known as INK4A and ARF), which encodes two key tumor suppressors, p16^{INK4a} and ARF [102]. p16^{INK4a} is an inhibitor of CDK4 and CDK6, and ARF increases p53 stability by inactivating the E3 ubiquitin ligase MDM2 [103]. The CDKN2A locus is usually expressed at very low levels in young tissue cells, but increases with age. However, the molecular mechanism of CDKN2A de-repression is not fully understood.

1.1.1.2.2 Oncogene-induced senescence (OIS)

Normal cells undergo cell senescence to against activation of many oncogenes, which is the fail-safe mechanism to maintain genomic integrity and to prevent tumorigenesis [104]. Activation of oncogenes helps aberrant cells to overcome tumor suppressor mechanisms . However, over-expression of mutant RAS induces distinct cellular senescence phenotype in primary cells, which is known as oncogene-induced cellular senescence [105]. More than 50 oncogenes have been found to induce the occurrence of cell senescence by over-expression [106]. Although the exact processes by which oncogene over-expression can induce cell senescence remain largely unknown, accumulation of DNA damage are often associated with over-expression of oncogenes in cells [107]. These DNA damage can activate the p53 protein by activating the DDR signaling pathway and promote the onset of cell senescence [108]. Oncogene-induced senescence is independent of telomere length, and cells that over-express telomerase cannot bypass this type of senescence [109]. Over-expression of oncogenes leads to abnormal DNA replication and high ROS levels, resulting in a large accumulation of DNA damage. Thus, the DDR signaling pathway is activated, which can subsequently activate p16, ARF and p53, to induce cell senescence [110]. Several studies that looked at signaling pathways suggested that mechanisms of OIS execution are not conserved in different cell types. In mice cells, the ARF-p53 pathway is a key activator of oncogene-induced senescence, and $p16^{INK4a}$ has a weak role in inducing cell senescence [111, 112]. However, in human cells, the DDR-p53 pathway plays a more important role than the ARF-p53 pathway, and the role of Rb-$p16^{INK4a}$ signaling pathway in inducing human cell senescence is more efficient. Deletion of $p19^{ARF}$ completely bypassed OIS in mice cells but not in human cells. But Human cells needed functional $p16^{INK4a}$ protein for Ras V12 induced OIS activation [47, 113]. Although the functions of cytokines in inducing OIS in vivo are not completely explored, recent studies have demonstrated that secreted cytokines and chemokines play a vital role in OIS activation. Over-expression of CXCR2 by itself was sufficient to induce senescence in fibroblast cells. Insulin-like growth factor binding protein 7 (IGFBP7) is required for BRAF-induced cell senescence [114, 115]. IL-6 and IL-8 are found to be involved in BRAF-induced cell senescence [56]. Interestingly, higher level of IL-6 is identified in premalignant lesions. This may due to successful activation of OIS but failure prevention of malignant transformation [56].

1.1.1.2.3 Oxidative stress-induced senescence

Cells grown in vitro encounter conditions are very different from those encountered in vivo. Many different types of cellular stimuli, such as excess nutrients and oxygen levels, chemotherapy drugs, loss of telomere protection, DNA damage, and oncogene activation, can lead to increased levels of cellular reactive oxygen species (ROS) [116]. Oxidative stress activate the p38/MAPK signaling pathway through RAS-RAF-MEK-ERK cascade induced high intracellular ROS levels, leading to increased transcriptional activity of p53 protein and up-regulation of p21^{CIP1}, thus inducing cell senescence [117]. On the other hand, oxidative stress can also lead to DNA breakage, activation of DDR signaling pathway. Activated DDR signaling pathway can potentially activate senescence through both p53/p21^{CIP1} and Rb/p16^{INK4a} pathways [118].

1.1.1.2.4 DNA damage induced senescence

As described above, telomere shortening induced replicative senescence, oxidative stress induced cell senescence and oncogene over-expression induced senescence all can activate DDR signaling pathway [90]. DDR signaling cascade involving Ataxia Telangiectasia-Mutated (ATM), Ataxia Telangiectasia and Rad3-Related (ATR), Checkpoint Homologs 1 and 2 (Chk1 and Chk2) and the p21^{CIP1}/p16^{INK4A}/p19^{ARF} tumor suppressor proteins [14, 119]. Many anti-cancer chemotherapeutic agents, such as PARP inhibitors, doxorubicin, and cisplatin, induce single- or double-strand DNA breaks and cause cells to undergo stress induced cell cycle arrest [120]. Persistent stress caused persistent cell cycle arrest will force these cells to undergo either apoptosis or senescence. Many studies have revealed p53-dependent mechanisms are critical in therapy-induced senescence . But some agents functions in p53-independent manners as well. For example, inhibitor of Aurora kinase A can induce senescence by blocking mitosis in cancer models regardless of their p53 status [121]. It has to be notice that therapy-induced senescence is not a universal response induced by all the anti-cancer chemotherapeutic agents.

1.1.1.2.5 The important role of p53 in cell senescence

The tumor suppressor p53 is an important transcription factor whose activity is precisely regulated by post-transcriptional modification. Since p53 can inhibit cell proliferation and induce apoptosis, it is considered to be one of the most powerful tumor suppressor genes [122]. Loss of p53 or mutant p53 is found in most human cancers. Interestingly, p53 presents in short-lived organisms that do not develop cancer, such as flies and worms, suggests that tumor suppression is not the only biological function of p53. Recent studies have also shown that p53 can affect development, reproduction, material metabolism, longevity and other biological process [123-126].

A chance discovery links p53 to cellular senescence. When Tyson and his colleagues tried to knock p53 into the mouse genome, they got an abnormally truncated version of p53 at the N-terminal. This truncated p53 mutant protein showed very strong constitutive p53 activity. And the mice with this mutant p53 exhibited a series of characteristics related to aging and significantly shortened lifespan. In 2004, a truncated mouse model with truncated p53, DNp53 or p44 subtype was developed in Scrable laboratory. This mouse line shows many significant defects in the growth process, and was associated with shorter life span and accelerated aging [126]. p53 up-regulated modulator of apoptosis (PUMA) is a pro-apoptotic protein and has been identified as a target gene of p53. In the case of p53 mutation, inhibition of PUMA can reverse the loss of stem cells and improve the aging phenotype [127].

Studies have shown that the human p53 activity is based on the phosphorylation/de-phosphorylation of Ser15 residue [79]. The same regulatory mechanism exists in mice, but the phosphorylation site is Ser18 residue. ATM phosphorylates p53 at site in response to the DNA damage response. In 2006, Armata and his colleagues analyzed the phenotype of knock-in mice in which p53 Ser18 site was replaced by non-phosphorylated alanine. These mice showed signs of accelerated aging, indicating that normal p53 activity could protect tissue cells from aging-related damage [128]. Another mouse model inserted with p53 and p19^{ARF} provides new evidence for anti-aging activities. This transgenic mouse has a long genome sequence containing p53 and p19^{ARF}, allowing high expression of both genes while maintaining endogenous regulatory mechanisms for p53 and p19^{ARF} [129]. Phenotype analysis showed that these mice lived longe. Although p19^{ARF} may function independently of p53, it can also increase p53 activity by preventing MDM2-mediated p53 degradation in proteasome.

These findings indicate that loss of p53 is detrimental to aging. Induction of p53 is essential for the occurrence of aging, especially after p53 is activated by DDR [130]. Variety of p53 target genes and regulators have been shown to be closely related to cell senescence, including microRNAs [131]. But its molecular mechanisms have not been fully elucidated. CDKN1A/p21^{CIP1}, one of the most mature p53 target genes, has been confirmed to be up-regulated in the process of replicative senescence. p21^{CIP1} is one of the earliest identified downstream targets of p53 and an important protein in p53 mediated cell senescence [132]. It was found that embryonic fibroblasts derived from p21^{CIP1} knockout mouse could not occur p53-dependent G1 arrest after DNA damage [133]. These studies demonstrate that p53-induced cell cycle arrest is dependent on $p21^{CIP1}$, and also indicate that $p21^{CIP1}$ plays an important role in cell senescence.However, p53-induced high expression of $p21^{CIP1}$ is not the only cause of cell senescence or the complex phenotypes of cell senescence [134].

Some studies have also shown that p53 can regulate cell senescence through the mTOR signaling pathway [135]. This p53/mTOR regulatory axis is usually caused by nutrient depletion [136]. When nutrients are adequate, active mTOR promotes cell growth and anabolism. In contrast, when nutrients are deficient or depleted, mTOR can be rapidly inactivated to promote catabolism and growth arrest. Recent studies have shown that the administration of mTOR inhibitors can extend the life span of mammals. It is shown that mTOR signaling pathway can be inhibited by p53 in different ways. p53 can directly inhibit mTOR activity by regulating sestrins [137]. In addition, p53 promotes the expression of AMP-activated protein kinase (AMPK), which in turn inactivates mTOR [138]. Moreover, p53 can also up-regulate PTEN to block the PI3K signaling pathway and further inhibit mTOR signaling [139].

1.1.1.3 Cell senescence, aging and age-related diseases

Cell senescence is often related to aging and age-related diseases. But many studies also showed that cell senescence is also involved in many physiological processes.

1.1.1.3.1 Cell senescence and aging

The idea that cell senescence contributes to organismal aging rises from several observations including the fact that cells explanted from aged donors went through fewer population doublings than those from younger individuals [58]. Now cell senescence is believed as a hallmark of aging. The tissue cells undergo cell senescence response to various endogenous or exogenous stimuli declines organ function. Studies have shown that injection of serum from young mice into old mice improves their learning and memory abilities. Conversely, injection of serum from old mice into young mice impairs their learning and memory abilities. These observations indicate that cell senescence plays an important role in the individual aging.

Another line of evidence that supports development of age-associated senescence in organisms is reduction of telomere length with increasing age. Many studies have found senescent cells in tissues. And their number, as determined by different senescence markers, increase in the tissues of older humans, primates and rodents.

1.1.1.3.2 Cell senescence is the essential mechanism in development

Recent researches have shown that cell senescence is one of the important mechanisms during embryonic development. Using mouse embryos, researchers found that cell senescence occurred extensively in different cells in various organs [140]. Cell senescence in the embryonic stage is strictly dependent on $p21^{CIP1}$, rather than p53-dependent or DNA damage dependent [141]. Senescence cells in the embryonic stage express high levels of $p21^{CIP1}$ regulated by the TGF-β/SMAD and PI3K/FOXO signaling pathways. Embryonic cell senescence plays an important role in organ remodeling. These findings point to a new direction of cell senescence. Cell senescence occurs not only during stress response and aging, but also during early embryonic development, contributing to physiology and health.

1.1.1.3.3 Cell senescence is a self-defense mechanism

When oncogene over-activation occurs, cell senescence can be induced by p53/p21^{CIP1}, p38/MAPK and other pathways. Senescent cells can be eliminated to prevent malignant transformation [142]. On the other hand, with the increasing number of cell division, a great number of damage is accumulated in the cell [143]. These accumulated damages may induce the cell to undergo a transformation into a cancer cell. But cells cannot divide permanently and enter the cellular senescence process, which removes the cells with damages. Therefore, cellular senescence is considered to be one of the self-defense mechanisms of cells, preventing damage from entering the daughter cells and affecting the whole organ or individual [18].

1.1.1.3.4 Cell senescence and tissue regeneration

Cell senescence can occur not only in somatic cells, but also in stem cells, which is crucial for maintaining the homeostasis of tissue renewal and tissue regeneration after injury [144]. Stem cell senescence has the following characteristics: (1) loss of self-renewal ability, which leads to the depletion of stem cell pool [145]; (2) decreased response to exogenous stimulus signals [146]; (3) abnormal in stem cells differentiation [98]. The damaged cells will be removed immediately when the organ get damaged. Then the stem cells are activated to produce new functional cells to replace the damaged cells. But if the stem cells undergo cellular senescence, they cannot consistently and correctly differentiate into functional cells with normal biological functions. This will eventually lead to the decline the function of tissues.

1.1.1.3.5 Cell senescence and disease

Cell senescence has been shown to be associated with number of human diseases, particularly with age-related diseases [147]. Studies have revealed that the roles of cell senescence are not congruity in different disease.

Cancer is known as age-related disease. In the early stage of tumorigenesis, the expression of oncogenes increases gradually. Cell senescence can be induced when its expression level increases to a certain extent [148]. Senescent cells can be further cleared by the immune system, preventing the spread of precancerous cells. On the other hand, senescent cells secrete a large number of inflammatory cytokines and change the cellular microenvironment [149]. These factors contain high levels of IL-6, TGF-β, MMPs, etc. If senescent cells are not eliminated, senescent cells can continuously secrete the above-mentioned cytokines, which can promote the development of cancer [150].

Alzheimer's disease (AD), a common neurodegenerative disease, has also been shown to be associated with cell senescence [151]. Senescent cells have been identified in the brain tissue of Alzheimer's patients. Studies have demonstrated that cell senescence is related to Tau tangles, which are one of the two pathological features of AD [152].

Atherosclerosis is another common disease of aging. Cell senescence plays a very important role in the pathogenesis of atherosclerosis [153]. Senescent cells produce the initial plaques that enter the blood vessel wall through SASP mediated mononuclear cells in the blood. The senescent endothelial cells are easily removed, resulting in vessel leakage [154].

Cutaneous fibrosis is a part of wound healing and is similar as liver fibrosis. The extracellular matrix protein family (CCN) is essential for inducing the senescence of dermal fibroblasts [155]. CCN1 activates NADPH oxidase 1 (NOX1) by RAC1 to activate DDR signaling pathway, ERK and p38 MAPK signaling pathways, which lead to the up-regulation of p53 and p16 [156]. Topical treatment with recombinant and purified CCN1 protein can reduce fibrosis during wound healing [157]. CYR61 knockout mouse models have demonstrated that loss of CYR61 does not activate dermal fibroblast senescence, which is involved in skin healing, but leads to fibrosis progression [155]. These studies suggest that cellular senescence is involved in limiting the initial wound fibrosis response.

1.1.2 CDK5 regulatory subunit associated protein 2 (Cdk5rap2)

Cyclin-dependent kinase 5 regulated subunit related protein 2 (Cdk5rap2) also known as CEP215, is a centrosomin family protein that is widely found in various cells [158]. Cdk5rap2 was initially identified based on its interaction with p35, the activator of Cdk5 [159, 160]. Cdk5rap2 is expressed ubiquitously in all human tissues, with highest expressed in brain and spine during embryonic development [161]. In 2005, Bond et al utilized a positional cloning strategy to identify that Cdk5rap2 is a gene in the MCPH3 locus linking Cdk5rap2 to primary microcephaly (MCPH) [162], a rare autosomal recessive neurodevelopmental disorder affecting ~1:30,000 to 1:250,000 individuals worldwide [163]. Individuals with primary microcephaly are born with a significant reduction in brain size, resulting in reduced head circumference between 4 and 12 standard deviations below the norm and severe mental retardation [164]. This reduction in brain size is believed to result from asymmetric division of neuronal progenitor cells, causing reduced number of neurons in embryonic development [165]. Previous studies have reported two different mutations, $T_{243}A$ and IVS26-$A_{15}G$, in the Cdk5rap2 gene in two northern Pakistani microcephaly pedigrees [166]. Both of these two mutations result in truncated protein products of 81 and 1338 amino acid residue peptides, respectively. Disruption of Cdk5rap2 in mice reveals a primary microcephaly phenotype [167].

These landmark findings are vital for understanding the molecular mechanisms by which MCPH3/Cdk5rap2 controls brain size.

1.1.2.1 The structure of Cdk5rap2

Cdk5rap2 is a 1893 amino acid residue protein that contains an N-terminal microtubule interaction site important for the -tubulin ring complex formation (γTuRC, 59-133aa; CM1), two predicted structural maintenance-of-chromosomes (SMC) sites (137-499aa, 1395–1653aa) important for chromatid cohesion, and DNA recombination during meiosis and mitosis, a Ser-rich motif for interaction with plus-end binding protein EB1 (926-1208aa), an interaction site with pericentrin (within 1726-1893aa), a C-terminal Cnn Motif 2 (CM2) domain for Golgi complex interaction and binding to calmodulin (within 1861-1870aa) and a C-terminal interaction site with Cdk5R1 (also known as p35), an activator or modulator of Cdk5 (Figure 2) [158].

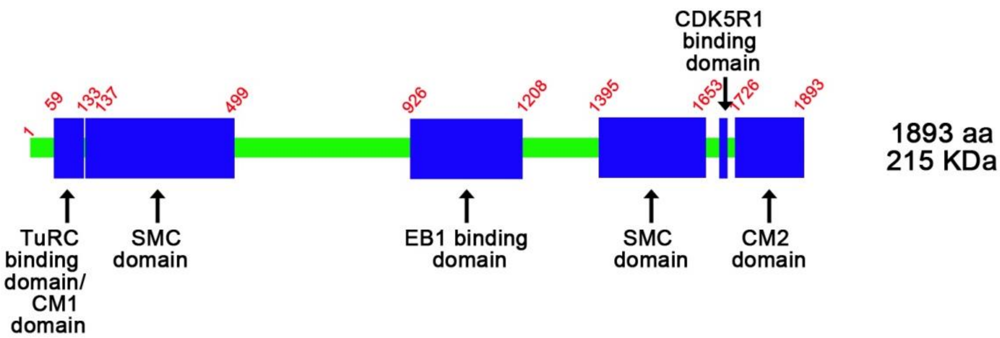

Figure 2: Schematic diagram of Cdk5rap2 protein domains.

Cdk5rap2 also contains coiled helical domains forming filament-like structures, which are the characteristics of perenentriolar matrix scaffold proteins . By comparing with NCBI's conserved domain database, it was found that Cdk5rap2 had homology with SMC proteins involved in cell division and chromosome distribution. There are two SMC domains in Cdk5rap2, known as SMC1 and SMC2 (figure 2). Further sequence alignment revealed the presence of Walker A domain in SMC1 of Cdk5rap2 and a Walker B domain in SMC2. SMC domain allows proteins to interact with C-terminal and N-terminal domains to form homologous dimers or heterodimers. Cdk5rap2 may form homologous dimers or heterodimers by similar biological mechanisms.

1.1.2.2 The biological function of Cdk5rap2

Studies have found that Cdk5rap2 mainly exists in centrosomes, microtubules and Golgi complex (Figure 3), and plays a very important role in maintaining the integrity of centrosomes structure and function [168]. Cdk5rap2 has also been implicated in biological processes such as DNA damage repair, cell cycle regulation, and Wnt signaling pathway.

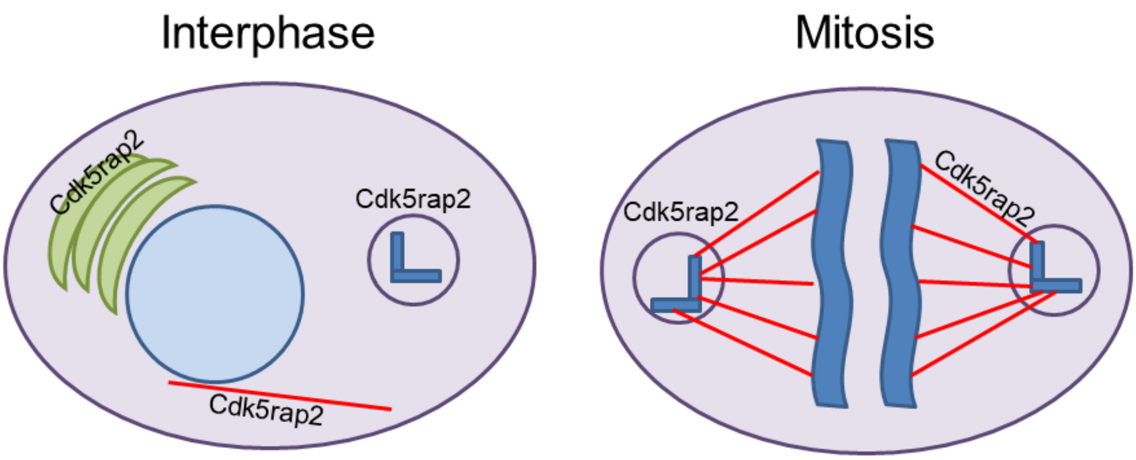

Figure 3: Cdk5rap2 is mainly presented at centrosome, microtubules and Golgi complex.

1.1.2.2.1 Cdk5rap2 and centrosome

Cdk5rap2 levels at the centrosome which plays a key role in the control of the temporal and spatial distribution of microtubule networks have been found to be regulated in a cell cycle-dependent manner in fibroblasts (low levels in interphase, high levels in prophase until telophase) [169, 170]. Disrupted Cdk5rap2 function inhibits centrosomal microtubule nucleation, which leads to disorganization of interphase microtubule arrays and formation of anastral mitotic spindles. RNAi knockdown and mutation of Cdk5rap2 reveals diverse centrosomal functions and its requirement for neural progenitor division or survival. Cdk5rap2 has a Drosophila orthologue, centrosomin (Cnn), which is required for centrosome assembly [171]. Loss of zygotic Cnn expression in flies perturbs development of the gut and the nervous system. Lizarraga et al reported an increase of asymmetric and a decrease of symmetric cell proliferation in a Cdk5rap2$^{an/an}$ mouse model [167]. In other mouse models, such a shift from symmetric to asymmetric proliferation has been shown to lead to a depletion of the progenitor pool, a reduction of brain size, and an increase of precursor and neuronal cell death [172].

1.1.2.2.2 Cdk5rap2 and cell cycle regulation

Although Cdk5rap2 has been proved to mainly present at centrosomes, Golgi complex and microtubules, one study found that Cdk5rap2 can act as a transcription factor to regulate the expression of MAD2 and BubR1 in Hela cells [173]. The MAD2 and BubR1 are important regulatory proteins for cell cycle checkpoints. Cdk5rap2 silencing cells also showed low levels of MAD2 and BuBR1. Low expression of MAD2 and BuBR1 leads to the inability of cell cycle checkpoints to be activated, allowing CDC20 to be located on the chromosome. Although chromosome mis-segregation occurs during cell division upon loss of Cdk5rap2, the cell cycle checkpoints is not activated and arrest cell cycles. Cells can ignore these errors and successfully complete cell division. This finding also explains the absence of Cdk5rap2 expression in some tumor cells.

1.1.2.2.3 Cdk5rap2 and Wnt signaling pathway

The Wnt signaling pathway is an important regulatory mechanism to maintain cell biological function and cell survival [174]. Dishevelled (DVL) protein is one of key molecules mediated Wnt signaling pathways [175]. DVL promotes the phosphorylation of GSK3β and blocks its activity, which in turn increases the level of β-catenin in cells [176, 177]. High levels of β-catenin then translocate into the cell nucleus and activate downstream genes expression.

A study published on PNAS in 2016 showed that Cdk5rap2 can bind to DVL protein [178]. This Cdk5rap2: DVL binding can be significantly enhanced by the centrosome-specific kinase NEK2. NEK2 phosphorylates DVL and activates the Wnt signaling pathway. Cdk5rap2 acts as a scaffold protein in this process.

1.1.2.3 Cdk5rap2 and human diseases

Primary microcephaly (MCPH) is a rare autosomal recessive neurodevelopmental disorder. Patients with MCPH are often born with significant reduction of brain size and reduced in occipital prefrontal circumference (OFC) and brain volume. Individual patients may have a lower normal range of OFC at birth but will undergo "secondary microcephaly" within first year after birth. Many patients exhibit mental retardation, including speech delays, hyperactivity and attention deficits, aggression, delayed developmental milestones, and seizures. In addition, abnormal height and weight and congenital hearing loss are detected in some patients.

At least 8 genes have been proved to be mutated in primary microcephaly patients and were given the name MCPH1~MCPH8 [179]. Each of these loci has been mapped to their corresponding gene in separate studies which are MCPH1/microcephalin, MCPH2/WDR62, MCPH3/Cdk5rap2, MCHP4/CEP152, MCHP5/ASPM, MCHP6/CENP-J, MCHP7/STIL and MCHP8/CEP135. Interestingly, all these eight MCPH genes code centrosome associated proteins. Cdk5rap2 loss of function mutation mice model (Cdk5rap2$^{an/an}$ mouse) can fully simulate the pathological characteristics of MCPH. Neural progenitor cells of this mice model show split centrosomes, resulting in multipolar spindle in mitosis. Cdk5rap2 loss of function mutation also causes the progenitor cells to undergo prolonged mitosis and leads to the cell death.

Interestingly, mouse embryonic fibroblast (MEF) cells derived from another Cdk5rap2 mutant mice model display a growth arrest phenotype [170]. MEF with mutant Cdk5rap2 cells is arrest between passage 8 and passage 10. After passage 4 a higher percentage of cells were needed to seed a culture. Following passage 8 and passage 10, MEF with mutant Cdk5rap2 remain viable but would no longer grow to confluence. These observations suggest that Cdk5rap2 is not only involved in development of nervous system but also in other tissues. This is further confirmed by identification of Cdk5rap2 mutation in Seckel syndrom[180] and primordial dwarfism [181]. Different from microcephaly, adults with Seckel syndrome or primordial dwarfism show short stature. And Cdk5rap2 mutant mice models always have smaller body size and lighter body weight. However, the biological functions of Cdk5rap2 and its mechanisms in tissue development other than nervous system remain largely unknown.

1.1.3 Wnt signaling pathway and β-catenin

In 1982, the Wnt gene was discovered in mouse breast cancer cells [182]. The gene was then given the name Int1 as its activation depended on the insertion of a mouse breast cancer-related virus gene. Subsequent studies have shown that Int1 plays an important role in the normal embryonic development of mice, which is equivalent to the Wingless gene of fruit flies and control the axial development of embryos [183]. Since then, a large number of studies have suggested the importance of Int1 gene in the embryonic development of the nervous system, so Wingless was combined with Int1 to be called Wnt gene. The human Wnt gene is located at 12q13.

Wnt signaling pathway consists of two pathways which are canonical Wnt signaling pathway and non-canonical Wnt signaling pathway [184]. Studies have shown that β-catenin is the effector of canonical Wnt signaling pathway. The level of β-catenin is accumulated in cytoplasm and translocated into cell nuclei to promote expressions of downstream target genes [185].

1.1.3.1 Canonical Wnt signaling pathway

The transduction of the canonical Wnt signaling pathway depends on a continuous process which is regulated at multiple levels. The canonical Wnt signaling pathway has two states: on-state and off-states [186]. In off-state, each receptor of the signaling pathway is inactivated. The level of β-catenin is low under the control of destruction complex consist of GSK3β, CK1, APC and Axin. GSK3β phosphorylates β-catenin and subsequently leads to the ubiquitination on β-catenin. Ubiquitinated β-catenin then is degraded by proteasomes. DDK, the endogenous negative regulator of Wnt signaling pathway can binds to LRP receptor and inhibits downstream signaling transduction (Figure 4A).

In on-state, the Wnt protein binds to Frizledled and LRP receptors and the intracellular tail of LRP will be phosphorylated. This modification further leads to the interaction of LRP and Axin in a Wnt dependent manner. Then dishevelled (DVL) protein is phosphorylated and subsequent causes phosphorylation at an inhibitory serine residue (Ser9) on GSK-3β that deactivates the catalytic capability of GSK-3β. Deactivation of GSK-3β on longer phosphorylates β-catenin resulting in the accumulation of non-phosphorylated β-catenin. Non-phosphorylated β-catenin is released from destruction complex leading to accumulation of β-catenin in the cytoplasm. Then, β-catenin translocates into cell nucleus and interacts with TCF/LEF transcription factors to induce the expressions of downstream target genes (Figure 4B).

In the off-state, TCF/LEF forms a complex with Groucho, inhibiting the expressions of target genes. As long as β-catenin translocates into cell nucleus, TCF/LEF can be re-transformed into a transcriptional activator and the expression of this gene can be activated. Many genes have identified as a downstream target of Wnt signaling pathway. Most of these genes are contribute to cell proliferation and cell survival, including CyclinD1, WISP1, c-myc, COX-2, etc [187-189].

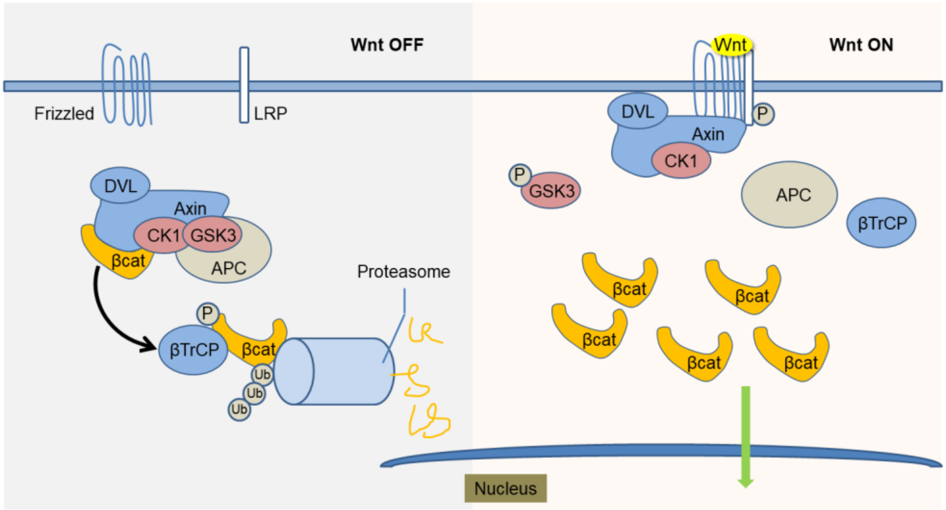

Figure 4: Schematic diagram of Wnt signaling pathway. (A) The off-state of Wnt signaling pathway. **(B)** The on-state of Wnt signaling pathway.

1.1.3.2 Non-canonical Wnt signaling pathway

In non- canonical Wnt signaling pathway, Wnt stimulates polarity formation in planar cells by activating the small GTPase Rho and Rac [190]. This causes the cytoskeleton to be rearranged, resulting in a lateral asymmetry of the cells. Wnt may also stimulate the release of intracellular calcium by the heterotrimeric G protein. In addition, there is an alternative mechanism that Wnt can activate Ror and Ryk tyrosine kinase receptors, which control the activity of JNK and Src kinases, respectively [191].

1.1.3.3 Crosstalk between Wnt and NF-κB signaling pathways

Both the Wnt signaling pathway and the NF-κB signaling pathway are conserved signaling pathways that regulate biological processes throughout the development and adulthood of mammals [192]. Abnormalities in either of these two signaling pathways result in variety of pathologies, such as cancer, inflammatory and immune diseases, and metabolic diseases [193-195].

Both Wnt signaling pathway and NF-κB signaling pathway regulate cell proliferation, cell survival and cell differentiation through different target genes [196, 197]. In addition to these common functions, the Wnt signaling pathway is critical for development and tissue regeneration, and the NF-κB signaling pathway is also critical in regulating inflammation [198, 199]. Recent studies have proved that crosstalk between these two signaling pathways influences their biological functions [200]. These two signaling pathways intersect to form biologically more complex and stable regulatory networks. Proteins in the Wnt signaling pathway regulate cellular function by interacting with the NF-κB signaling pathway. NF-κB also affects the activity of the Wnt signaling pathway.

1.1.3.3.1 The positive effects of Wnt signaling pathway on NF-κB signaling pathway

Present studies have elucidated that the Wnt signaling pathway positively regulates the NF-κB signaling pathway. β-TrCP, encoded by the BTRC gene, is an E3 ubiquitin ligase receptor that mediates ubiquitination and proteasomal degradation of β-catenin and IκB-α [201]. Activation of Wnt signaling pathway by overexpression of β-catenin or Wnt enhances the expression of β-TrCP, and subsequently facilitating the degradation of IκB-α and increasing the nucleus transportation of NF-κB without affecting the activity of IKK [202]. In vascular smooth muscle cells, Wnt1 activates the expression of β-TrCP and the activity of NF-κB through β-catenin/TCF4 [203]. In addition, β-catenin/TCF can also up-regulate and stabilize the mRNA of β-TrCP and accumulate its protein level through promoting the transcription of its target gene CRDBP [204]. In colon cancer, the induction of BTRC and CRDBP expression is associated with the activation of β-catenin and NF-κB [205].

Stimulation of TLR3 has been shown to drive the transformation of breast cancer cells to cancer stem cells by activating both the Wnt and NF-κB signaling pathways, suggesting a synergistic effect between the two pathways [206]. Evidence showed that oncogenic mutated scaffold protein CARMA1 caused the stability of β-catenin and associated B cell receptor (BCR) signaling with NF-κB signaling, thereby coupling the Wnt and NF-κB signaling pathways in diffuse large B cell lymphoma [207]. High level of β-catenin induces the expressions of cononical Wnt target genes, and enhances the expression of immunosuppressor IL10 [208]. Together with NF-κB, β-catenin induces a cancer cell favorable microenvironment.

Besides, the β-catenin:TCF/LEF complex has been shown to bind to the promoter of NF-κB target gene, such as C-reactive protein (CRP) and MMP13 [209]. In HEK293T cells and HepG2 cells treated with TNF-α, both β-catenin and p50 are required for CRP expression [210]. Depletion of β-catenin in human bronchial epithelial cells results in the inactivation of LPS induced NF-κB signaling pathway and the expression of pro-inflammatory cytokines [211]. In contrast, over-expression of TCF4 in human chondrocytes enhances NF-κB activity and promotes the expression of various MMPs and pro-inflammatory cytokines [212]. These results indicate that there is a synergistic effect between β-catenin and NF-κB.

1.1.3.3.2 The negative effects of Wnt signaling pathway on NF-κB signaling pathway

On the other hand, some studies have found that β-catenin can form a complex with RelA and p50 to inhibit the binding of NF-κB at promoter region of target genes, causing the reduced expression of target gene [213]. The protein pull down assay shows that β-catenin does not interact with NF-κB. The interaction is detected by adding cell lysate into the reaction, indicating an indirect interaction. Active β-catenin inhibits the expression of NF-κB target gene FAS, which may further promote tumorigenesis by inhibiting FAS-mediated cell apoptosis [214]. Some other studies also show a negative regulation mediated β-catenin on the expressions of NF-κB signaling pathway target genes [215, 216].

This inhibitory mechanism is also found in many non-tumor cell types, such as chondrocytes, epithelial cells, osteoblasts, and hepatocytes [208, 217-219]. Stimulation by Wnt3a or Wnt7B or over-expression of β-catenin inhibits the expressions of IL-6 and MMPs mediated by IL-1β. In intestinal epithelial cells, over-expression of constitutively active mutant form of β-catenin or activation of β-catenin by inhibition of GSK3β results in decreased NF-κB activity and reduced expression of IL-6 and IL-8, two target genes of NF-κB signaling pathway [220]. The negative regulatory effect of Wnt signaling on NF-κB signaling pathway is also observed in the liver cells derived from β-catenin conditional knockout mice [221]. Absence of β-catenin increases RelA levels. In dendritic cells, the expression of TLR4 was enhanced by the knockdown of β-catenin [222].

1.1.3.3.3 The effect of GSK3β on NF-κB signaling pathway

In addition to regulating the NF-κB signaling pathway by regulating the protein levels of β-catenin, GSK3β also regulates NF-κB signaling pathway through β-catenin independent manner. Overexpression of GSK3β has been shown to inhibit TNF-α- induced NF-κB activation. GSK3β stabilizes IκB and inhibits NF-κB signaling. Besides, GSK3β directly phosphorylates RelA and negatively controls the basal activity of NF-κB [223]. Inhibition of GSK3β enhances the expression of IL-10 mediated by CREB in monocytes treated with TLR agonists [224]. This is believed by affecting the interaction of RelA, CREB and CBP to inhibit the production of pro-inflammatory cytokines mediated by NF-κB. Inhibition of GSK3β enhances the binding of CBP to CREB.

1.1.3.4 Wnt signaling pathway and cell senescence

The Wnt signaling pathway plays an important role in the cell senescence. In senescent cells, the Wnt signaling pathway is often inhibited, and reactivation of the Wnt signaling pathway can significantly reverse the senescence related phenotypes [225]. Knockout sFRP3, an endogenous inhibitory protein of the Wnt signaling pathway successfully restore the body and brain volume in BubR1H/H accelerated aging mice model [226]. In addition, knockout of sFRP3 also restored the proliferation of nerve progenitor cells in the dentate gyrus of the hippocampus in BubR1H/H mice. Wnt signaling pathway is also proved to be important in maintaining the number of thymic epithelial cells. Inactivation of the Wnt signaling pathway leads to cell senescence in thymic epithelial cells [227].

Studies also have shown that the expression of Wnt2 and downstream target genes of canonical Wnt signaling pathway are suppressed in senescent cells [228]. Inactivation of Wnt signaling pathway occurs in the early stage of cell senescence. In addition, β-catenin synergized with N-Ras can immortalize melanocytes by inhibiting p16^{INK4a} [229]. These studies indicate that Wnt signaling pathway plays an important role in cell senescence.

1.1.4 Wild-type p53-induced phosphatase 1 (Wip1) in cell senescence and aging

Wild-type p53-induced phosphatase 1 (Wip1) is a member of the PP2C family of Ser/Thr protein phosphatases encoded by PPM1D gene [230]. The expression of this gene is induced in a p53-dependent manner in response to various environmental stresses [231]. While being induced by p53, Wip1 negatively regulates the activity of p53 by de-phosphorylation mechanism, and in turn suppresses p53-mediated apoptosis and cell senescence [232, 233]. Wip1 is characterized to have distinct oncogenic properties mediated by inhibitory functions on several tumor suppressor pathways, including ATM, CHK2, p38/MAPK and p53 [234, 235].

Studies have proved that Wip1 is also a target gene of NF-κB signaling pathway [236]. There is an evolutionarily conserved κB site in the promoter region of PPM1D gene. NF-κB binds to this specific DNA sequence to induce Wip1 expression. Treatment with IMD-0354, the inhibitor of NF-κB results in a reduction of Wip1 mRNA level and total protein level. Activation of NF-κB induces Wip1 expression.

Recent evidence indicates that the expression of Wip1 is impaired during aging in some tissues [40, 237]. Wip1 knockout mice showed a reduction in longevity [238]. An mRNA expression analysis reveals that Wip1 is dramatically down-regulated with aging in mice. Primary cells derived from Wip1 deficient mice show reduced proliferation capability. Higher levels of $p16^{INK4a}$ and ARF are found in Wip1 deficient mice compared to wild type littermates [239]. Wip1 knockout mice exhibit hyper-activation of p53 induced cell senescence, resulting in depletion of a pool of adult stem cells in the brain [233]. Deletion of p53 but not CDKN2A rescues the phenotype of NSC in Wip1 knockout mice. Such an accumulated stress response by loss of Wip1 function and subsequent relief of stress signaling inhibition may also be responsible for the premature aging phenotype of Wip1 deficient mice.

Not surprisingly, human mesenchymal stem cells (hMSCs) undergo premature senescence in culture. Stable expression of Wip1 in hMSCs lowers the stress response and overcomes premature senescence, which maintains the multi-differentiation potential [240]. This suggests that modulation of the stress response by Wip1 expression in hMSCs is important for their stemness.

1.2 Loss of Cdk5rap2 compromises centromeric chromatin integrity through downregulation of CENP-A

1.2.1 Centromere and Centromere protein A (CENP-A)

1.2.1.1 Centromere

The centromere is the specialized DNA sequence of a chromosome that links a pair of sister chromatids [241]. Centromeres were first thought to be genetic loci that direct the behavior of chromosomes.

The centromere is a large chromatin containing protein complex that forms the assembly site for the mitotic kinetochore, a giant protein complex that binds spindle microtubules to segregate the chromatids during mitosis (Figure 5) [242]. In addition to microtubule attachment, kinetochores also control mitotic checkpoint activation, preventing abnormal chromosome segregation in the presence of unattached kinetochores which equate to unattached chromosomes.

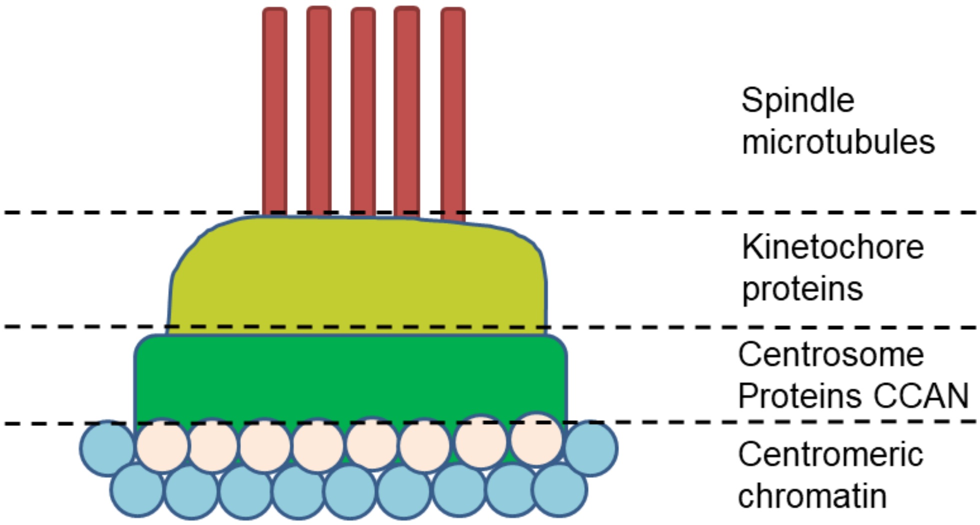

Figure 5. Schematic diagram of the centromere/kinetochore in mitosis.

Numerous proteins are persistently located at centromere with proper organization throughout the cell cycle. These proteins mostly are centromere specific and are collectively called the constitutive centromere-associated network [243]. In contrast, kinetochore proteins are only recruited to the centromere position before and during mitosis to enable chromosome alignment segregation. Although widely diverse structures of centromeres are identified in different eukaryotes, its function for kinetochore assembly and provide a site to bind microtubules so that chromosomes can be equally segregated in mitosis is highly conserved in evolution.

Many researches have shown that without the centromere, kinetochore will be no longer formed and the chromosomes will not be segregated precisely [244]. Thus, the centromere/kinetochore can be regarded as a single protein complex, which has crucial importance for mitotic chromosome segregation and thus prevent the genomic instability [242].

1.2.1.2 Centromere protein A (CENP-A)

Eukaryotic DNA sequence is packaged by histone proteins to constitute nucleosomes. These proteins are histone protein H2A, H2B, H3, and H4, forming an octamer with DNA [245]. But in centromeric region, the components of nucleosomes are quite unique from the rest of the chromosome.

Centromeric nucleosomes contain a histone H3 variant called centromere protein A (CENP-A), which is only specific present at centromere in place of histone H3 [246]. The human CENP-A gene encodes a 140-residue protein while histone H3 is 136 amino acids. The amino acids sequence of CENP-A is about 48% identical to histone H3. Several key differences between CENP-A and histone H3 confer the unique functions of CENP-A at centromere. The most divergent domain at N-terminal 40 amino acids of CENP-A are usually post-translational modified which is known to effect the function of CENP-A at nucleosome [247]. Two residue insertion in the histone fold domain of CENP-A effects CENP-A nucleosome stability [248]. Importantly, the CENP-A targeting domain (CATD) is essential for the function and structure of CENP-A, including binding of the CENP-A chaperone Holliday junction recognition protein (HJURP) and the centromere protein CENP-N [249]. The extended hydrophobic C-terminal tail of six amino acids in CENP-A is essential for the interaction with centromere protein CENP-C [250, 251].

Post-transcriptional modifications, such as mono-, bi- and tri-methylation and acetylation are very common on histone H3. As with the modifications on histone H3 at non-centromere region, multiple post-transcriptional modifications on CENP-A has been identified and is closely related to its function. H3K4me2 is a centromere-specific modification that has been shown to promote CENP-A assembly into chromatin [252]. In Drosophila, CENP-A stability is maintained by ubiquitination through CUL3/RDX ubiquitin ligase [253]. In addition, targeting of transcriptional activators to human artificial chromosome (HAC) centromeres affects the kinetochore formation and CENPA assembly [254]. But the mechanism of this process is unknown.

In human cells, functional centromeres consistently have CENP-A. CENP-A assembly at centromere starts after anaphase, and finishes before the end of G1 phase [255]. This CENP-A assembly process is regulated by many cell-cycle kinases. CENP-A assembly occurs prematurely upon CDK1 inhibition [256]. Blocking of APC activity causes the failure of CENP-A assembly at centromere [257]. Holliday junction recognition protein (HJURP) is the chaperone of CENP-A. HJURP directly binds to CENP-A through recognition of the CATD domain of CENP-A [258, 259]. Tethering LacI-HJURP fusion protein to Lac operators at ectopic chromosomal loci consequently assemble CENP-A and form largely functional kinetochores, suggesting an importance of HJURP in centromere CENP-A assembly [260].

CENP-A is the core inner protein for other centromere protein assembly. CENP-A nucleosomes direct the recruitment centromere proteins to form functional centromere through both direct and indirect binding with higher order protein complexes (Figure 6). CENP-N binds CENP-A nucleosomes by CATD domain of CENP-A, while CENP-C binds to the C-terminal tail of CENP-A [250, 261]. The conserved domains in the CENP-C protein provide specificity for CENP-C recruitment to centromeres. Replacement of CENP-A with H3/CENP-A chimeras lacking the C-terminal region of CENP-A reduces the CEN-C recruitment at centromere in human cells [262]. The recruitment of CENP-B at centromere requires the CENP-A N-terminal tail. Incomplete decrease in CENP-A protein levels does not affect the localization of CENP-B at centromere [251]. But completely loss of CENP-A leads to approximately 50% mis-localizaiton of CENP-B at centromere.

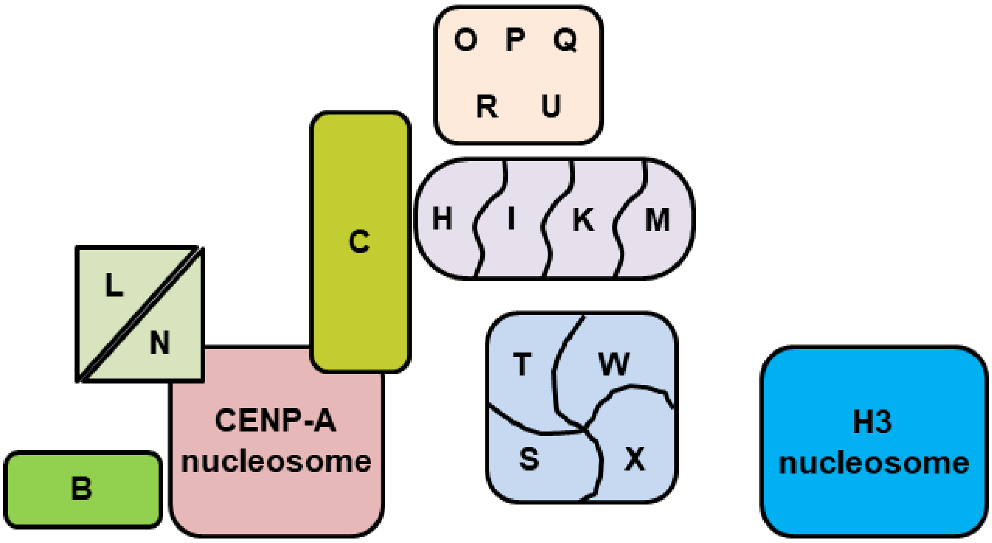

Figure 6. Schematic diagram of centromere architecture.

The appropriate CENP-A expression has to be precisely regulated. Over-expression of CENP-A causes the ectopic localization of CENP-A at noncentromeric regions, which in turns leads to ectopic kinetochore formation and numerous mitotic errors [263]. However, loss of CENP-A impairs the recruitments of outer centromere proteins. These impairments will further disrupt the centromere architecture and kinetochore. Obviously, loss of CENP-A causes the failure of centromere and kinetochore formation, leading to unable attachment of chromosomes to the spindle microtubules and deficient chromosome alignment and segregation in mitosis [264].

1.3 Hypothesis & Objectives

Cdk5rap2 is one of primary microcephaly genes regulates centrosome function and spindle microtubule organization in mitosis. However, loss-of-function mutations of Cdk5rap2 are also found in Seckel syndrome and primordial dwarfism patients with short stature suggesting that Cdk5rap2 is also involved in non-nervous system development. MEF cells derived from mutant Cdk5rap2 mice arrest cell proliferation in culture which is a major characteristic of cell senescence. Thus, it is important to investigate whether Cdk5rap2 is involved in cell senescence and the molecular mechanisms by which Cdk5rap2 regulates cell senescence.

Cdk5rap2 is a transcriptional factor of MAD2 and BubR1. It is possible that Cdk5rap2 may regulate other genes expression. Since we identified CENP-A might be a target gene of Cdk5rap2 in Hela cells, and CENP-A is critical for chromosome alignment and segregation in mitosis, we hypothesized that loss of Cdk5rap2 causes genomic instability could partly be due to down-regulation of CENP-A.

Primary objectives of the current study are:

(1) Investigate the involvement of Cdk5rap2 in cell senescence and the molecular mechanisms by which Cdk5rap2 regulates cell senescence.

(2) Investigate the role of Cdk5rap2 in CENP-A expression and its effect on genomic instability.

Chapter Two: Loss of Cdk5rap2 triggers cellular senescence via β-catenin-mediated downregulation of WIP1

2.1 Abstract

Cdk5rap2 is expressed ubiquitously in human tissues and loss-of-function mutations in Cdk5rap2 have been linked to primary microcephaly and primordial dwarfism, a developmental disorder characterized by small body size and other growth abnormalities. However, the mechanisms by which Cdk5rap2 loss-of-function causes developmental disorders remain obscure. In this study, we show that loss of Cdk5rap2 triggers premature cell senescence via GSK3β/β-catenin-mediated downregulation of WIP1. Such senescence is associated with proliferation defect as manifested by increased population of cells at G0/G1 and reduced population at S phase in Cdk5rap2-depleted BJ-5ta human fibroblasts and small body size in Cdk5rap2an/an mice. In BJ-5ta cells, Cdk5rap2 loss induces p53 Ser15 phosphorylation, which does not correlate with activation of p53 kinases but rather correlates with decreased level of the p53 phosphatase, WIP1. Ectopic WIP1 expression reverses the senescent phenotype in Cdk5rap2-depleted cells, indicating that senescence in these cells is linked to WIP1 downregulation. Cdk5rap2 interacts with GSK3β, causing increased inhibitory GSK3β Ser9 phosphorylation and inhibiting the activity of GSK3β, which phosphorylates β-catenin, tagging β-catenin for degradation. Thus, Cdk5rap2 loss decreases GSK3β Ser9 phosphorylation and increases GSK3β activity, reducing nuclear β-catenin, which affects the expression of the NF-κB target gene, WIP1. Consequently, depletion of Cdk5rap2 or β-catenin causes WIP1 downregulation. Inhibition of GSK3β activity restores β-catenin and WIP1 levels in Cdk5rap2-depleted cells, reducing p53 Ser15 phosphorylation and preventing senescence in these cells. Conversely, inhibition of WIP1 activity increases p53 Ser15 phosphorylation and senescence in Cdk5rap2-depleted cells lacking GSK3β

activity. Premature cell senescence through GSK3β/β-catenin downregulation of WIP1 may contribute to developmental disorders associated with Cdk5rap2 loss-of-function.

2.2 Introduction

Cyclin-dependent kinase 5 (Cdk5) regulatory subunit associated protein 2 (Cdk5rap2) was originally identified based on its ability to interact with the Cdk5 regulatory subunit, p35 [159]. Cdk5rap2 localizes to the centrosome in a dynein-dependent manner [265] and regulates centriole engagement and centrosome cohesion during the cell cycle [266-268]. Cdk5rap2 moved into the spotlight as loss-of-function mutations in Cdk5rap2 cause primary microcephaly (MCPH), an autosomal recessive neurodevelopmental disorder characterized by small brain and cognitive deficit [162, 269]. In fact, Cdk5rap2 is most abundant at the luminal surface of the brain's ventricular zone, particularly in cells lining the ventricular wall where neural stem and progenitor cells reside. However, since Cdk5rap2 is also expressed in other tissues, it is not surprising that loss-of-function mutations in Cdk5rap2 are further associated with other developmental disorders such as cochlear and retinal developmental defects [270], primordial dwarfism [181, 271], as well as Seckel syndrome, a heterogeneous, autosomal recessive disorder characterized by prenatal proportionate short stature, severe microcephaly, intellectual disability, and characteristic 'bird-headed' facial features [180]. However, the molecular mechanisms by which Cdk5rap2 loss-of-function mutations cause these developmental disorders remain elusive.

Cellular senescence is a state of stable cell cycle arrest in which cells remain viable and metabolically active [5]. In addition to cell cycle arrest, cell senescence is characterized by increased senescence-associated β-galactosidase (SA-β-gal) activity [272], formation of senescence-associated heterochromatin foci (SAHF) [273] and morphological transformation [20]. Senescence is triggered by a number of cellular stresses [108, 274-276]. For example, activated oncogenes such as H-RAS^{G12V} and B-RAF^{V600E} induce senescence by evoking sustained anti-proliferative response [47], a mechanism that acts as an initial barrier in preventing normal cell transformation into malignant cells. H-RAS^{G12V}-induced senescence is associated with accumulation of DNA damage foci and activation of the p53 kinases, ataxia telangiectasia mutated (ATM), checkpoint kinase 1 (Chk1) and/or checkpoint kinase 2 (Chk2), suggesting that aberrant oncogene activation induces a DNA damage response (DDR) [47, 108]. Cell senescence can also be induced by telomere attrition and oxidative stress among others. The molecular mechanisms of senescence have been studied extensively using a variety of cell types. Phosphorylation of the tumor suppressor protein, p53, at Ser15 by p53 kinases such as ATM, Chk1 and/or Chk2 is one of the key events in p53-associated cell senescence [277, 278]. Apparently, p53 Ser15 phosphorylation stabilizes p53 by inhibiting its interaction with Mdm2, an E3 ubiquitin ligase that catalyzes polyubiquitination and subsequently induces proteasome degradation of p53 [236]. However, p53 Ser15 phosphorylation is also required for p53 activation [279, 280], which blocks cell cycle progression by inducing p21^{CIP1} expression[281]. Aside from phosphorylation by kinases, p53 Ser15 phosphorylation is also regulated by p53 phosphatases such as wild-type p53-induced phosphatase 1 (WIP1). In fact, WIP1 has been associated with p53-mediated cell senescence [282, 283]. For example, hematopoietic stem cells (HSC) from WIP1$^{-/-}$ mice exhibit senescent phenotypes, impairing repopulating activity [283]. Mouse embryonic fibroblasts (MEFs) [283] and mesenchymal stem cells [284] from WIP1$^{-/-}$ mice also undergo premature senescence. In primary chondrocytes, reduced WIP1 is associated with senescent phenotype, which is reversed by ectopic WIP1 expression [285]. *WIP1,* which contains an NF-κB binding site in its promoter region, is a downstream gene target of NF-κB [236]. Interestingly, β-catenin associates with NF-κB and induces the expression of NF-κB target genes[200].

Our investigations examine the possibility that WIP1 expression is regulated by β-catenin. Since β-catenin is phosphorylated by GSK3β that earmarks β-catenin for ubiquitination-mediated degradation by the proteasome pathway [286], we further examined whether GSK3β controls our presumed β-catenin-mediated WIP1 expression. To explore these possibilities, we used two model systems: (i) the Cdk5rap2$^{an/an}$ mouse model [167], which carries exon 4 inversion in *Cdk5rap2.* Cdk5rap2$^{an/an}$ exhibits primary microcephaly that is comparable to that of the human disease, displaying proliferation and survival defects in neuronal progenitor cells [167]. Cdk5rap2$^{an/an}$ homozygotes are spontaneously aborted, appearing to exhibit late embryonic lethality, and (ii) BJ-5ta normal human diploid foreskin fibroblast cells. BJ-5ta cells, which were immortalized through forced expression of the hTERT component of telomerase, maintains many characteristics of normal primary cells such as karyotype, growth rate, morphology, tissue-specific markers and contact inhibition. Altogether, we demonstrate that loss of Cdk5rap2 triggers premature cell senescence via elevation of GSK3β activity that causes β-catenin-mediated downregulation of WIP1 and subsequent upregulation of p53 Ser15 phosphorylation. Proliferation defect and senescent phenotypes in Cdk5rap2-depleted BJ-5ta cells are recapitulated in Cdk5rap2$^{an/an}$ as reduced embryonic body weights and reduced MEF growth rate, and increased SA-β-gal staining and reduced PCNA but increased p21^{CIP1} levels in MEFs, respectively.

2.3 Materials and methods

2.3.1 Materials

hTERT-immortalized BJ-5ta human foreskin fibroblast cells and adenovirus carrying H-Ras^{G12V} and GFP alone were obtained from Drs. Tara Beattie and Karl Riabowol, respectively, at the University of Calgary. HEK293 cells were from ATCC (Manassas, VA, USA). The Cdk5rap2 antibody (A300-554A) was from Bethyl Laboratories (Montgomery, TX, USA). p21^{CIP1} (sc-271610), p16^{INK4a} (sc-468), p53 (sc-393031), Ras (sc-35), histone H3 (sc-517576) and actin (sc-8432) antibodies, and protein A/G PLUS-agarose (sc-2003) were from Santa Cruz Biotech (Manassas, VA, USA). phosphoSer15-p53 (#9284), GSK3β (#12456), phosphoSer9-GSK3β (#5558), ATM (#92356), phosphoSer1981-ATM (#13050), Chk1 (#2360), phosphoSer345-Chk1 (#2348), Chk2 (#6334), phosphoThr68-Chk2 (#2197), β-catenin (#8480), GST (#2624) and Ki-67 (#9129) antibodies were from Cell Signaling (Danvers, MA, USA). WIP1 antibody (ab236515) was from Abcam (Cambridge, MA, USA). The HRP-conjugated anti-rabbit (#7074) and anti-mouse (#7076) secondary antibodies were from Cell Signaling (Danvers, MA, USA). Primers and siRNAs were synthesized at the University of Calgary Core DNA services or GenePharma, Shanghai, China. Goat anti-mouse or anti-rabbit secondary antibodies conjugated with Alexa-488 or -594 were from Invitrogen (Carlsbad, CA, USA). Myc-tagged Cdk5rap2 and Flag-tagged GSK3β expression vectors, and pReceiver-M02 carrying WIP1 were from GeneCopoeia (Rockville, USA). GSK3β protein (14-306) was from Upstate Biotech. (Lake Placid, NY, USA).

2.3.2 Cells and cell culture

BJ-5ta immortalized human diploid foreskin fibroblast cells (ATCC-CRL-4001) and immortalized human embryonic kidney (HEK) 293 cells (ATCC-CRL-1573) were purchased from American Type Cell Collection (ATCC). BJ-5ta cells were grown in Eagle's Minimum Essential Medium (EMEM, Invitrogen, Carlsbad, CA, USA) supplemented with 10% fetal bovine serum (FBS, Gibco, Grand Island, NY, USA), 50 U/mL penicillin, and 50 μg/mL streptomycin (Invitrogen). HEK293 cells were grown in high glucose Dulbecco's MEM supplemented with 10% FBS. All the cells were maintained in a humidified atmosphere with 5% CO_2 and 95% air at 37 ℃ and media was changed every 2-3 days or as required. Plastic tissue culture plates were supplied by Corning Canada.

2.3.3 Freezing and thawing of cells

Cultured cells were harvested by incubating with trypsin-EDTA (Gibco) for detachment and centrifuged at 800 rpm for 5 minutes. Then cells were re-suspended in a medium containing 10% FBS and 10% sterile dimethylsulfoxide (DMSO, Sigma, St. Louis, MO, USA) to to yield approximately $1\text{-}2\times10^6$ cells/ml. One milliliter aliquots of cell suspension were transferred to cryovials (thermo Fisher, Waltham, MA, USA) and vials were placed at -80 ℃ overnight. Frozen cells were then kept in liquid nitrogen for long-term storage.

To thaw the cells, vials of frozen cells were removed from liquid nitrogen and placed in a 37 ℃ water bath until completely thawed. The thawed cell suspension was quickly transferred to 15ml centrifugal tube and mix with 4ml fresh culture media. The cells were collected by centrifugation at 800 rpm for 5 minutes. The supernatant were discarded. The cells were re-suspended with fresh culture media and transferred to plates containing fresh culture media supplemented with 10% FBS and incubated at 37 ℃ incubator with 5% CO_2. When the cells settle down and attach to the plate, the medium was replaced with fresh complete growth medium and were returned to the incubator for growing.

2.3.4 Splitting of cells

Cells reaching confluence were detached from the plate using trypsin-EDTA solution at 37 ℃ for 2-5 minutes after washing them three times with sterile PBS. The cells were harvested by triturating with an appropriate volume of culture media containing 10% FBS and seeded onto new tissue culture dishes. BJ-5ta cells were split at 1:2-1:4 ratios and HEK293 cells were split at 1:4-1:6, depending on the growth rate of the cells and the purpose of the experiments.

2.3.5 Animals

The Cdk5rap2$^{+/an}$ breeding pairs were purchased from JAX laboratory (Bar Harbor, ME, USA) and fed with commercial mice chow, provided water ad libitum and kept on a 12:12 hr light-dark cycle. Cdk5rap2$^{+/+}$, Cdk5rap2$^{+/an}$ and Cdk5rap2$^{an/an}$ embryos were isolated from pregnant Cdk5rap2$^{+/an}$ mice. All animal studies conformed to regulatory standards and were approved by the University of Calgary Health Sciences Animal Care Committee.

2.3.6 Genotyping

Genomic DNAs were extracted from mice using the Extracta DNA prep kit (Quantabio, Edmonton, AB. Canada). Tissue samples were added to 50-100 µl of extraction buffer, incubated at 95 ℃ for 30 min, and stabilized with an equal volume of stabilization buffer. DNA sample (1 µl) was added to 10 µl of Quantabio's AccuStart II PCR SuperMix containing 100 nM of the appropriate DNA primers. The forward primers used were:

Table 1. Primers for genotyping.

Primer	Sequence
wt Cdk5rap2-F	GAAACCAGGGTGACA GGTACA
an Cdk5rap2-F	AGATGTCATGTCTAAAGCAATCACT
universal primer-R	CCTTTGTCTTTCTGCCCTGA;

Based on the expected size of each fragment, the wt *Cdk5rap2* allele corresponds to a 581 bp band whereas the mutant an *Cdk5rap2* allele corresponds to a 500 bp band. The reaction mixtures were input into a Bio-Rad thermocycler using PCR settings recommended by the Jackson Laboratory.

2.3.7 Isolation of primary MEFs

Primary MEFs were isolated from E12.5 Cdk5rap2$^{+/+}$, Cdk5rap2$^{+/an}$ and Cdk5rap2$^{an/an}$ embryos as described previously [287]. Briefly, embryos were washed with 1x PBS, decapitated and eviscerated then washed again with PBS. Embryos were minced using sterile forceps and placed in 3–5 ml of 0.05% trypsin-EDTA, pipetted up and down to get cells into suspension and incubated at 37°C for 5 min. Cell suspensions were transferred to tubes containing MEF medium (DMEM-high glucose supplemented with 10% FBS, 50 U/ml penicillin and 50 mg/ml streptomycin (Invitrogen, Carlsbad), and 2 mM GlutaMAX) then centrifuged at 1,000 rpm for 5 min. Cell pellets were resuspended in fresh media and plated in 10 cm cell culture dishes. Primary MEFs were cultured in DMEM supplemented with 10% FBS and 50 U/ml penicillin and 50 mg/ml streptomycin (Invitrogen, Carlsbad) under hypoxic condition (5% O_2 and 5% CO_2 incubator). All experiments were performed in passage P2-P7 MEFs.

2.3.8 Plasmid/siRNA transfection and adenovirus infection

Cells cultured ~18 hours and at about 60% confluency were transfected with indicated siRNA using Lipofectamine 2000 (Invitrogen) in serum-free medium, which was replaced with complete medium 5 hours post-transfection.

Table 2. siRNA sequences for gene depletion

Control siRNA	CGUACGCGGAAUACUUCGAUU
Cdk5rap2 siRNA#1	GGACGUGUUGCUUCAGAAAUU
Cdk5rap2 siRNA#2	GAGUCAGCCUUCUGCUAAAUU
Wip1 siRNA	CCAAUGAAGAUGAGUUAUAUU
GSK3β siRNA	AGGAGACCACGACCUGUUAAUU
β-catenin siRNA	CTCGGGATGTTCACAACCGAA

Cells were harvested at different time points as indicated. Adenovirus infection was carried out at a MOI of 50-100. Media was then replaced with EMEM containing 10% FBS 24 hours post infection and cells were incubated until the indicated time.

2.3.9 RNA extraction and real-time qRT-PCR

Total RNA was extracted using TRIzol reagent (Invitrogen, Carlsbad, CA, USA) according to the manufacturer's protocol, and transcribed into cDNA using high-capacity cDNA reverse transcription kit (Thermo Fisher, Waltham, MA). Real-time qRT-PCR was performed using power SYBR® green PCR master mix (Thermo Fisher, Waltham, MA), and an Applied Biosystems 7500 real-time PCR machine using a standard protocol. The PCR conditions were 35 cycles at 94 ℃ for 20 seconds, 60 ℃ for 20 seconds and 72 ℃ for 35 seconds. The primer sets used were:

Table 3. Primers for examination of Wip1 expresion.

Primer	Sequence
WIP1-F	GGGAGTGATGGACTTTGGAA
WIP1-R	CAAGATTGTCCATGCTCACC
GAPDH-F	GGAGCGAGATCCCTCCAAAAT
GAPDH-R	GGCTGTTGTCATACTTCTCATGG

GAPDH was used for normalization.

2.3.10 Isolation of nuclear fraction

Lysates of BJ-5ta cells transfected with Cdk5rap2 siRNA or control siRNA were centrifugated at 800 rpm for 10 min. The resulting pellets were resuspended in cell lysis buffer containing 10 mM HEPES; pH 7.5, 10 mM KCl, 0.1 mM EDTA, 1 mM dithiothreitol (DTT), 0.5% Nonidet-40 (NP-40), 0.5 mM PMSF, and the protease inhibitor cocktail, then incubated on ice for 30 min with intermittent mixing, and centrifuged at 12,000 xg at 4 ℃ for 15 min. The pellets were washed three times with cell lysis buffer, and resuspended and incubated in nuclear extraction buffer containing 20 mM HEPES (pH 7.5), 400 mM NaCl, 1 mM EDTA, 1 mM DTT, 1 mM PMSF and protease inhibitor cocktail for 30 min. Nuclear fractions were harvested by centrifugation at 12,000 xg for 15 min at 4 ℃.

2.3.11 Western blot analysis

Cell lysates (50 μg) were resolved by SDS-PAGE, transferred to nitrocellulose membrane, and immunoblotted for Cdk5rap2, $p21^{CIP1}$, $p16^{INK4a}$, p53, phospho-p53, Ras, histone, GSK3β, phosphoSer9-GSK3β, ATM, phosphoSer1981-ATM, Chk1, phosphoSer345-Chk1, Chk2, phosphoThr68-Chk2, β-catenin, WIP1 and actin. Following incubation with HRP-conjugated anti-rabbit or anti-mouse secondary antibody, immunoreactive bands were detected using the

ECL reagent (GE Healthcare, Little Chalfont, Buckinghamshire, UK). Western blot images were obtained using the ChemiDoc™ Imager (Bio-Rad) set at optimal exposure. No enhancements were performed.

2.3.12 Immunofluorescence microscopy

Cells transfected with Cdk5rap2 or control siRNA on coverslips were fixed with 4% paraformaldehyde/PBS for 10 min, permeabilized using 0.1% Triton X-100/PBS for 10 min, then blocked in 2% BSA/PBS for 1 hour at room temperature. Cover slips incubated with the indicated primary antibody for 1 hour followed by 20 min incubation with secondary antibodies were washed with 1x PBS, counterstained with DAPI and mounted on glass slides using ProLong™ Diamond Antifade Mountant (P36961, Invitrogen, Carlsbad, CA, USA). Images were captured using a Zeiss Axiovert 200 microscope. BJ-5ta cells transfected with Cdk5rap2 siRNA #2 were analyzed for Ki-67 positive cells 3 days post-transfection.

2.3.13 Senescence-associated β-galactosidase staining

Cells were fixed using 3% paraformaldehyde in PBS (pH 6.0) and stained with 1 mg/ml 5-bromo-4-chloro-indolyl-β-D-galactopyranoside (X-gal) solution containing 5 mM potassium ferrocyanide, 5 mM potassium ferricyanide, 150 mM NaCl, and 2 mM $MgCl_2$ in PBS (pH 6.0) for 16-20 hrs at 37 ℃.

2.3.14 Cell viability and cell cycle analyses

BJ-5ta cells transfected with Cdk5rap2 siRNA #2 or control siRNA were seeded into 96-well plates at 5,000 cells per well 24 hours post transfection, then analyzed for cell viability at days 0, 2 and 4 using Cell Counting Kit-8 (CCK-8, Dojindo). For analysis of cell cycle distribution, cells transfected with Cdk5rap2 siRNA #2 or control siRNA were fixed using cold 2% formaldehyde and stained with 7-AAD (5 μg/μl) then subjected to flow cytometry.

2.3.15 Immunoprecipitation

HEK293 cells tranfected with Myc-tagged Cdk5rap2 or Flag-tagged GSK3β or both for 48 hrs were lysed in ice-cold lysis buffer containing 50 mM Tris/pH 8.0, 150 mM NaCl, 1% NP-40, 10 mM EDTA, 5% glycerol, 1 mM phenylmethylsulfonylflouride (PMSF), 10 μg/ml aprotinin, and 10 μg/ml leupeptin. Lysates were then clarified by centrifuged at 13,000 rpm for 25 min at 4 ℃. For immunoprecipitation under denaturing condition, 1% SDS was added in the lysis buffer. Lysates were pre-cleared by adding normal mouse or rabbit IgG + sepharose A/G beads and incubating at 4 ℃ for 2 hrs followed by centrifugation at 14,000 rpm for 10 min. One-tenth of the lysates from each sample was retained and used to assess input or total cell lysate in western blots. Pre-cleared cell lysates were subjected to immunoprecipitation using Myc or Flag antibody conjugated to protein A/G agarose beads. After incubating the mixture overnight at 4 ℃, immunoprecipitates were washed with lysis buffer three times at 4 ℃.

2.3.16 Measurement of GSK3β activity

GSK3β activity was measured using the GSK-3β activity assay kit (Sigma, ON, Canada) following the manufacturer's protocol. Briefly, cells transfected with Cdk5rap2 or control siRNA were lysed in ice-cold lysis buffer containing 50 mM Tris/pH 8.0, 150 mM NaCl, 1 % NP-40, 10 mM EDTA, 5% glycerol, 1 mM phenylmethylsulfonylflouride (PMSF), 10 μg/ml aprotinin and 10 μg/ml leupeptin. Cell lysates (300 μg) were incubated with 2 μl of anti-GSK-3 and 30 μl EZview Red protein-G affinity gel beads at 4 ℃ for 3 hrs. The beads were recovered by centrifugation at 8,000 xg for 30 sec and washing with 500 μl of ice-cold lysis buffer. The immunoprecipitates were mixed with 20 μl of reaction mixture containing 25 Ci ^{32}P-ATP and 5 μl of GSK-3β substrate solution, incubated at 37 ℃ for 30 minutes, then spotted onto P81 phosphate cellulose membranes. Membranes were washed 4 times with 0.5% phosphoric acid and once with acetone. Counting of incorporated radioactivity was performed using a Beckman scintillation counter.

2.3.17 Expression and purification of GST-Cdk5rap2

GST-Cdk5rap2 was cloned into pFastBac vectors from which baculovirus was generated according to the Bac-to-Bac® baculovirus protein expression system (Thermo Fisher, Waltham, MA). Sf9 insect cells were infected with P2 baculovirus carrying GST-Cdk5rap2 for 24 hrs. GST-Cdk5rap2 was purified by affinity chromatography using a glutathione (GSH)-conjugated agarose column (Sigma-Aldrich, St. Louis, MO). Sf9 cell lysates expressing GST-Cdk5rap2 were incubated with GSH-agarose for 1 hour at 4˚ C and washed with 1x PBS containing 1% Triton X-100. Bound proteins were eluted with 10 mM reduced GSH in 50 mM Tris elution buffer (pH 8).

2.3.18 GST pull down assay

GST-Cdk5rap2 (1 mole) bound to glutathione-agarose beads was mixed with GSK3β (2 g) at 4 ℃ for 2 hrs. The pulled-down complex was washed 4 times with ice-cold GST lysis buffer (20 mM Tris-HCl (pH 8.0), 200 mM NaCl, 1 mM EDTA (pH 8.0), 0.5% NP-40, 2 μg/μl aprotinin, 1 μg/μl leupeptin, 0.7 μg/ml pepstatin and 25 μg/ml PMSF) by centrifugation at 2,500 rpm for 10 min and analyzed by SDS-PAGE and immunoblotting for GST and GSK3β.

2.3.19 Generation of promoter constructs of wt WIP1 (pGL3-WIP1) and WIP1 with NF-κB binding site deletion (pGL3-WIP1-ΔκB)

Using genomic DNAs isolated from HEK293 cells as a template, the WIP1 promoter region was amplified by PCR using the primer set: WIP1-F1 and WIP1-R1. The promoter region for WIP1-ΔκB was generated by PCR using two different sets of primers WIP1-F1 and WIP1-R2, and WIP1-F2 and WIP1-R1, with overlapping fragments (lowercase letters) in WIP1-R2 and WIP1-F2. Two PCR products were annealed and used as templates for subsequent 8 fusion PCR cycles [288]. PCR products were then purified using the GeneJET PCR Purification Kit (Thermo Fisher, Waltham, MA) and used as templates for PCR amplification using the WIP1-F1 and WIP1-R2 primer set. Generated WIP1 and WIP1-ΔκB promoter PCR products were cloned into pGL3-basic luciferase reporter vector (Promega, Madison, WI, USA) using XhoI and BglII restriction enzyme sites and designated as pGL3-WIP1 and pGL3-WIP1-ΔκB, respectively. Successful cloning was confirmed by DNA sequencing.

Table 4. Primers for pGL3-WIP1 and pGL3-WIP1-ΔκB vector construction.

Primer	sequence
WIP1-F1	ACATTTTCTTGAGCTGATTTTGCTT
WIP1-F2	ACCGAGACTGTGCAGCTGACGGTTAAGTGCTT
WIP-R1	TCGGAGAAGACGCTCACTCC
WIP-R2	GTTTAAAAAGCACTTAACCGTCAGCT

2.3.20 Luciferase assay

To measure luciferase activity, HEK293 cells were co-transfected with the indicated siRNA, pGL3-WIP1 or pGL3-WIP1-ΔκB and pTK-Renilla luciferase vector using lipofectamine

2000 (Invitrogen, Carlsbad, CA, USA). Cell extracts were prepared 48 hours after transfection and luciferase activity was measured using the Dual-Luciferase Reporter assay system (Promega, Madison, WI, USA). Renilla luciferase served as an internal control for normalization.

2.3.21 Statistical analysis

All data are expressed as mean ± standard deviation of at least three biological replicates. The statistical analyses were done using student's t-tests for two samples and one-way analysis of variance (ANOVA) for differences among groups using GraphPad Prism software. A probability of $p < 0.05$ was taken to be statistically significant.

2.4 Results

2.4.1 Loss of Cdk5rap2 induces cellular senescence

To investigate how Cdk5rap2 loss-of-function may cause proliferation defects associated with developmental disorders, we examined the effect of Cdk5rap2 depletion in BJ-5ta human fibroblasts by siRNA. As shown in Figure 1, knocking down Cdk5rap2 using two different siRNAs (#1 and #2; Figure 7A) triggers the formation of senescence-associated heterochromatin foci (SAHF) as demonstrated by staining with DAPI (Figure 7B) and SAHF colocalization with heterochromatin protein 1γ (HP1γ, Figure 7C), a SAHF marker [289]. Senescence induced by activated H-RAS^{G12V} oncogene [142] was used as positive control to detect SAHF and HP1γ staining.

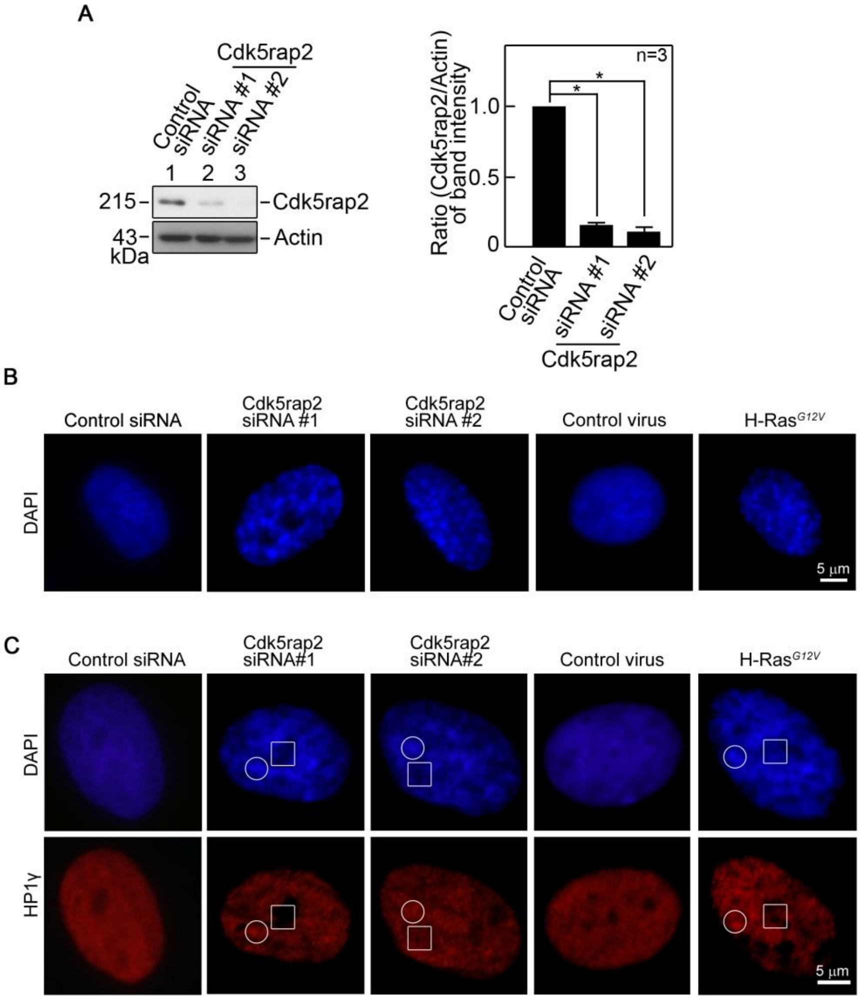

Figure 7. Cdk5rap2 loss triggers SAHF formation.

A. Depletion of Cdk5rap2 in BJ-5ta human diploid foreskin fibroblasts. Lysates of cells transfected with Cdk5rap2 siRNA for 3 days were analyzed by SDS-PAGE and immunoblotting for Cdk5rap2 (left panel). Actin blot was used as loading control. Representative blots are from one of three independent experiments (n=3) showing similar results. Ratios of levels of Cdk5rap2 vs actin (right panel) were calculated following densitometric analysis of blots using NIH Image J 1.61. Standard deviation for the 3 independent sets of experiments was calculated based on the ratios of the densitometric levels of Cdk5rap2 vs actin, with values from cells transfected with control siRNA normalized to 1.0. *$p<0.001$. B and C. Cdk5rap2 loss causes formation of SAHF. BJ-5ta cells transfected with Cdk5rap2 siRNA for 3 days were stained with DAPI (B) and HP1γ antibody (C), and subjected to microscopic examination. SAHF formation induced by infecting adenovirus carrying H-RASG12V into BJ cells was used as positive control. Representative images of control and Cdk5rap2-depleted cells, and cells infected with adenovirus carrying GFP alone or H-RASG12V are shown with DAPI and HP1γ stain-enriched and -devoid regions highlighted with open circles and squares, respectively.

To support the suggestion that Cdk5rap2 depletion causes premature cellular senescence, cells transfected with Cdk5rap2 siRNA #2 (Figure 8) were monitored for the appearance of SAHF-positive cells and the expression of the senescence-associated biomarkers[289], p21^{CIP1} and p16^{INK4a}, over 5 days post transfection. As shown in Figure 8A, the number of SAHF positive cells increases markedly in the first 3 days after transfection with Cdk5rap2 siRNA #2, reaching peak levels on days 3-5, a period when no or only a modest number of SAHF positive cells was observed in those transfected with control siRNA. The increase in number of SAHF positive cells upon Cdk5rap2 depletion coincides with increased expression of p21^{CIP1} and p16^{INK4a} (Figure 8B). Together with the noticeable staining for SA-β-gal, another marker of cellular senescence [290], 3 days post- transfection with Cdk5rap2 siRNA #2 (Figure 8C), our findings indicate that loss of Cdk5rap2 induces cellular senescence.

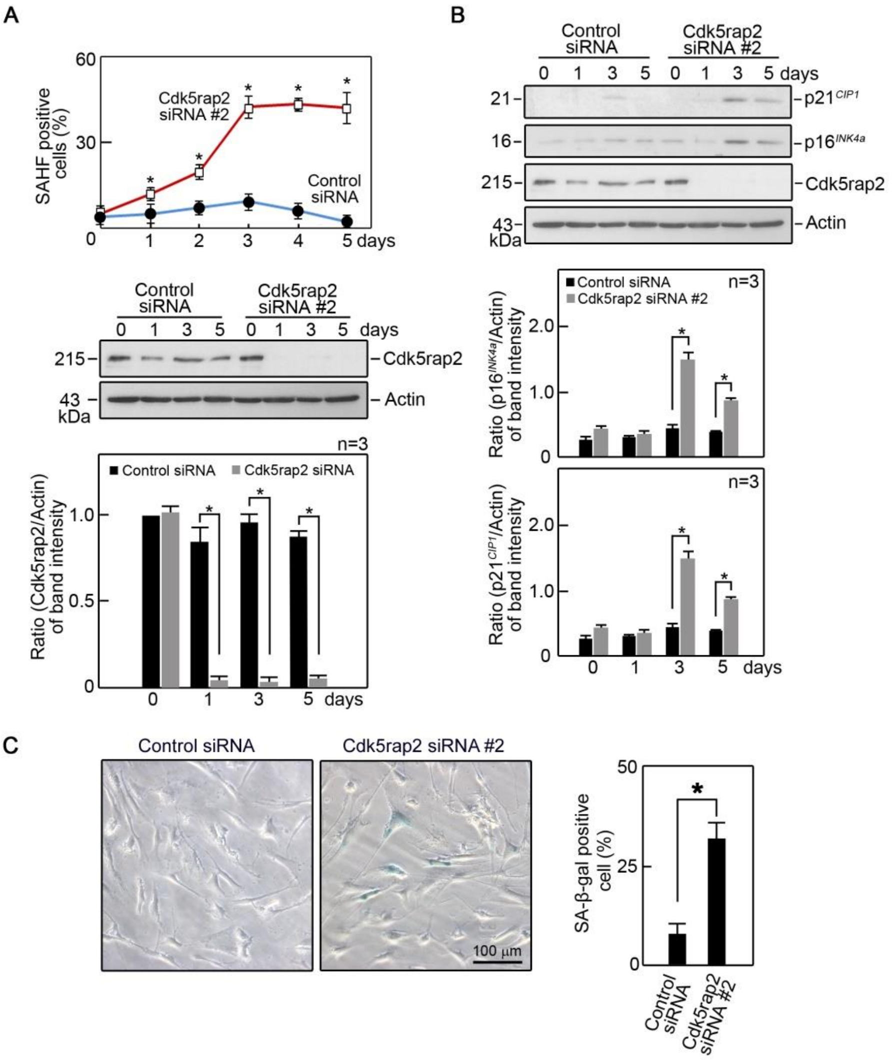

Figure 8. Increased number of SAHF positive Cdk5rap2-depleted cells coincides with expression of $p21^{CIP1}$ and $p16^{INK4a}$.

BJ-5ta cells transfected with Cdk5rap2 siRNA #2 for 5 days were analyzed (i) for SAHF positive cells (A, upper panel) and by SDS-PAGE and immunoblotting for (ii) Cdk5rap2 and actin (A, middle panel), and (iii) p21CIP1 and p16INK4a as well as Cdk5rap2 and actin (B, upper panel). The number of SAHF positive cells was assessed in ~200 cells per treatment group in each of 3 independent experiments (n=3). *$p<0.01$. Actin was used as loading control for immunoblotting. Representative blots are from one of three independent experiments (n=3) showing similar results. Ratios of levels of Cdk5rap2, p21CIP1 and p16INK4a vs actin and standard deviation for the 3 independent sets of experiments (A, lower panel and B, middle and lower panels) were calculated as described for Cdk5rap2 vs actin in Figure 1, with values from cells transfected with control siRNA at day 0 normalized to 1.0. *p<0.02. C. Cells transfected with Cdk5rap2 siRNA #2 or control siRNA were subjected to SA-β-gal staining 3 days post-transfection. Representative images (left panel) are from one of three independent experiments (n=3) showing similar staining patterns. The number of SA-β-gal positive cells was assessed in ~200 cells per treatment group in each of the 3 independent experiments (n=3). *p=0.0005.

Increased levels of SAHF as well as p21^{CIP1} and p16^{INK4a}, which are also molecular inhibitors of cell cycle Cdks, upon loss of Cdk5rap2 led us to test whether loss of Cdk5rap2 affects cell proliferation. Indeed, we found that cells transfected with Cdk5rap2 siRNA #2 proliferate at a slower rate compared to cells transfected with control siRNA (Figure 9A). Flow cytometry analysis show greater population of cells at G_0/G_1 but reduced population of cells at S in those transfected with Cdk5rap2 siRNA #2 compared to those transfected with control siRNA (Figure 9B). In addition, reduced number of Ki-67 positive cells was observed in those transfected with Cdk5rap2 siRNA #2 compared to those transfected with control siRNA (Figure 9C). Altogether, these findings indicate that Cdk5rap2 loss triggers senescence-associated proliferation arrest.

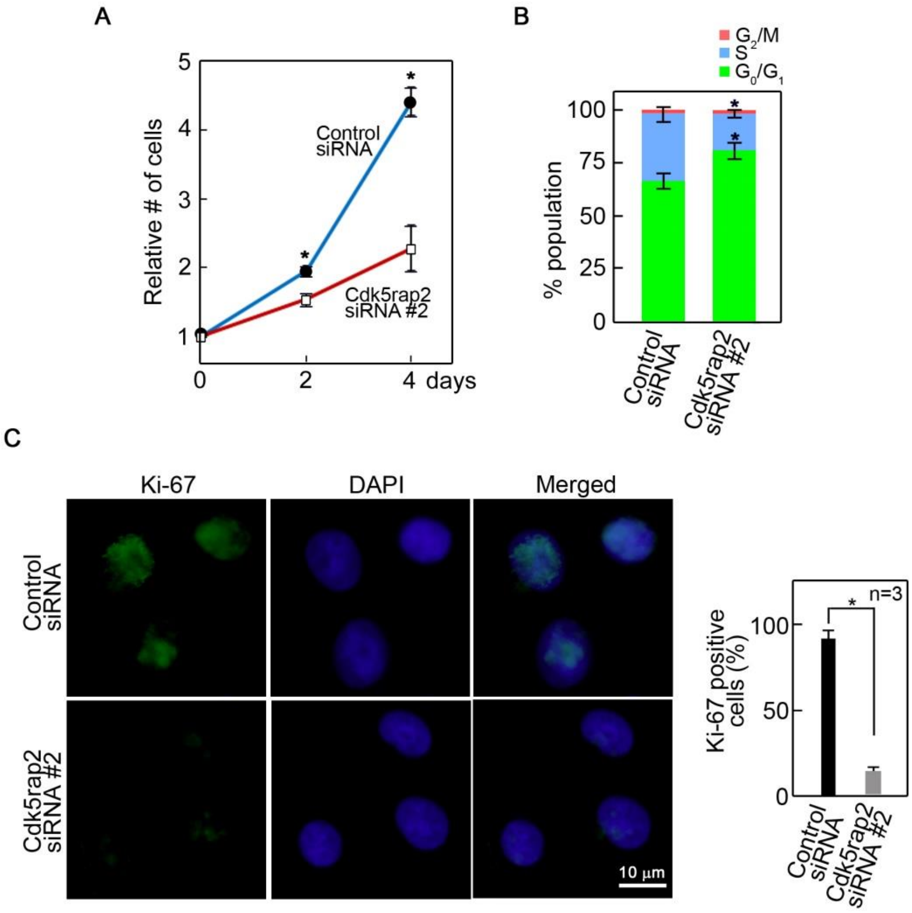

Figure 9. Cdk5rap2 loss causes decreased cell proliferation.

BJ-5ta cells transfected with Cdk5rap2 siRNA #2 were subjected to (A) cell viability assay, (B) cell cycle distribution analysis by flow cytometry, and (C) measurement of Ki-67 positive cells as described in Materials and Methods. Data represent means ± SD from three separate experiments (n=3). *p<0.01 (in A and B). The percentage (%) of Ki-67 positive cells (C, right panel) were assessed in ~200 cells per treatment group in each of the 3 independent experiments (n=3). *p=0.001.

2.4.2 Mouse embryonic fibroblast cells (MEFs) isolated from Cdk5rap2$^{an/an}$ mice, which have reduced body weights, exhibit senescence-associated phenotypes

The availability of Hertwig's anemia (an) mutant mice (Cdk5rap2$^{an/an}$) that carry exon 4 inversion in the *Cdk5rap2* gene, allowed us to test whether such Cdk5rap2$^{an/an}$ mutation affects body weight and whether the senescent-associated phenotypes observed in Cdk5rap2-depleted BJ-5ta cells are also exhibited by Cdk5rap2$^{an/an}$ MEFs. Since Cdk5rap2$^{an/an}$ mice have high incidence of death in late embryonic stages, we initially isolated embryonic day 12.5 (E12.5) Cdk5rap2$^{+/+}$, Cdk5rap2$^{+/an}$ and Cdk5rap2$^{an/an}$ embryos from pregnant Cdk5rap2$^{+/an}$ mice and body weights were compared. As shown in Figure 10A, within the same litter, the Cdk5rap2$^{an/an}$ embryo weighs less than the Cdk5rap2$^{+/+}$ and Cdk5rap2$^{+/an}$ embryos. E17.5 embryos from different litters also show lower average weights of Cdk5rap2$^{an/an}$ compared to Cdk5rap2$^{+/+}$ and Cdk5rap2$^{+/an}$ embryos (Figure 10B, left panel). Similar observations were further noted for average weights of E12.5 to E17.5 Cdk5rap2$^{+/+}$, Cdk5rap2$^{+/an}$ and Cdk5rap2$^{an/an}$ embryos (Figure 10B, right panel). Next, MEFs isolated from E12.5 Cdk5rap2$^{+/+}$, Cdk5rap2$^{+/an}$ and Cdk5rap2$^{an/an}$ embryos were examined for the appearance of SA-β-gal positive cells (Figure 10C, left panel). Analysis of SA-β-gal staining show that the number of SA-β-gal positive cells in Cdk5rap2$^{an/an}$ MEFs is remarkably greater than those in Cdk5rap2$^{+/+}$ and Cdk5rap2$^{+/an}$ MEFs (Figure 10C, right panel). In addition, Cdk5rap2$^{an/an}$ MEFs exhibit decreased proliferation (Figure 10D), which coincides with reduced PCNA but increased p21^{CIP1} levels (Figure 10E) compared to Cdk5rap2$^{+/+}$ and Cdk5rap2$^{+/an}$ MEFs. Thus, the senescence-associated phenotypes that we observed in Cdk5rap2-depleted BJ-5ta cells is recapitulated in *ex vivo* Cdk5rap2$^{an/an}$ MEFs.

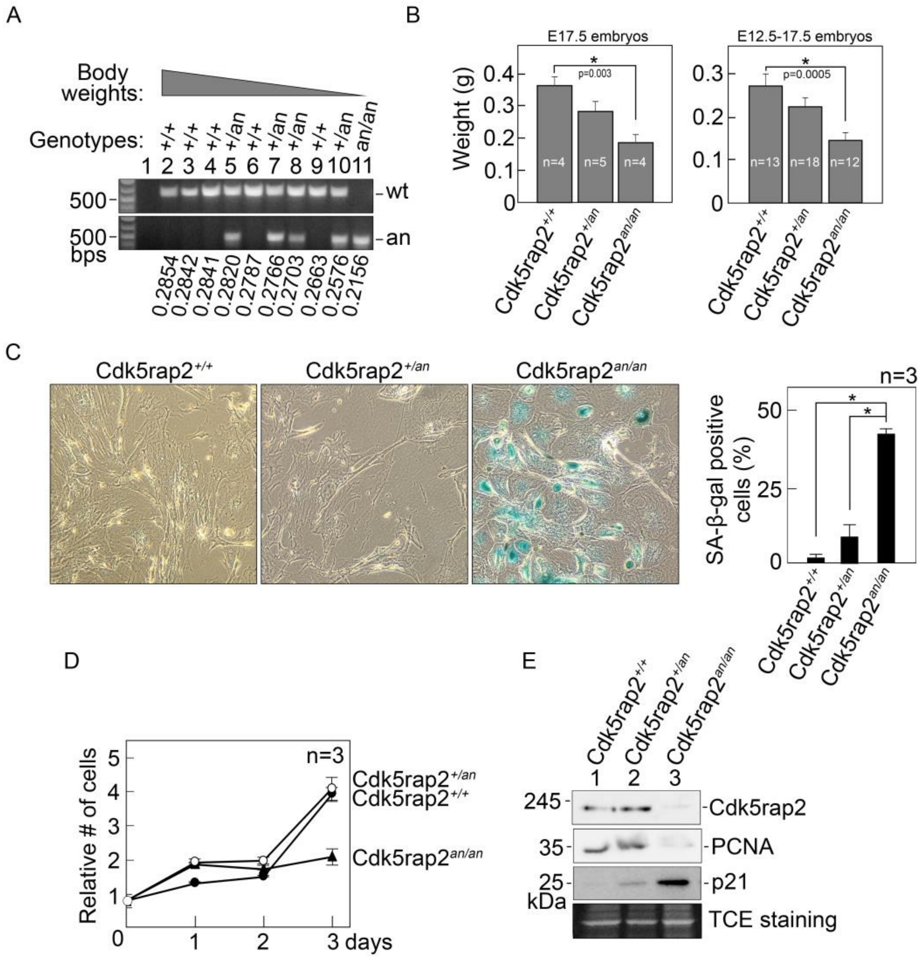

Figure 10. Cdk5rap2$^{an/an}$ embryos have reduced body weight and Cdk5rap2$^{an/an}$ MEFs show senescent phenotype.

A. Genomic DNAs from E12.5 Cdk5rap2$^{+/+}$, Cdk5rap2$^{+/an}$ and Cdk5rap2$^{an/an}$ littermates obtained from a Cdk5rap2$^{+/an}$ pregnant mouse were subjected to genotyping by PCR as described in Materials and Methods. Lane 1 is a negative control where no PCR template was added. Embryos were numbered (2-11) according to their weights (heaviest to lightest). B. Average weights of isolated E17.5 (left panel) and E12.5 to E17.5 (right panel) Cdk5rap2$^{+/+}$, Cdk5rap2$^{+/an}$ and Cdk5rap2$^{an/an}$ embryos from different litters are shown. C. MEFs isolated from Cdk5rap2$^{+/+}$, Cdk5rap2$^{+/an}$ and Cdk5rap2$^{an/an}$ embryos were subjected to SA-β-gal staining. Representative images (left panel) are from one of three independent experiments (n=3) showing similar staining patterns. The number of SA-β-gal positive cells was assessed in ~200 cells per treatment group in each of the 3 independent experiments (n=3). *p=0.0002. D. Growth of MEFs obtained from Cdk5rap2$^{+/+}$, Cdk5rap2$^{+/an}$ and Cdk5rap2$^{an/an}$ embryos was analyzed by cell viability assay. E. Lysates of MEFs isolated from Cdk5rap2$^{+/+}$, Cdk5rap2$^{+/an}$ and Cdk5rap2$^{an/an}$ embryos were analyzed by SDS-PAGE and immunoblotting for Cdk5rap2, PCNA and p21^{CIP1}. TCE staining was used to assess protein loading.

2.4.3 Cell senescence due to loss of Cdk5rap2 is linked to elevated p53 Ser15 phosphorylation via WIP1 downregulation

p53 plays a key role in triggering the expression of SA-β-gal. In addition, upon DNA damage and other types of stress that induce cellular senescence [279, 291], p53 is phosphorylated at Ser15 by protein kinases such as ATM, Chk1, and Chk2 [236]. Thus, we examined the status of p53 Ser15 phosphorylation in BJ-5ta cells depleted of Cdk5rap2. By immunoblotting using a phosphoSer15 p53 antibody, we observed that loss of Cdk5rap2 causes noticeable increase in p53 Ser15 phosphorylation, which coincides with elevation of p21^{CIP1} level (Figure 11A). Next, we tested whether senescence due to Cdk5rap2 loss involves ATM, Chk1 and/or Chk2 activation. Phosphorylation of ATM Ser1981, Chk1 Ser345 and Chk2 Thr68 was examined in Cdk5rap2-depleted cells by immunoblotting. Cells infected with H-RAS^{G12V} oncogene[142] was used as a positive control to detect senescence-associated activation of ATM, Chk1 and Chk2. Interestingly, we did not detect phosphorylation/activation of ATM, Chk1 and Chk2 in Cdk5rap2-depleted cells (Figure 11B). Unexpectedly, we observed reduced level of Cdk5rap2 in cells infected with activated H-RAS^{G12V}. The mechanism by which this happens requires further investigation but is beyond the scope of the current study. Since phosphorylation of p53 Ser15 is also regulated by protein phosphatases such as WIP1, a critical senescence regulator [282, 283] that has been associated with p53 Ser15 dephosphorylation, we examined the possibility that loss of Cdk5rap2 affects WIP1 expression. By qRT-PCR and immunoblotting, we found that WIP1 phosphatase is downregulated at both the mRNA (Figure 11C, left panel) and protein (Figure 11C, right upper and lower panels) levels in cells depleted of Cdk5rap2. Taken together, our findings indicate that cellular senescence due to loss of Cdk5rap2 may be induced by activation of p53 via downregulation of WIP1, and that p53-mediated senescence due to Cdk5rap2 loss is independent of ATM, Chk1 and Chk2 activation.

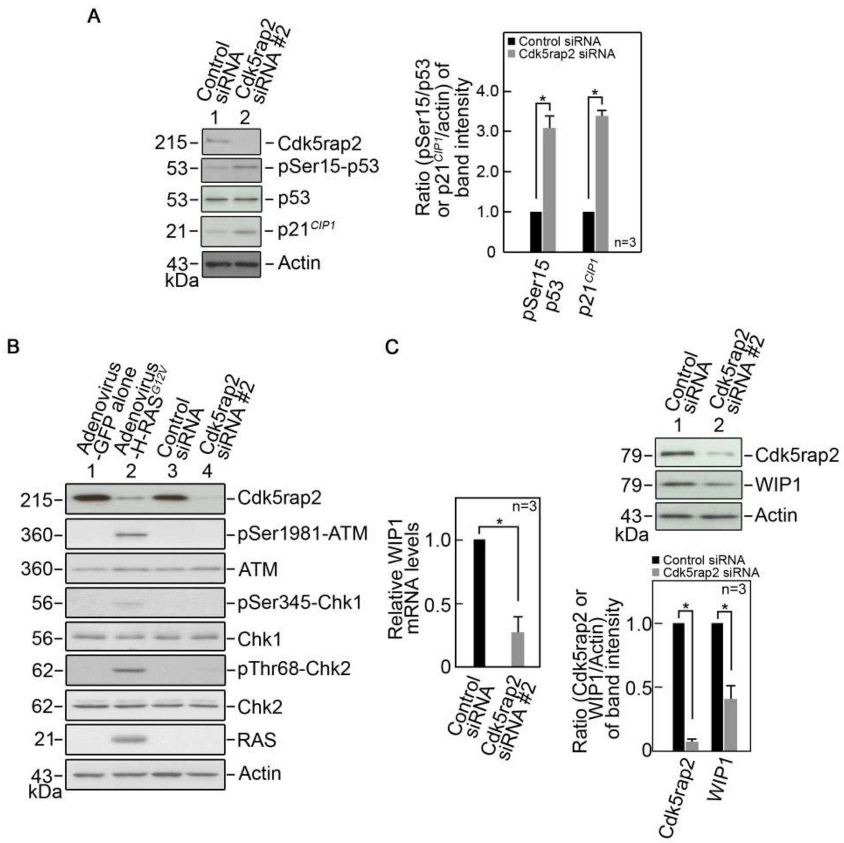

Figure 11. Cdk5rap2 loss triggers cellular senescence through downregulation of WIP1-mediated p53 activation.

A. BJ-5ta cells depleted of Cdk5rap2 show increased p53 phosphorylation at Ser15, which coincides with increased level of p21^{CIP1}. Lysates of cells transfected with Cdk5rap2 siRNA #2 for 3 days were analyzed by

SDS-PAGE and immunoblotting for Cdk5rap2, phosphoSer15 p53 (pSer15-p53), p53, p21^{CIP1} and actin (A, left panel). Actin blot was used as loading control. Representative blots are from one of three independent experiments (n=3) showing similar results. Ratios of levels of phosphoSer15 p53 (pSer15-p53) and p21^{CIP1} vs actin and standard deviation for the 3 independent sets of experiments (A, right panel) were calculated as described for Cdk5rap2 vs actin in Figure 1, with values from cells transfected with control siRNA normalized to 1.0. *p<0.005. B. Lysates of cells infected with adenovirus carrying H-RAS^{G12V} or transfected with Cdk5rap2 siRNA #2 for 3 days were analyzed by SDS-PAGE and immunoblotting for Cdk5rap2, phosphoSer1982-ATM (pSer1982-ATM), ATM, phosphoSer345-Chk1 (pSer345-Chk1), Chk1, phosphoThr68-Chk2 (pThr68-Chk2), Chk2, H-RAS and Actin. Actin blot was used as loading control. C. Cdk5rap2 loss represses WIP1 mRNA and protein expression. Levels of WIP1 mRNA in cells transfected with Cdk5rap2 siRNA #2 were determined by qRT-PCR using isolated total RNA as template. GAPDH was used for normalization. Relative levels of WIP1 mRNA (left panel) were calculated using the $2^{-\Delta\Delta CT}$ method. Relative levels from cells transfected with control siRNA were normalized to 1.0. Data represent means ± SD of calculated ratios from three independent experiments (n=3). *p=0.002. WIP1 protein expression was analyzed by immunoblotting (upper right panel). Actin blot was used as loading control. Representative blots from one of three independent experiments (n=3) showing similar results are shown. Ratios of levels of WIP1 vs actin and standard deviation for the 3 independent sets of experiments (lower right panel) were calculated as described for Cdk5rap2 vs actin in Figure 1, with values from cells transfected with control siRNA normalized to 1.0. *p<0.01.

While we note that p53-associated cell senescence induced by loss of Cdk5rap2 is distinct from the p53-mediated senescence induced by activated H-RAS^{G12V}, which is often associated with activation of the DNA damage response (DDR) [108, 119, 278], we sought to examine the possibility that senescence induced by Cdk5rap2 loss involves DDR. To do so, we performed immunofluorescence microscopy to test whether loss of Cdk5rap2 in BJ-5ta cells triggers the formation of γH2AX foci, which was assessed by staining with histone H2AX phosphoSer139 antibody (Figure 12). Cells infected with activated H-RAS^{G12V} and cells treated with 4Gy ionizing radiation (IR), which show 96.7% and 100%, respectively, of cells positive for γH2AX foci served as positive controls. Cells infected with an empty vector and cells transfected with control siRNA served as negative controls. Examination of Cdk5rap2-depleted cells revealed no γH2AX foci, indicating that p53-associated senescence that is linked to WIP1 downregulation in Cdk5rap2-depleted cells does not involve DDR activation.

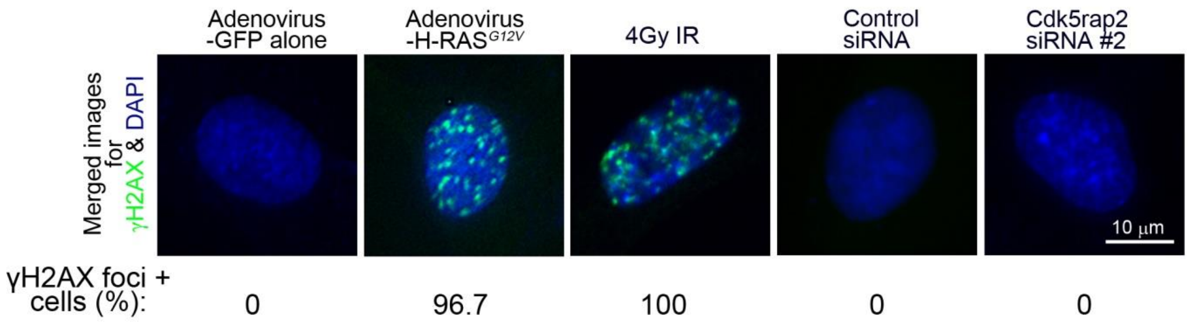

Figure 12. Cdk5rap2-depleted cells have no detectable γH2AX foci.

BJ-5ta cells transfected with Cdk5rap2 siRNA #2 for 3 days were stained with DAPI and γH2AX antibody. Cells infected with adenovirus carrying H-RAS^{G12V} and cells treated with 4Gy IR were used as positive controls for γH2AX detection. Merged images of γH2AX and DAPI staining are shown. Representative images are from one of three independent experiments showing similar staining patterns. The indicated percentage (%) of γH2AX positive cells was assessed in ~200 cells per treatment group in each of the 3 independent experiments (n=3).

To examine the idea that WIP1 loss in Cdk5rap2-depleted cells accounts for the sustained p53 Ser15 phosphorylation that leads to cellular senescence, BJ-5ta cells depleted of WIP1 by siRNA were analyzed by SDS-PAGE and immunoblotting for WIP1, p53 phophoSer15, total p53 and $p21^{CIP1}$ as well as SA-β-gal staining. Consistent with our observations in Cdk5rap2-depleted cells, WIP1-depleted cells show p53 Ser15 phosphorylation and elevation of $p21^{CIP1}$ level (Figure 13A), and increased number of SA-β-gal positive cells (Figure 13B).

A

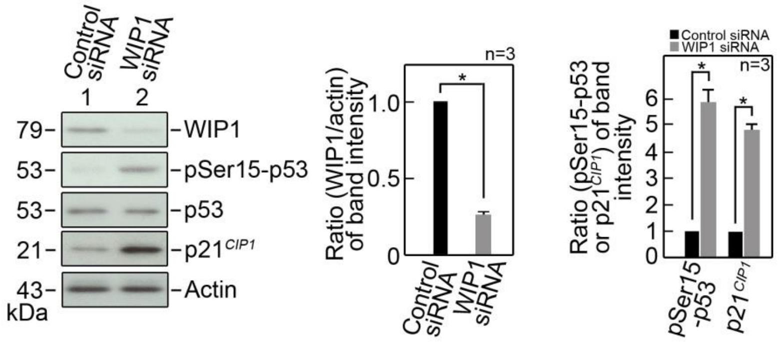

B

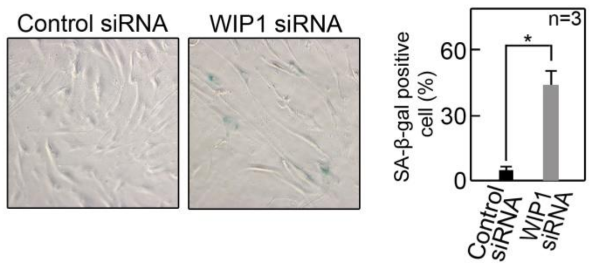

Figure 13. WIP1 loss triggers cellular senescence through p53 activation.

BJ-5ta cells transfected with WIP1 siRNA were analyzed by (A) SDS-PAGE and immunoblotting for WIP1, phophoSer15-p53, p53, and $p21^{CIP1}$ (left panel), and (B) SA-β-gal staining (left panel). Actin was used as loading control for immunoblotting. Representative blots are from one of three independent experiments (n=3) showing similar results. Ratios of levels of WIP1 vs actin (A, middle panel) and phophoSer15-p53 vs p53 and $p21^{CIP1}$ vs actin (A, right panel) and standard deviation for the 3 independent sets of experiments were calculated as described for Cdk5rap2 vs actin in Figure 1, with values from cells transfected with control siRNA normalized to 1.0. *p<0.005. Representative images of SA-β-gal staining in B (left panel) are from one of three independent experiments (n=3) showing similar staining patterns. The number of SA-β-gal positive cells (B, right panel) was assessed in ~200 cells per treatment group in each of the 3 independent experiments (n=3). *p=0.00016.

To establish a link between senescence induced by Cdk5rap2 loss and downregulated WIP1 expression, BJ-5ta cells were co-transfected with Cdk5rap2 siRNA #2 and pReceiver-M02 vector carrying WIP1. As shown in Figure 7, ectopic WIP1 overexpression in Cdk5rap2-depleted cells (Figure 14A) reverses the appearance of SA-β-gal positive cells induced by Cdk5rap2 loss (Figure 14B), supporting our view that senescence due to loss of Cdk5rap2 is linked to downregulated WIP1 expression.

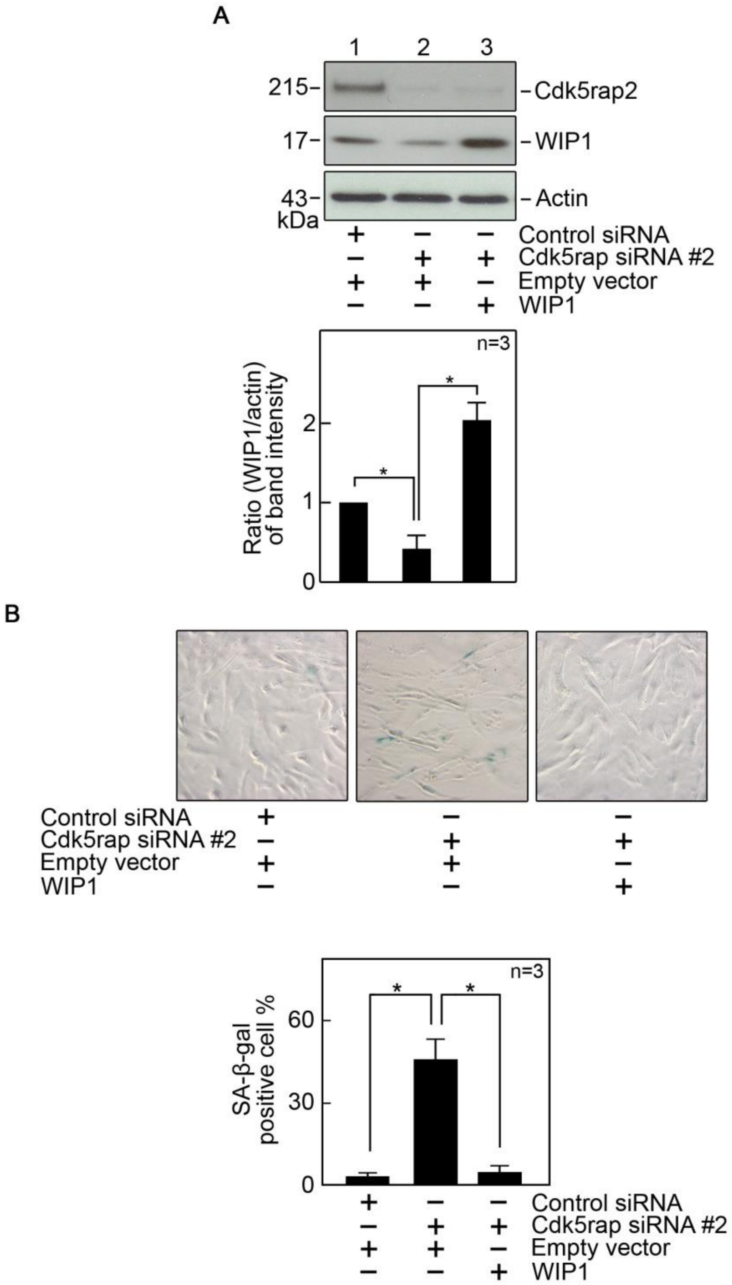

Figure 14. Ectopic expression of WIP1 reverses the senescent phenotypes observed in cells depleted of Cdk5rap2.

Lysates of BJ-5ta cells co-transfected with Cdk5rap2 siRNA #2 and pReceiver-M02 carrying WIP1 were analyzed by SDS-PAGE and immunoblotting for Cdk5rap2 and WIP1 (A, upper panel), and SA-β-gal staining (B, upper panel) 72 hrs post-transfection. Actin was used as loading control for immunoblotting. Representative blots are from one of three independent experiments (n=3) showing similar results. Ratios of levels of WIP1 vs actin and standard deviation for the 3 independent sets of experiments (A, lower panel) were calculated as described for Cdk5rap2 vs actin in Figure 1, with values from cells co-transfected with control siRNA and empty vector normalized to 1.0. *$p<0.05$. Representative images of SA-β-gal staining in B (upper panel) are from one of three independent experiments (n=3) showing similar staining patterns. The number of SA-β-gal positive cells (B, lower panel) was assessed in ~100 cells per treatment group in each of the 3 independent experiments (n=3). *$p<0.001$.

2.4.4 Cdk5rap2 regulates WIP1 expression through β-catenin

As indicated above, we found that loss of Cdk5rap2 causes downregulation of WIP1 expression at both the mRNA and protein levels. The WIP1 promoter contains a nuclear factor-κB (NF-κB) binding site [236] (Figure 15A) through which NF-κB positively regulates WIP1 expression [236], and β-catenin associates with NF-κB, affecting the expression of NF-κB target genes [200]. These apparent interactions led us to test whether loss of Cdk5rap2, which causes reduced WIP1 level, influences β-catenin expression. As shown in Figure 15B, loss of Cdk5rap2 reduces β-catenin level in the nucleus where β-catenin associates with NF-κB. Depletion of β-catenin by siRNA downregulates WIP1 level (Figure 15C), suggesting that Cdk5rap2 loss may reduce WIP1 level through downregulation of β-catenin.

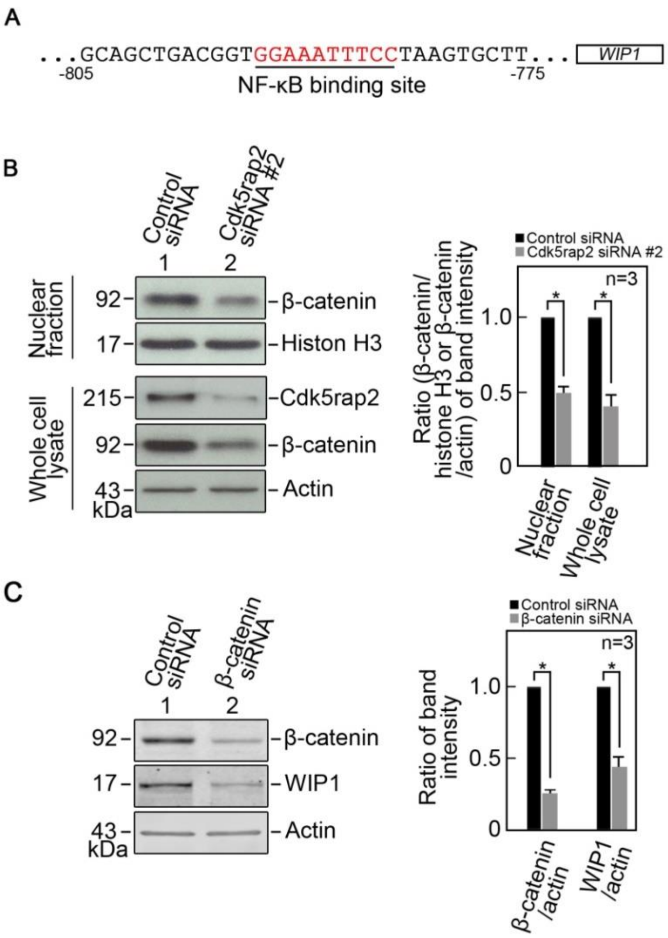

Figure 15. Cdk5rap2 loss reduces β-catenin level.

A. The WIP1 promoter contains an NF-κB binding site [236]. BJ-5ta cells transfected with Cdk5rap2 siRNA #2 (B), or β-catenin siRNA (C) for 3 days were analyzed by SDS-PAGE and immunoblotting. Nuclear fractions and whole cell lysates in (B) were probed for β-catenin and histone H3 (nuclear fraction) or Cdk5rap2 and actin (whole cell lysate), and whole cell lysates in (C) were probed for β-catenin, WIP1 and actin. Actin blot was used as loading control. Representative blots are from one of three independent experiments (n=3) showing similar results. Ratios of levels of β-catenin vs histone H3 (in nuclear fraction) or actin (in whole cell lysate) in (B) and β-catenin or WIP1 vs actin in (C), right panels, and standard deviation for the 3 independent sets of experiments were calculated as described for Cdk5rap2 vs actin in Figure 1, with values from cells transfected with control siRNA normalized to 1.0. *$p<0.05$ (in B). *$p<0.005$ (in C).

2.4.5 Cdk5rap2 interacts with glycogen synthase kinase-3β (GSK3β) and such interaction inhibits GSK3β activity

Because GSK3β phosphorylates β-catenin, targeting β-catenin for ubiquitination-mediated degradation by the proteasome pathway [286], we examined whether Cdk5rap2 interacts with GSK3β and affects GSK3β activity. To do so, lysates of BJ-5ta cells co-transfected with Myc-tagged Cdk5rap2 and FLAG-tagged GSK3β were subjected to immunoprecipitation using FLAG or Myc antibody then analyzed for Cdk5rap2 and GSK3β co-immunoprecipitation by immunoblotting both immunoprecipitates with Myc and FLAG antibodies. Fig. 16A shows reciprocal co-immunoprecipitation of Cdk5rap2 and GSK3β. To determine whether Cdk5rap2 interacts directly with GSK3β, GST-Cdk5rap2 purified from baculovirus-infected Sf9 insect cells was bound to GSH-agarose beads then mixed with purified GSK3β. Analysis of the GST pulled-down complex by SDS-PAGE and immunoblotting using GST or GSK3β antibody show the presence of both GST-Cdk5rap2 and GSK3β (Figure 16B), indicating direct interaction between these proteins. GSH-agarose-bound GST mixed with GSK3β was used as negative control. We then sought to determine whether Cdk5rap2 interaction with GSK3β affects GSK3β activity. Since GSK3β phosphorylation at Ser9 inhibits its activity [282, 292], we first examined whether Cdk5rap2 loss influences the state of GSK3β Ser9 phosphorylation. As shown in Figure 16C, cells transfected with Cdk5rap2 siRNA #2 have reduced GSK3β Ser9 phosphorylation compared to cells transfected with control siRNA, suggesting that Cdk5rap2 interaction with GSK3β could affect GSK3β activity. Indeed, by *in vitro* GSK3β kinase assay, we found that the GSK3β immunoprecipitate from cells transfected with Cdk5rap2 siRNA #2 show greater

GSK3β activity compared to cells transfected with control siRNA (Figure 16D). To examine a link between increased GSK3β activity and reduced β-catenin and WIP1 levels in Cdk5rap2-depleted cells, we tested whether inhibition of GSK3β with TWS119 restores β-catenin and WIP1 levels in these cells. Western blot analysis shows that TWS119 restores β-catenin and WIP1 levels in cells transfected with Cdk5rap2 siRNA #2 (Figure 16E), supporting a link between increased GSK3β activity and reduced β-catenin and WIP1 levels upon loss of Cdk5rap2.

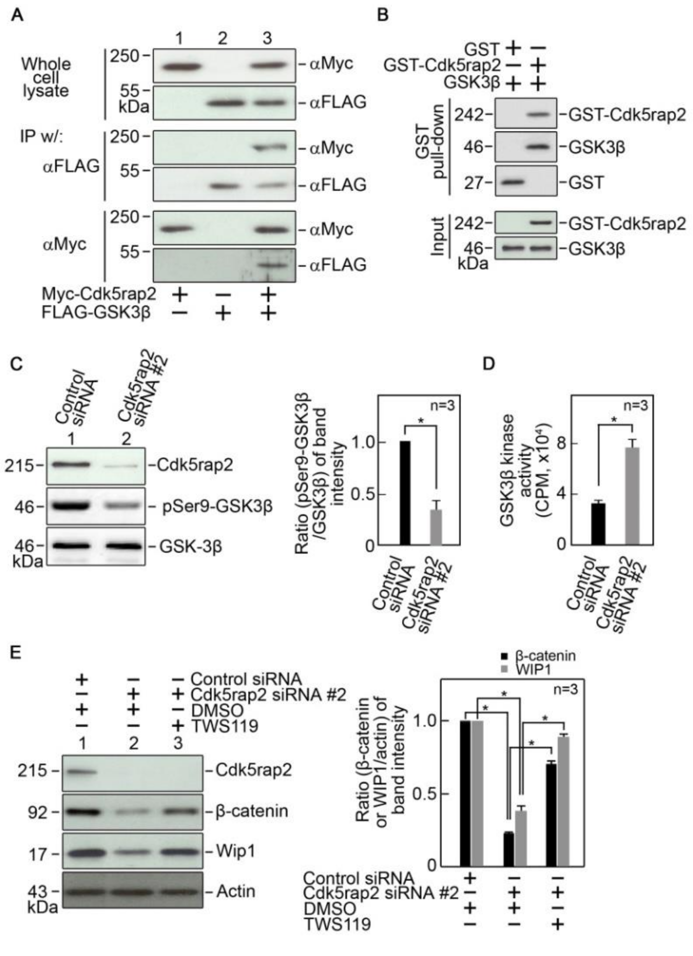

Figure 16. GSK3β interaction with Cdk5rap2 inhibits its kinase activity.

A. Lysates of BJ-5ta cells co-transfected with Myc-tagged Cdk5rap2 and FLAG-tagged GSK3β (upper panel) were subjected to immunoprecipitation (IP) using FLAG antibody (middle panel) or Myc antibody (lower panel) then analyzed for Cdk5rap2 and GSK3β co-immunoprecipitation by immunoblotting both IPs with Myc and

FLAG antibodies. B. Cdk5rap2 directly interacts with GSK3β. GST-Cdk5rap2 bound to GSH-agarose beads was mixed with GSK3β as described in Materials and Methods. The resulting complexes were washed extensively then analyzed by SDS-PAGE and immunoblotting for GST and GSK3β. C. Lysates of cells transfected with Cdk5rap2 siRNA #2 for 3 days were analyzed by SDS-PAGE and immunoblotting for Cdk5rap2, phosphoSer9-GSK3β and GSK3β (left panel). Representative blots are from one of three independent experiments (n=3) showing similar results. Ratios of levels of phosphoSer9-GSK3β vs GSK3β and standard deviation for the 3 independent sets of experiments (right panel) were calculated as described for Cdk5rap2 vs actin in Figure 1, with values from cells transfected with control siRNA normalized to 1.0. *p=0.01. D. Lysates of cells transfected with Cdk5rap2 siRNA #2 for 3 days were subjected to IP using GSK3β antibody. The IPs were then examined for *in vitro* GSK3β kinase activity as described in Materials and Methods. Data represent means ± SD from three independent experiments (n=3). *p=0.0027. E. Inhibition of GSK3β activity with TWS119 in cells depleted of Cdk5rap2 restores β-catenin and WIP1 expression (left panel). Representative blots from one of three independent experiments (n=3) showing similar results are shown. Ratios of levels of β-catenin and WIP1 vs actin and standard deviation for the 3 independent sets of experiments (right panel) were calculated as described for Cdk5rap2 vs actin in Figure 1, with values from cells transfected with control siRNA and treated with DMSO normalized to 1.0. *p<0.05.

2.4.6 Cdk5rap2 loss induces senescence through upregulation of GSK3β activity and subsequent downregulation of β-catenin-mediated WIP1 expression

Our next step was to examine whether inhibition of GSK3β with TWS119, which restores β-catenin and WIP1 levels in BJ-5ta cells depleted of Cdk5rap2, inhibits senescence in these cells. We found that treatment of BJ-5ta cells with TWS119, which increases β-catenin and

WIP1 levels and reduces p53 Ser15 phosphorylation in cells transfected with Cdk5rap2 siRNA #2 (Figure 17A), results in loss of SA-β-gal staining in these cells (Figure 17B), suggesting that inhibition of GSK3β prevents senescence in Cdk5rap2-depleted cells through upregulation of β-catenin and WIP1 and subsequent inactivation of p53. We then examined the effect of inhibition of WIP1 activity with GSK2830371 in Cdk5rap2-depleted cells treated with TWS119. Figure 10A shows that GSK2830371 has no effect on β-catenin and WIP1 levels in these cells but causes an increase in p53 Ser15 phosphorylation and thus, as shown in Figure 17B, an increase in SA-β-gal staining. These findings support our view that GSK3β acts upstream of β-catenin as well as WIP1 and, therefore, while GSK3β inhibition prevents senescence in Cdk5rap2-depleted cells by increasing β-catenin and WIP1 levels, reducing p53 Ser15 phosphorylation, direct inactivation of WIP1 in cells lacking Cdk5rap2 and GSK3β activity results in p53 Ser15 phosphorylation and increased senescence.

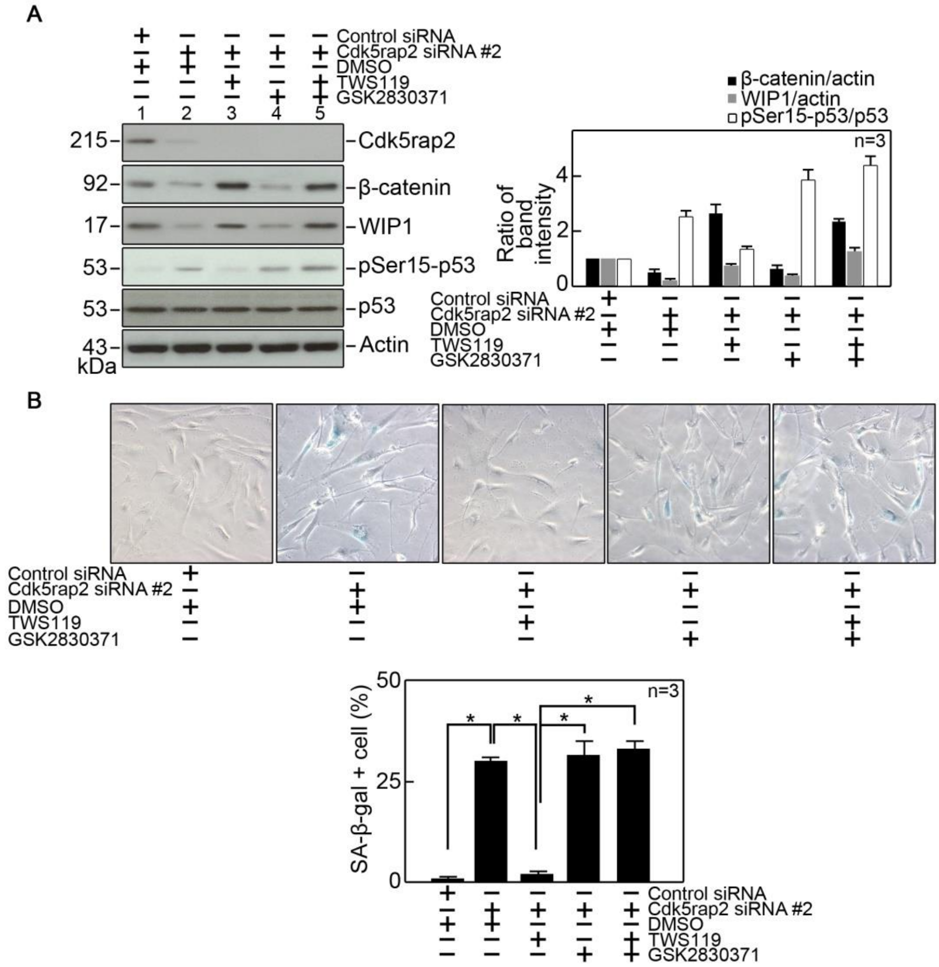

Figure 17. Inhibition of GSK3β in Cdk5rap2-depleted cells inhibits senescence that is induced upon inhibition of WIP1 activity.

A. BJ-5ta cells transfected with Cdk5rap2 siRNA #2 were treated with TWS119 and/or GSK2830371, a potent inhibitor of WIP1 activity. Cell lysates were then analyzed by SDS-PAGE and immunoblotting for Cdk5rap2, β-catenin, WIP1, phosphoSer15-p53, p53 and actin (left panel). Actin blot was used as loading control. Representative blots from one of three independent experiments (n=3) showing similar results are shown. Ratios of levels of β-catenin and WIP1 vs actin and phosphoSer15-p53 vs p53, and standard deviation for the 3 independent sets of experiments (right panel) were calculated as described for Cdk5rap2 vs actin in Figure 1, with values from cells transfected with control siRNA and treated with DMSO normalized to 1.0. *p<0.05. B. Representative images of SA-β-gal staining (upper panel) are from one of three independent experiments (n=3) showing similar staining patterns. The number of SA-β-gal positive cells (lower panel) was assessed in ~100 cells per treatment group in each of the 3 independent experiments (n=3). *$p<0.05$.

Promoter bashing analysis by transfecting a luciferase reporter vector carrying wt WIP1 promoter (pGL3-WIP1, Figure 11A) into cells transfected with Cdk5rap2 siRNA #2 (Figure 11B) or β-catenin siRNA (Figure 11C) show reduced luciferase activity in these cells compared to cells transfected with control siRNA (Figure 11, B &C). Conversely, transfection with WIP1 lacking its NF-κB binding site (pGL3-WIP1-ΔκB; Figure 11A) has no effect on luciferase activity in Cdk5rap2- or β-catenin-depleted cells. Treatment with TWS119 restored luciferase activity in Cdk5rap2-depleted cells transfected with pGL3-WIP1 (Figure 11B, right panel), further suggesting that senescence due to Cdk5rap2 loss is controlled by GSK3β through regulation of the WIP1 promoter via β-catenin.

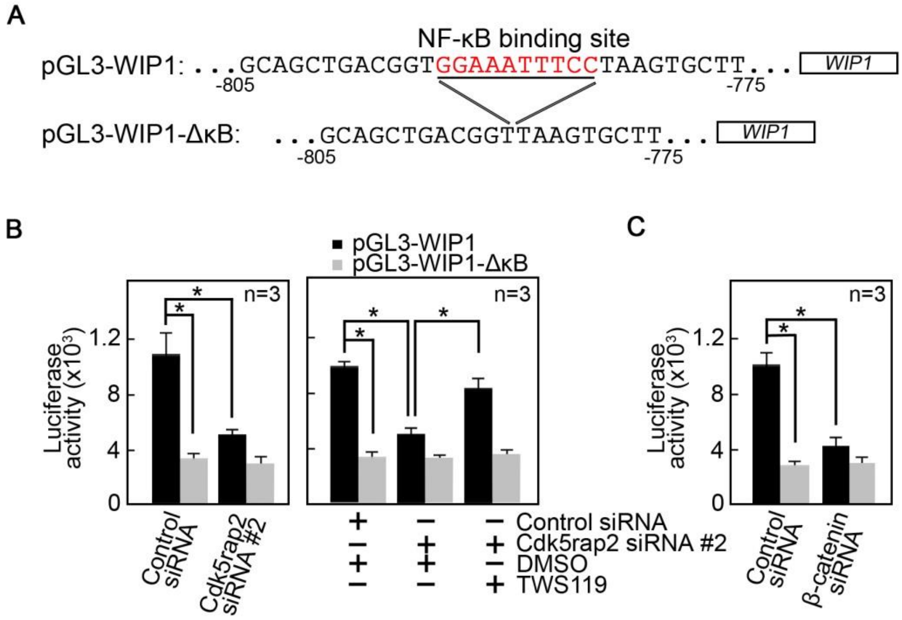

Figure 18. Cdk5rap2 regulates WIP1 promoter activity via β-catenin.

A. Sequence of pGL3 luciferase reporter vector carrying WIP1 or WIP1-ΔκB promoter. B and C. Loss of Cdk5rap2 (B, left and right panels) or β-catenin (C) inhibits WIP1 promoter activity as measured by luciferase reporter activity but inhibition of GSK3β with TWS119 in Cdk5rap2-depleted cells restores WIP1 promoter activity (B, right panel). Data represent means ± SD from three (n=3) independent experiments. *p<0.05.

2.5 Discussion

In this study, we provide for the first time the evidence that Cdk5rap2 loss induces premature cellular senescence through regulation of GSK3β activity that controls β-catenin-mediated downregulation of WIP1. We prove this by using BJ-5ta cells as well as Cdk5rap2$^{an/an}$ mice embryos and their corresponding *ex vivo* MEF cells. After recovering from cryopreservation, BJ-5ta cells were used for up to 10 additional population doublings to ensure that there is no further change in these parameters. We started our experiment by eliminating the possibility of siRNA off-target effect. To do so, we used two different Cdk5rap2 siRNAs (#1 and #2) and confirmed whether Cdk5rap2 depletion by these siRNAs gives rise to similar results: i.e., formation of SAHF as demonstrated by staining with DAPI and colocalization with HP1γ. For subsequent experiments, siRNA #2, which causes greater depletion of Cdk5rap2 was used. Premature cellular senescence due to Cdk5rap2 loss was verified by the increase in number of SAHF positive cells, upregulation of the senescence-associated genes, p21^{CIP1} and p16^{INK4a} [293], and increased staining for SA-β-gal. In addition, defect in proliferation due to Cdk5rap2 loss was demonstrated by reduced cell proliferation, which was determined by increased population of cells at G_0/G_1 and reduced population of cells at S phase. In the Cdk5rap2$^{an/an}$ mouse model, cell proliferation defect is manifested by reduced embryo body size as measured by body weight. In addition to E12.5, we also analyzed E17.5 embryos as well as E12.5, E14.5, E15.5 and E17.5 together to assess the significance of the reduced body weight of Cdk5rap2$^{an/an}$ compared to Cdk5rap2$^{+/+}$ and Cdk5rap2$^{+/an}$. We note that the senescence phenotypes observed in Cdk5rap2-depleted BJ-5ta cells are recapitulated in *ex vivo* MEFs isolated from Cdk5rap2$^{an/an}$ embryos. Previously, a frameshift loss-of-function mutation in Cdk5rap2, designated as E385fsX4 [162] and later corrected to R1334SfsX5 [233], was reported in northern Pakistani microcephaly pedigrees. A mouse model that carries this mutation has been generated [170], and MEFs isolated from these mice are viable but do not grow to confluence after passages 8 to 10 [170]. This observation is consistent with our view that Cdk5rap2 loss triggers premature cellular senescence.

Loss of Cdk5rap2 causes an increase in p53 Ser15 phosphorylation, one of the early events leading to cellular senescence [279, 291]. Unexpectedly but interestingly, we found that increased 53 Ser15 phosphorylation is not due to activation of the p53 kinases, ATM, Chk1, or Chk2 [236], but rather due to downregulation of WIP1 phosphatase expression. Indeed, WIP1-mediated p53 dephosphorylation at Ser15 has been associated with cellular senescence [282, 283]. It is known that p53 phosphorylation at Ser15 stabilizes p53 by inhibiting its interaction with Mdm2, an E3 ubiquitin ligase that catalyzes polyubiquitination and subsequently induces proteasome degradation of p53[236]. However, increased level of p53 was not detected in cells depleted of Cdk5rap2, which showed elevated p53 Ser15 phosphorylation. Since p53 Ser15 phosphorylation is required for p53 activation [279, 280], it is possible that loss of Cdk5rap2 induces activation of p53 via Ser15 phosphorylation. Indeed, elevated level of p21^{CIP1}, a major transcriptional target of p53, was observed upon Cdk5rap2 depletion. Examination of Cdk5rap2-depleted cells revealed no γH2AX foci, indicating that p53-associated senescence that is linked to WIP1 downregulation in these cells is independent of DDR activation. This is consistent with the lack of activation of ATM, Chk1 or Chk2 in p53-associated cell senescence induced by loss of Cdk5rap2. Our findings that knocking down WIP1 causes increased p53 Ser15 phosphorylation and number of SA-β-gal positive cells, and that ectopic expression of WIP1 in cells depleted of Cdk5rap2 reverses such phenotypes establish a link between cellular senescence due to Cdk5rap2 loss and downregulation of WIP1. In fact, WIP1$^{-/-}$ mice exhibit aging phenotypes in their hematopoietic stem cells, including impaired repopulating activity [283], and WIP1$^{-/-}$ MEFs [283] and mesenchymal stem cells [284] exhibit premature senescence. In addition, reduced level of WIP1 in primary chondrocytes triggers the onset of senescence and loss of the chondrocyte phenotype, while ectopic expression of WIP1 delays such onset, retaining their proliferative capacity [285].

Our observation that Cdk5rap2 loss causes downregulation of WIP1 mRNA and protein levels together with the fact that the WIP1 promoter contains an NF-κB binding site [236] through which NF-κB positively regulates WIP1 expression [236], and β-catenin associates with NF-κB to induce the expression of NF-κB target genes[34] led to our view that Cdk5rap2 loss reduces WIP1 level through downregulation of β-catenin. In addition, our notion that the level of β-catenin is regulated by GSK3β activity is based on the fact that GSK3β phosphorylates β-catenin, targeting β-catenin for ubiquitination-mediated degradation by the proteasome pathway [286] and inhibiting translocation of β-catenin into the nucleus [294]. Our finding that Cdk5rap2 interacts with GSK3β and such interaction inhibits GSK3β activity elucidates the molecular mechanism by which β-catenin level is downregulated upon Cdk5rap2 loss. Indeed, the harmonizome database [181], and immunoprecipitation and mass spectrometry analyses [181] show that GSK3β binds to Cdk5rap2. Additional evidence that reflects their interaction include from their colocalization in centrosome, duplication of which is synchronized with the cell cycle. Thus, although GSK3β, which promotes mitotic progression, is mainly distributed throughout the cytoplasm, a subpopulation of GSK3β localizes at the centrosome [180]. Recently, the phosphorylated form of GSK3β has been mapped to the centrosome [285], where Cdk5rap2 exists [158, 295] and regulates centriole engagement and cohesion during the cell cycle [170]. In this study, inhibition of GSK3β activity due to interaction with Cdk5rap2 was demonstrated by increased inhibitory phosphorylation at GSK3β Ser9 and a corresponding decline in GSK3β activity as determined by *in vitro* kinase assay of GSK3β immunoprecipitates. Since AKT (protein kinase B), which regulates centrosome composition and integrity during mitosis [296], can phosphorylate

GSK3β at Ser9 [176, 177], it is possible that GSK3β is recruited to the centrosome where it interacts with Cdk5rap2, facilitating inhibitory phosphorylation of GSK3β Ser9 by AKT. However, upon Cdk5rap2 loss, unphosphorylated and active GSK3β could be released from the centrosome and phosphorylate β-catenin, targeting β-catenin for ubiquitination-mediated degradation by the proteasome pathway. Reduced level of β-catenin and subsequent downregulation of WIP1 expression, increased p53 Ser15 phosphorylation and upregulation of p21^{CIP1} ultimately induces cellular senescence. Using the TWS119 GSK3β inhibitor that restores β-catenin and WIP1 levels in Cdk5rap2-depleted cells, we established a link between increased GSK3β activity and decreased β-catenin and WIP1 levels upon loss of Cdk5rap2. The fact that TWS119 restores luciferase activity in Cdk5rap2-depleted cells transfected with the WIP1 promoter (pGL3-WIP1) and luciferase activity is also reduced in β-catenin-depleted cells transfected with pGL3-WIP1 further suggest that senescence caused by Cdk5rap2 loss is controlled by GSK3β through β-catenin regulation of the WIP1 promoter. Taken together, our studies reveal that loss of Cdk5rap2 triggers premature cellular senescence via β-catenin-mediated downregulation of WIP1. Such senescence is associated with proliferation defect as manifested by increased population of cells at G_0/G_1 and reduced population at S phase in BJ-5ta cells as well as small body size in Cdk5rap2$^{an/an}$ mice. As Cdk5rap2 loss-of-function has been associated with primary microcephaly [162, 269], cochlear and retinal developmental defects[270], primordial dwarfism [181, 271] and Seckel syndrome, a heterogeneous, autosomal recessive disorder characterized by prenatal proportionate short stature, severe microcephaly, intellectual disability, and characteristic 'bird-headed' facial features [180], it is possible that premature cellular senescence contributes to these developmental disorders. Results from our studies provide novel insight into the molecular mechanisms by which Cdk5rap2 loss-of-function causes cell senescence, which may lead to developmental disorders.

2.6 Acknowledgements

We thank (i) Dr. Karl Riabowol at University of Calgary, Calgary, Canada, for providing us adenovirus carrying Ras V12 and control empty adenovirus, (ii) Dr. Tara Beattie at the University of Calgary for providing us the BJ-5ta cells.

Chapter Three: Loss of Cdk5rap2 compromises centromeric chromatin integrity through downregulation of CENP-A

3.1 Abstract

Centromeres are chromosomal loci where kinetochores assemble to ensure faithful chromosome segregation during mitosis. CENP-A defines the loci by serving as an epigenetic marker that recruits other centromere components such as CENP-C for a functional structure. However, the mechanism that controls CENP-A regulation of centromeric integrity remains to be explored. Separate studies, showing that loss of either CENP-A or the Cdk5 regulatory subunit associated protein 2 (Cdk5rap2), which has been shown to play key roles in mitotic progression, triggers the occurrence of lagging chromosomes, prompted us to investigate a potential link between these proteins. Here, we demonstrate that Cdk5rap2 loss causes reduced CENP-A expression while ectopic Cdk5rap2 expression in cells depleted of endogenous Cdk5rap2 restores CENP-A expression. Indeed, we show that Cdk5rap2 is a nuclear protein that acts as a positive transcriptional regulator of CENP-A. Cdk5rap2 interacts with the CENP-A promoter and upregulates CENP-A transcription. Furthermore, Cdk5rap2 loss causes reduced centromeric CENP-A and CENP-C, which are both known to induce kinetochore recruitment. Aside from manifesting lagging chromosomes, cells depleted of Cdk5rap2, and thus CENP-A, show increased micronuclei and chromatin bridge formation. Altogether, our findings indicate that centromeric chromatn integrity is maintained by CENP-A under the control of Cdk5rap2.

3.2 Introduction

Precise segregation and distribution of chromosomes into daughter cells during cell division are key cellular processes where errors trigger cell death or disease such as cancer [297, 298]. Centromeres are defined as chromosomal loci that nucleate kinetochore assembly for chromosome attachment to spindle microtubules and chromosome separation during cell division [299]. Although eukaryotic centromeres are organized into highly-ordered short tandem repeats [300], they differ significantly among and within species [299]. Thus, in spite of being highly functionally conserved, no specific DNA sequence for the common centromere has been identified thus far [299]. In addition, centromeres are known to be specified epigenetically in most species [301, 302] by accumulating the histone H3 variant, CENtromeric Protein A (CENP-A), resulting in interspersed H3 and CENP-A nucleosomes within the chromosome loci[303-306]. CENP-A disposition is critical for recruitment of other centromere components such as CENP-C and CENP-N [250, 307], which are necessary for proper centromere formation and chromosome segregation [242]. Thus, it is not surprising that CENP-A knock-down cells display lagging chromosomes [77, 308, 309].

Cyclin-dependent kinase 5 regulatory subunit associated protein 2 (Cdk5rap2), which is also known as CEP215, was originally identified based on its ability to interact with the Cdk5 regulatory subunit, p35 [159]. The human Cdk5rap2 gene (accession #: NP_060719) consists of 38 exons, encoding a protein that is made up of 1893 amino acid residues. Cdk5rap2 is composed of (i) a CM1 domain (residues 58–90) [310] that binds γ-tubulin complexes, (ii) two predicted structural maintenance of chromosome (SMC) domains (one each in the N- and C-terminals, corresponding to residues 137–470 and 1399–1646, respectively) [162] that are known to play a role in chromatid cohesion and DNA recombination during meiosis and mitosis [311-313], (iii) a serine-rich EB1 binding region (residues 926–1208)[314], (iv) a p35 interacting domain (residues 1682–1827) [159, 161], (v) a pericentrin binding domain (residues 1726–1893) [295], and (vi) a Cnn Motif 2 (CM2) domain (residues 1861-1870) for Golgi complex interaction and binding to calmodulin [295]. Cdk5rap2 is ubiquitously expressed in human and in embryonal mouse tissues [159, 162]. Subcellular localization of Cdk5rap2 in cultured cells such as murine fibroblasts [170], human embryonic kidney HEK239 cells [295, 314]; human cervical HeLa cells [295, 314] and human osteosarcoma U2OS cells [314] showed its presence in growing tips of microtubules[314] and in centrosomes [295], particularly in the pericentriolar material (PCM) [315, 316]. The level of PCM Cdk5rap2 is regulated in a cell cycle-dependent manner with the highest level observed during mitosis [170]. In this process, Cdk5rap2 was found to play a role in spindle formation [162] and implicated to be required for the spindle checkpoint signaling pathway [173]. As with CENP-A knock-down cells, cells lacking Cdk5rap2 show lagging chromosomes, suggesting a role for Cdk5rap2 in proper chromosome segregation [173]. However, why and how loss of Cdk5rap2 triggers the occurrence of lagging chromosomes remains unexplored.

In this study, we examined a potential link between Cdk5rap2 and CENP-A, and their involvement in mitosis, specifically in chromosome segregation. Interestingly, we found that Cdk5rap2 regulates the expression of *CENP-A*. We determined that Cdk5rap2 localizes in the nucleus where it acts as a transcriptional activator for *CENP-A*. Indeed, we found that (i) loss of Cdk5rap2 causes reduced level of CENP-A, and expression of Cdk5rap2 in cells depleted of endogenous Cdk5rap2 increases CENP-A level, (ii) Cdk5rap2 interacts with the CENP-A promoter and upregulates CENP-A transcription, and (iii) Cdk5rap2 loss causes decreased level of CENP-A as well as the CENP-A-interacting protein, CENP-C, at the centromeres. Together with the appearance of lagging chromosomes, the notable formation of micronuclei and chromatin bridges upon loss of Cdk5rap2 suggests that CENP-A mediated centromeric chromatin integrity is under the control of Cdk5rap2.

3.3 Materials and Methods

3.3.1 Materials.

hTERT-immortalized BJ-5ta human foreskin fibroblast cells was obtained from Dr. Tara Beattie at the University of Calgary. SaOS-2 human osteosarcoma and HEK293 cells were from ATCC (Manassas, VA, USA). The Cdk5rap2 antibody (A300-554A) was from Bethyl Laboratories (Montgomery, TX, USA). CENP-A (ab13939) and CENP-C (ab193666) antibody was from Abcam (Cambridge, MA, USA). HA (sc-7392), H2AX (sc-54606) and actin (sc-8432) antibodies, normal IgG (sc-2025) and protein A/G PLUS-agarose (sc-2003) were from Santa Cruz Biotech. (Santa Cruz, CA, USA). c-Myc antibody (9E10) was from Thermo Fisher Scientific (Waltham, MA USA). The HRP-conjugated anti-rabbit (#7074) and anti-mouse (#7076) secondary antibodies were from Cell Signaling (Danvers, MA, USA). The goat anti-mouse Alexa-488 (ZF-0512) and goat anti-rabbit Alexa-594 (ZF-0516) are from ZSGB Biotech (Beijing, China). XhoI (#R0146) and HindIII (#R0104) restriction enzymes were from New England Biolabs (Beverly, MA, USA). The Dual-Luciferase® Reporter Assay System kit (E1910) was from Promega (Madison, WI, USA). PerfeCTa SYBR Green supermix (95054-500) was from Quanta Biosciences (Beverly, MA, USA). All primers and siRNAs were synthesized at the University of Calgary Core DNA services.

3.3.2 Cell culture

BJ-5ta cells were cultured in Eagle's minimal essential medium (EMEM, Lonza) with 10% fetal bovine serum (FBS, GIBCO), 50 U/ml penicillin and 50 mg/ml streptomycin (Invitrogen, Carlsbad, CA, USA). SaOS-2 human osteosarcoma and HEK293 human embryonic kidney cells were cultured in Dulbecco’s modified Eagle medium (DMEM, Invitrogen), containing 10 % FBS, 50 U/ml penicillin and 50 mg/ml streptomycin. Cells were maintained at 37 ℃ in a 5 % CO2 humidified incubator.

3.3.3 Plasmid or siRNA transfection

SaOS-2 cells and BJ-5ta cells were seeded 24 hours before transfection. Cdk5rap2 siRNA or control siRNA target sequence or pcDNA carrying HA-tagged Cdk5rap2(res) expression vector was transfected using Lipofectamine 2000 (Invitrogen) in serum-free medium, which was replaced with complete medium 5 hours post-transfection. Cells were harvested at different time points as indicated.

Table 5. siRNA sequences for gene depletion

Control siRNA	CGUACGCGGAAUACUUCGAUU
Cdk5rap2 siRNA#1	GGACGUGUUGCUUCAGAAAUU
Cdk5rap2 siRNA#2	GAGUCAGCCUUCUGCUAAAUU

3.3.4 RNA extraction and qRT-PCR

Total RNA was extracted using TRIzol reagent (Invitrogen, Carlsbad, CA, USA) according to the manufacturer’s protocol, and transcribed into cDNA using superscriptase II (Invitrogen).

Real-time PCR were performed using Power SYBR® Green PCR Master Mix (Thermo Fisher) on an Applied Biosystems 7500 Real-time PCR system using a standard protocol. The PCR conditions include 35 cycles of 94 ℃ for 20 seconds, 60 ℃ for 20 seconds and 72 ℃ for 35 seconds. The following primer sets were used:

Table 6. Primers for examination of gene expresion.

Primer	Sequence
Cdk5rap2-F	AAGATGCTCGAAAGAAGGTGC
Cdk5rap2-R	TTTCCAAACGCAACCGAAGAG
CENP-A-F	TTCACTCGTGGTGTGGACTT;
CENP-A-R	CGGCCTGCATGTAAGGTGA
GAPDH-F	TCCCTGAGCTGAACGGGAAG
GAPDH-R	GGAGGAGTGGGTGTCGCTGT

GAPDH was served as loading control for normalization.

3.3.5 Western blot analysis

Cell lysates were resolved by SDS-PAGE, transferred to a nitrocellulose membrane, and immunoblotted for Cdk5rap2, CENP-A, HA, H2AX, and actin. Following incubation with HRP-conjugated anti-rabbit or anti-mouse secondary antibody, immunoreactive bands were detected using the ECL reagent (GE Healthcare, Little Chalfont, Buckinghamshire, UK). Western blot images were obtained using the ChemiDoc™ Imager (Bio-Rad) and using the optimal exposure setup. No enhancements were performed.

3.3.6 Chromatin immunoprecipitation (ChIP) assay and ChIP-qPCR.

SaOS-2 cells were trypsinized, harvested and placed in a centrifuge tube. Cells were washed in PBS and fixed with 0.5% formaldehyde at room temperature for 10 min then quenched with the addition of 125 mM glycine. Fixed cells were suspended in sonication buffer (20 mM Tris-HCl pH 8.0, 1 mM EDTA, 1 mM DTT, 0.02 % SDS), and sonicated using the Bioruptor (Scientz, China) to fragment chromatin DNA. Soluble chromatin was recovered by centrifugation and diluted with twice its volume of IP buffer (30 mM Tris-HCl pH 8.0, 450 mM NaCl, 0.75 mM EDTA, 0.75 mM DTT, 1.5 % Triton X-100, 0.075 % SDS, 7.5 % glycerol). Input samples were taken from this preparation. Samples from this preparation were also subjected to immunoprecipitation using a Cdk5rap2 antibody that was pre-incubated with protein A/G PLUS-agarose. DNA-enriched IPs were de-crosslinked by incubation at 65oC. The purified DNA was analyzed by real-time PCR (Bio-Rad, Hercules, CA, USA) using PerfeCTa SYBR Green supermix. The following primer were used in ChIP assay:

Table 7. Primers for ChIP assay.

Primer	Sequence
Primer1-F	CCCAACAAAGGGAAGAGAGCA
Primer1-R	AGGACAGGGGAGACTGATGG
Primer2-F	CACACCATCCACGTTCCAAAC
Primer2-R	CCGCTCGCGTTCAAATCG
Primer3-F	ATCAGTCTCCCCTGTCCTCC
Primer3-R	CCATGACACGCCGCAGA
Primer4-F	GAGTCGCTGGATTCGGGTTT
Primer4-R	TTGATGGGAGGAAGCGCCTA

For ChIP-qPCR assay, crosslinked DNAs were subjected to immunoprecipitation for CENP-A or CENP-C. The ChIP was performed as described above. After ChIP, samples were diluted 1:100 in dH2O for qPCR. Data were analyzed using comparative $2^{-\Delta\Delta CT}$ quantitation.

The following primers used in ChIP-PCR assay:

Table 8. Primers for ChIP-PCR assay

Primer	Sequence
Centromere-F	ACGATCCTTTACAGAGCAGA
Centromere -R	ATTGACCTCAAAGCGGCTGA

3.3.7 Luciferase reporter assay

CENP-A promoter region (-330-+4) were amplified by PCR reaction using genomic DNA from SaOS-2 cells. The following primer were used for amplification:

Table 9. Primers for CENP-A promoter region amplification.

Primer	Sequence
CENPA-PRO-CL-F	ATCGCTCGAGATCAGTCTCCCCTGTCCTCC
CENPA-PRO-CL-R	ATCGAAGCTTATGACACGCCGCAGAGGGTG

PCR production was The PCR products were purified using GeneJET PCR Purification Kit (Thermo Fisher) and then cloned into pGL3-basic firefly luciferase reporter vector using XhoI and HindIII restriction enzyme sites. The insert sequence was confirmed by DNA sequencing and designated as pGL-3-basic-CENPA-promoter. To measure the luciferase activity, HEK293 cells were co-transfected with indicated siRNA, pGL-3-basic-CENPA-promoter and renilla luciferase vector using lipofectamine 2000 (Invitrogen). After 48 hours transfection, the luciferase activities were measured using Dual-Luciferase® Reporter Assay System (Promega) following manufacture’s protocol. Renilla luciferase served as an internal control for normalization

3.3.8 Ectopic expression of Myc-tagged full-length (1-1893), N-terminal (1-994) and C-terminal (991-1893) Cdk5rap2 and analysis of CENP-A expression.

Lysates of HEK293 cells transfected with a vector carrying full length or a fragment of Cdk5rap2 were resolved by 5-20% gradient SDS-PAGE and immunoblotted for Myc and CENP-A. Ratios of CENP-A/Myc-tagged Cdk5rap2 band intensities were calculated based on values obtained by densitometry analysis using the National Institutes of Health Image J 1.61 software.

3.3.9 Primary sequence and protein secondary structure analysis

Primary sequence analysis of Cdk5rap2 was performed using the Motif Scan-MyHits software. Protein secondary structure analysis was assessed using Secondary Structure Prediction-ExPASy: SIB Bioinformatics.

3.3.10 Immunofluorescence microscopy

SaOS2 cells transfected with Cdk5rap2 or control siRNA on coverslips were fixed for 48 hrs at room temperature. To stain centromeric CENP-A, cells were incubated with a mouse CENP-A antibody for 1 hr, washed, then incubated with a goat anti-mouse Alexa-488-conjugated secondary antibody for 20 min at room temperature. Coverslips were mounted on glass slides using ProLong™ Diamond Antifade Mountant (P36961, Invitrogen). Images were captured using Olympus FSX100 microscope, and the number of CENP-A-stained foci in these cells (n=86 for each group) were counted. DAPI was used to visualize the nucleus.

To assess for the formation of micronuclei and chromatin bridges, cells on coverslips were stained with DAPI and mounted on glass slides using ProLong™ Diamond Antifade

Mountant (P36961, Invitrogen, Carlsbad, CA, USA). Images were captured using Olympus FSX100 microscope.

3.3.11 Statistical analyses

All data are expressed as mean ± standard deviation of at least three biological replicates. The statistical analyses were done using student's t-tests for two samples and one-way analysis of variance (ANOVA) for differences among groups using GraphPad Prism software. A probability of $p < 0.05$ was taken to be statistically significant.

3.4 Results

3.4.1 Loss of Cdk5rap2 induces lagging chromosomes

It has been demonstrated that inhibition of Cdk5rap2 expression in HeLa cells causes lagging chromosomes [173]. We further examined the effect of Cdk5rap2 deficiency in SaOS-2 human osteosarcoma cells and found that cells depleted of Cdk5rap2 (Figure 19A) by two different siRNAs (#1 or #2) showed noticeable occurrence of lagging chromosomes (Figure 19B) while control cells mostly displayed proper chromosome separation. Two independent siRNAs, which were used to rule out the possibility of off-target effects, caused a similar extent of occurrence of lagging chromosome in Cdk5rap2-depleted cells. Our analysis revealed that in Cdk5rap2-depleted cells, 7/41 or 17 % of anaphase cells showed lagging chromosomes while only 3/52 or 5.7 % of control cells in anaphase exhibited lagging chromosomes.

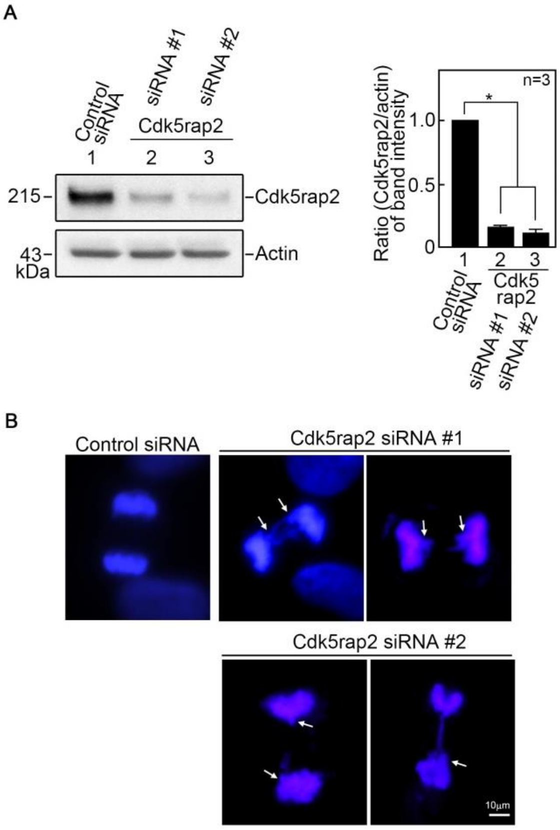

Figure 19. Loss of Cdk5rap2 causes lagging chromosomes.

(A) SaOS-2 cells transfected with Cdk5rap2 or control siRNA for 2 days were subjected to SDS-PAGE and immunoblotting for Cdk5rap2. Actin blot was used as loading control. Representative blots are from one of three independent experiments (n=3) showing similar result patterns. Ratios of levels of Cdk5rap2 vs actin were calculated following densitometric analysis of blots using NIH Image J 1.61. *p<0.01. (B) Two days after transfection, cells were stained with DAPI and subjected to microscopic examination. Representative images of control and Cdk5rap2-depleted cells are shown with arrows directed at lagging chromosomes.

3.4.2 Cdk5rap2 regulates CENP-A expression

The molecular mechanism by which loss of Cdk5rap2 triggers the occurrence of lagging chromosomes is undefined. As loss of CENP-A also causes the appearance of lagging chromosomes [308, 309], we asked whether loss of Cdk5rap2 alters CENP-A level. We examined

SaOS-2 cells depleted of Cdk5rap2 for levels of CENP-A protein and mRNA by immunoblot analysis and qRT-PCR, respectively. As shown in Figure 2, levels of CENP-A protein (Figure 20A) and mRNA (Figure 20B) were significantly reduced (p<0.01) in SaOS-2 cells depleted of Cdk5rap2 using two different siRNAs (#1 and #2) compared to corresponding cells transfected with control siRNA.

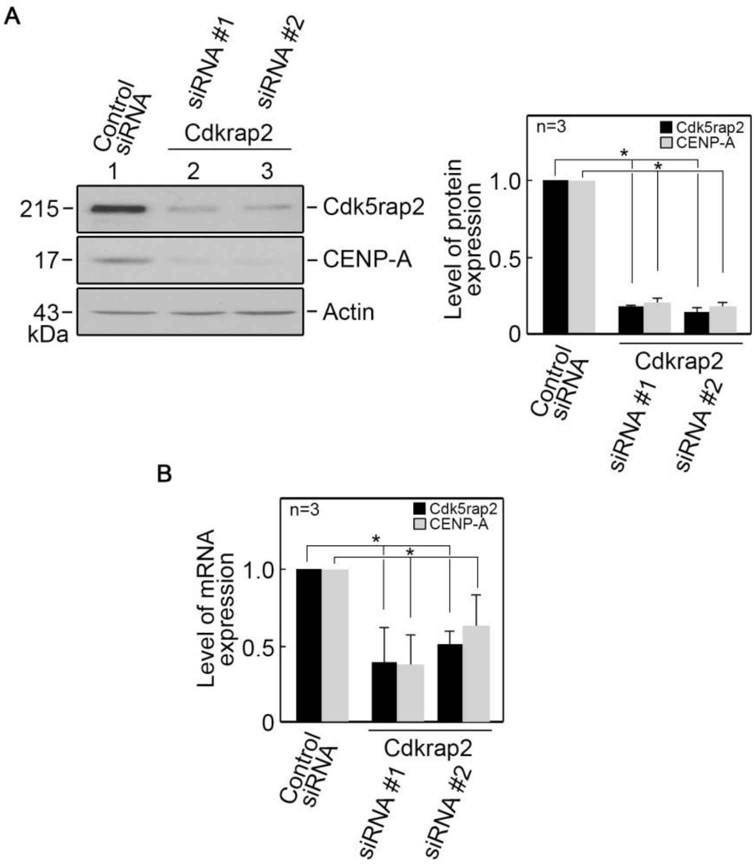

Figure 20. Loss of Cdk5rap2 results in reduced expression levels of CENP-A protein and mRNA.

(A) SaOS-2 cells seeded in 6 cm dishes were transfected with control or Cdk5rap2 siRNA (#1 or #2). After 48 hrs, cell lysates were subjected to SDS-PAGE and western blotting using Cdk5rap2 and CENP-A antibodies. Actin blot was used as loading control. Representative blots are from one of three independent experiments (n=3) showing similar result patterns. **(B)** Ratios of levels of Cdk5rap2 and CENP-A vs actin were calculated after densitometric analysis of blot images using NIH Image J 1.61. Levels of Cdk5rap2 and CENP-A mRNAs in transfected SaOS-2 cells were determined by qRT-PCR using isolated total RNA. **(C)** Ratios of levels of Cdk5rap2 and CENP-A vs GAPDH were calculated using the $2^{-\Delta\Delta CT}$ method. Protein and mRNA ratios obtained from cells transfected with control siRNA were normalized to 1.0. Ratios represent means ± SD of calculated ratios from three independent experiments (n=3). *p<0.01.

BJ-5ta human foreskin fibroblast cells depleted of Cdk5rap2 showed a similar decrease in levels of CENP-A protein (Figure 21 A) and mRNA (Figure 21 B).

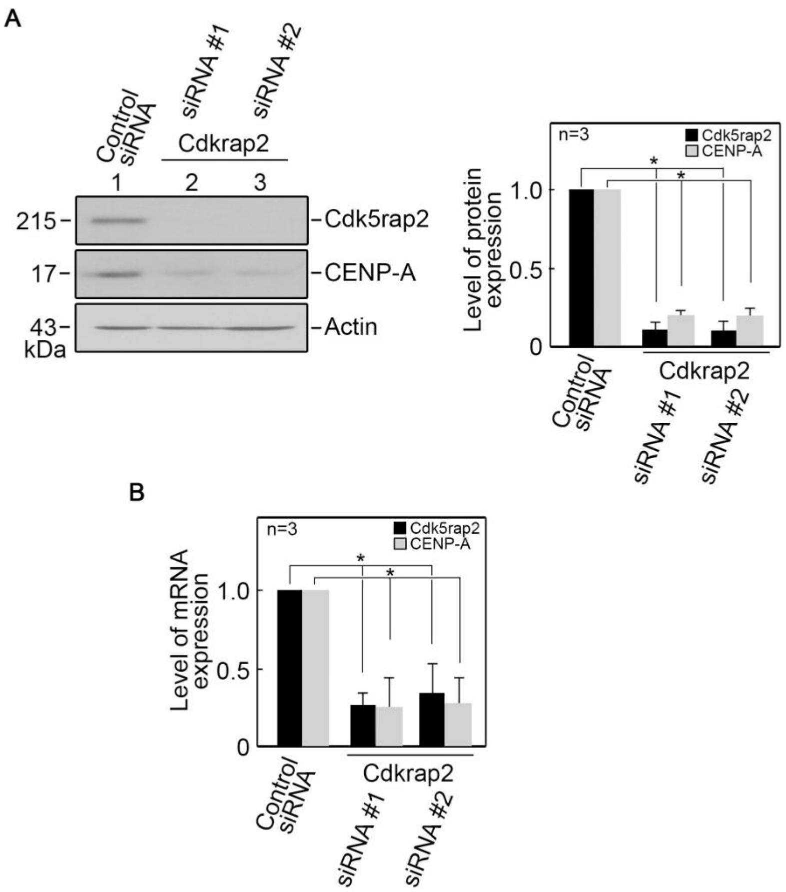

Figure 21. Loss of Cdk5rap2 results in reduced expression levels of CENP-A protein and mRNA in BJ-5ta cells.

(A) BJ-5ta cells seeded in 6 cm dishes were transfected with control or Cdk5rap2 siRNA (#1 or #2). After 48 hrs, cell lysates were subjected to SDS-PAGE and western blotting using Cdk5rap2 and

CENP-A antibodies. Actin blot was used as loading control. Representative blots shown are from one of three independent experiments (n=3) showing similar result patterns. **(B)** Ratios of levels of Cdk5rap2 and CENP-A vs actin were calculated after densitometric analysis of blot images using NIH Image J 1.61. Levels of Cdk5rap2 and CENP-A mRNAs were determined by qRT-PCR using total RNA isolated from transfected cells. **(C)** Ratios of levels of Cdk5rap2 and CENP-A vs GAPDH were calculated. Ratios obtained from cells transfected with control siRNA were normalized to 1.0. Ratios represent means ± SD of calculated ratios from three independent experiments (n=3). *p<0.001.

To substantiate the observed effect of Cdk5rap2 loss on CENP-A expression, we depleted endogenous Cdk5rap2 in SaOS-2 cells using Cdk5rap2 siRNA #1 then overexpressed exogenous Cdk5rap2 by transfection with an siRNA #1-resistant HA-tagged Cdk5rap2 construct [HA-Cdk5rap2(res)] in which the target recognition site of siRNA #1 is mutated. Figure 22A shows the Cdk5rap2 siRNA #1 target sequence, the corresponding endogenous Cdk5rap2 nucleotide and amino acid sequences, and the nucleotide substitutions in HA-Cdk5rap2(res) that do not alter the Cdk5rap2 amino acid sequence but confer resistance to Cdk5rap2 siRNA #1 [173]. As shown in Figure 22B, HA-Cdk5rap2(res) expression was not inhibited in the presence of Cdk5rap2 siRNA #1 (lane 3), indicating that HA-Cdk5rap2(res) was not targeted by the siRNA, which depleted endogenous Cdk5rap2 (lane 2). Our data also show that expression of exogenous Cdk5rap2 restored CENP-A expression, which was clearly reduced upon depletion of endogenous Cdk5rap2 (lane 2). Together, these findings indicate that Cdk5rap2 regulates CENP-A expression.

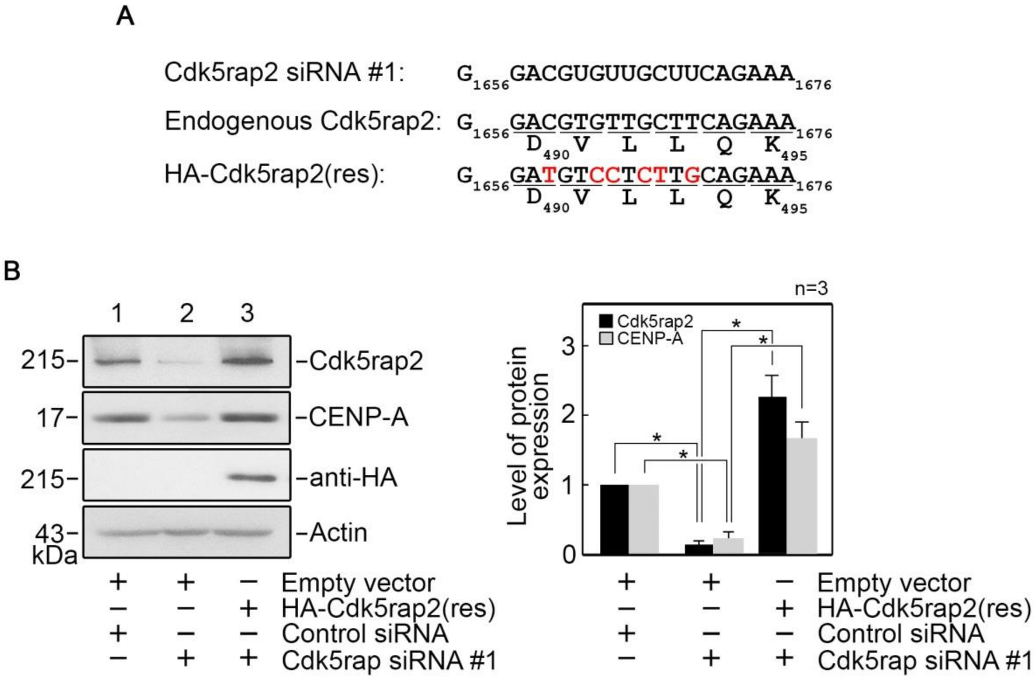

Figure 22. Expression of exogenous HA-Cdk5rap2(res) in cells depleted of endogenous Cdk5rap2 restores CENP-A expression.

(A) The Cdk5rap2 siRNA #1 target sequence, the corresponding endogenous Cdk5rap2 nucleotide (NM_018249.6) and amino acid (NP_060719) sequences, and the nucleotide substitutions in HA-Cdk5rap2(res) that do not alter the Cdk5rap2 amino acid sequence but confer resistance to Cdk5rap2 siRNA #1. **(B)** SaOS-2 cells seeded in 6 cm dishes were co-transfected with the indicated vector and siRNA. After 48 hrs, cell lysates were resolved by SDS-PAGE and immunoblotted for Cdk5rap2 and CENP-A. Actin blot was used as loading control. Blots shown represent results from one of three independent experiments (n=3) showing similar result patterns. Ratios of levels of Cdk5rap2 and CENP-A vs actin were determined after densitometric analysis of immunoblots. Ratios obtained from cells transfected with control siRNA were normalized to 1.0. Ratios represent means ± SD of calculated ratios from three independent experiments (n=3).

3.4.3 Cdk5rap2 is an upstream transcription regulator for *CENP-A*

We then asked whether Cdk5rap2 acts as a *CENP-A* transcription regulator. Cdk5rap2 has been shown to localize in the growing tips of microtubules and in centrosomes, particularly in the PCM [295, 314, 315], but its localization in the nucleus has not been demonstrated. Thus, we further examined SaOS-2 cells for the presence of Cdk5rap2 in the nucleus. By western blot analysis of subcellular fractions, we found that Cdk5rap2, indeed, localizes in the nucleus (Figure 23A).

To test whether Cdk5rap2 interacts with the upstream promoter region of *CENP-A*, we generated four different overlapping sets of primers that cover the +117 to -802 region of the putative *CENP-A* promoter (relative to the transcription start site identified in hg38_mane_ENST000 00335756.9 range=chr2:26785056-26794589, UCSC Genome Browser). We then performed ChIP analysis using a Cdk5rap2 antibody to immunoprecipitate Cdk5rap2-cross-linked chromatin fragments in SaOS-2 cells. ChIP-enriched DNA samples were subjected to PCR using the four different sets of primers to determine which set gives rise to a positive signal. As shown in Figure 23B, the primer set that covers the -330 to +4 region of the *CENP-A* promoter produced a positive 334 bp PCR product, suggesting that Cdk5rap2 binds to the -330 to +4 region of the *CENP-A* promoter. To further test whether the -330 to +4 region of the *CENP-A* promoter acts as a cis-element for Cdk5rap2 binding and subsequent transcriptional activation of *CENP-A*, we cloned this region of the *CENP-A* promoter into the pGL3 basic luciferase reporter vector, transfected it into HEK293 cells, and dual luciferase reporter assay was carried out. As shown in Figure 23C, depletion of endogenous Cdk5rap2 by siRNA #1 caused a 71% decrease (p=0.002) in *CENP-A* promoter activity while overexpression of exogenous HA-Cdk5rap2(res) caused an 89% increase (p=0.004) in *CENP-A* promoter activity. Taken together, these findings indicate that Cdk5rap2 acts as a transcriptional activator for *CENP-A*.

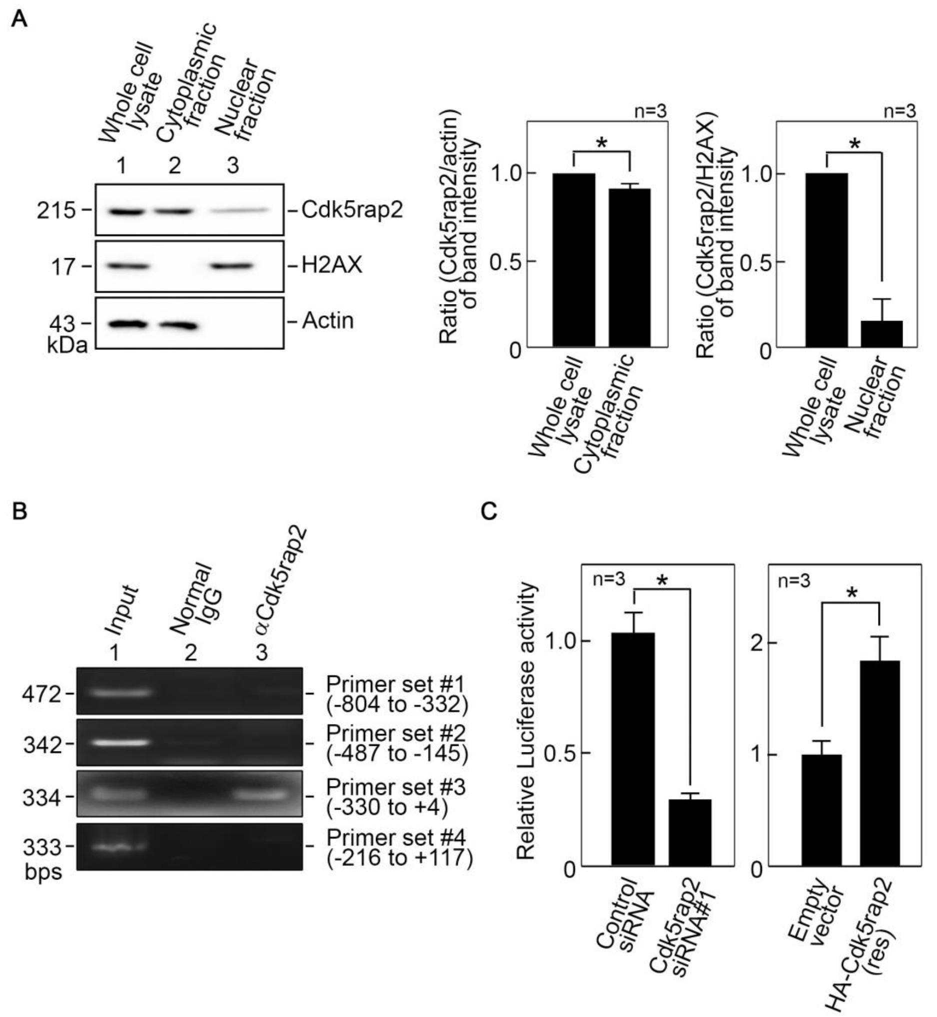

Figure 23. Cdk5rap2 localizes in the nucleus, interacts with the CENP-A promoter, and upregulates CENP-A transcription.

(A) Cdk5rap2 localizes in the nucleus. SaOS-2 cell lysates (lane 1) as well as cytoplasmic (lane 2) and nuclear (lane 3) fractions were resolved by SDS-PAGE and immunoblotted for Cdk5rap2 and histone H2AX, a nuclear marker, which also served as a loading control for the whole cell lysate and nuclear fraction. Actin was used as loading control also for the whole cell lysate and cytoplasmic fraction. The right panel shows the ratios of the levels of Cdk5rap2 vs actin or histone H2AX, which were determined after densitometric analysis of immunoblots. Ratios obtained from the whole cell lysates were normalized to 1.0. Ratios represent means ± SD of calculated ratios from three independent experiments (n=3). *p<0.05. **(B)** Cdk5rap2 binds to the -330~+4 region of the CENP-A promoter. ChIP analysis was performed as described in Materials and Methods. Normal IgG was used as negative control. The numbers for the 4 different overlapping promoter sets used indicate the positions of the N- and C-terminal forward and reverse promoters that were designed based on the CENP-A promoter region relative to its transcriptional start site. Data represent one of three independent experiments (n=3) showing similar results. **(C)** Cdk5rap2 depletion causes a decrease in CENP-A promoter activity while Cdk5rap2 overexpression causes an opposite effect. HEK293 cells transfected with pGL3 basic luciferase reporter vector containing the Cdk5rap2 promoter region (from -330 to +4) were depleted of Cdk5rap2 (left panel) or transfected with HA-tagged Cdk5rap2 (right panel). Luciferase assay was performed 48 hrs post-transfection. Values represent means ± SD from three separate experiments (n=3). Significance cut-off was set at p<0.05 for (A) and p<0.01 for (C).

To obtain a general idea on whether Cdk5rap2 regulates CENP-A expression through its N- or C-terminal region, we transfected HEK293 cells with full-length or N- or C-terminal regions (amino acid residues 1-994 and 991-1893, respectively) of Cdk5rap2. As expected, ectopic expression of Cdk5rap2 caused increased expression of CENP-A compared to cells transfected with an empty vector (Figure 24, left panel). However, ratios of CENP-A/Cdk5rap2 band intensities (Figure 24, right panel) were lower in cells overexpressing the N- or C-terminal regions of Cdk5rap2 compared to cells overexpressing full-length Cdk5rap2. These results indicate reduced CENP-A expression in the absence of either the Cdk5rap2 N- or C-terminal, and that each of these regions is important for Cdk5rap2-mediated CENP-A expression.

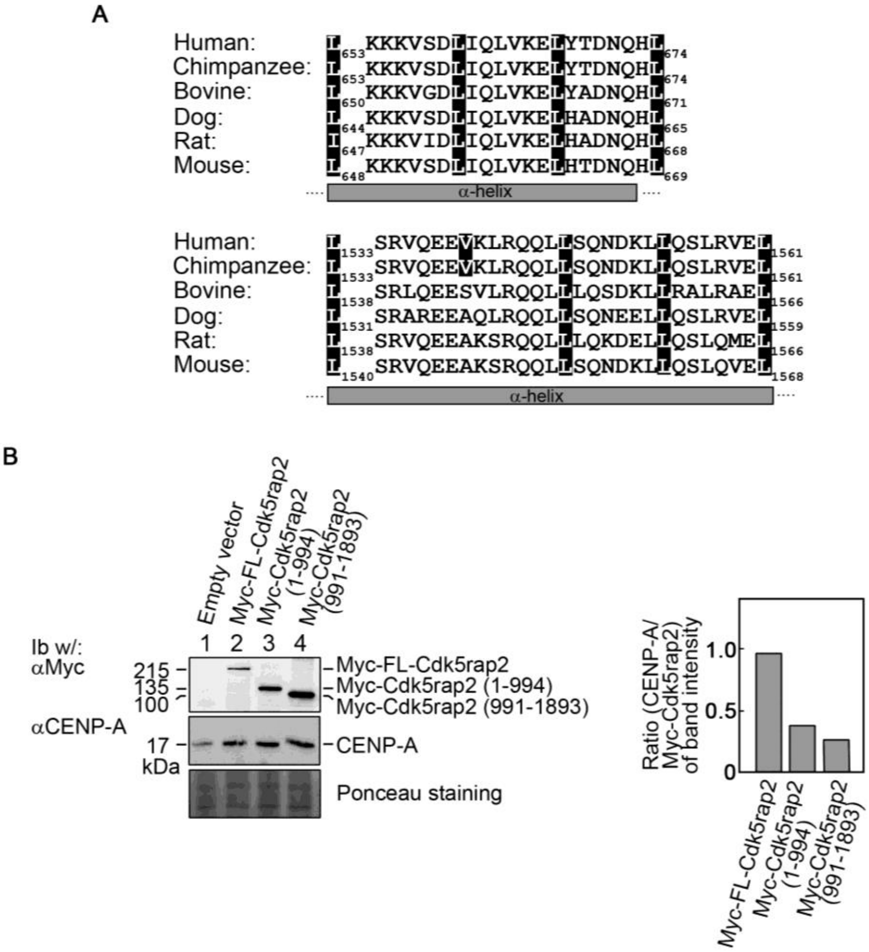

Figure 24. Both the N- and C-terminals in Cdk5rap2 contain sequences that are important for Cdk5rap2-mediated CENP-A expression.

(A) Sequence alignment of the Cdk5rap2 leucine zipper motifs in various species. The leucine residues in the leucine zipper motifs are highlighted in black for homology comparison. V, which has close structural similarity to L is highlighted as well. Basic amino acids (K, R and H) are shown in red. The grey boxes indicate α-helix motifs that contain the leucine zipper motifs. GenBank accession numbers are as follows: human, NP_060719; chimpanzee, NP_001035901; bovine, NP_001179098; dog, XP_855524; rat, NP_775157.2; mouse, NP_666102. **(B)** Lysates of HEK293 cells transfected with Myc-tagged full- length, N-terminal (amino acid residues 1-994) or C-terminal (amino acid residues 991-1893) Cdk5rap2, were resolved by 5-20% gradient SDS-PAGE and immunoblotted for Myc (upper panel) and CENP-A (middle panel). Representative blots from 3 independent experiments showing similar result patterns are shown. Data on the right represent ratios of CENP-A/Myc-tagged Cdk5rap2 band intensities based on densitometry analysis using the National Institutes of Health Image J 1.61 software. Values are means ± SD, n=3. *$p<0.05$.

3.4.4 Loss of Cdk5rap2 causes reduced enrichment of CENP-A and CENP-C at the centromere, and induces the formation of micronuclei and chromatin bridges

CENP-A in the centromeric chromatin recruits CENP-C via its C-terminal domain [250, 307], allowing centromere establishment and function. Therefore, we sought to determine whether loss of Cdk5rap2, which causes an overall decrease in cellular CENP-A level, results in reduced levels of both CENP-A and CENP-C at the centromeres. To do so, we performed ChIP using CENP-A or CENP-C antibody to immunoprecipitate CENP-A- and CENP-C-cross-linked centromere fragments, respectively, in SaOS-2 cells. The amount of captured centromere fragments, which reflects the levels of CENP-A and CENP-C at the centromere, were quantified by qPCR. As shown in Figure 25A, CENP-A enrichment at the centromere was reduced upon Cdk5rap2 depletion. Consequently, CENP-C enrichment at the centromere was also reduced albeit to a lesser extent (Figure 25A). CENP-A and CENP-C co-staining revealed that CENP-A foci, CENP-C foci as well as CENP-A/CENP-C co-localized foci were all less in Cdk5rap2 depleted cells (Figure 25B).

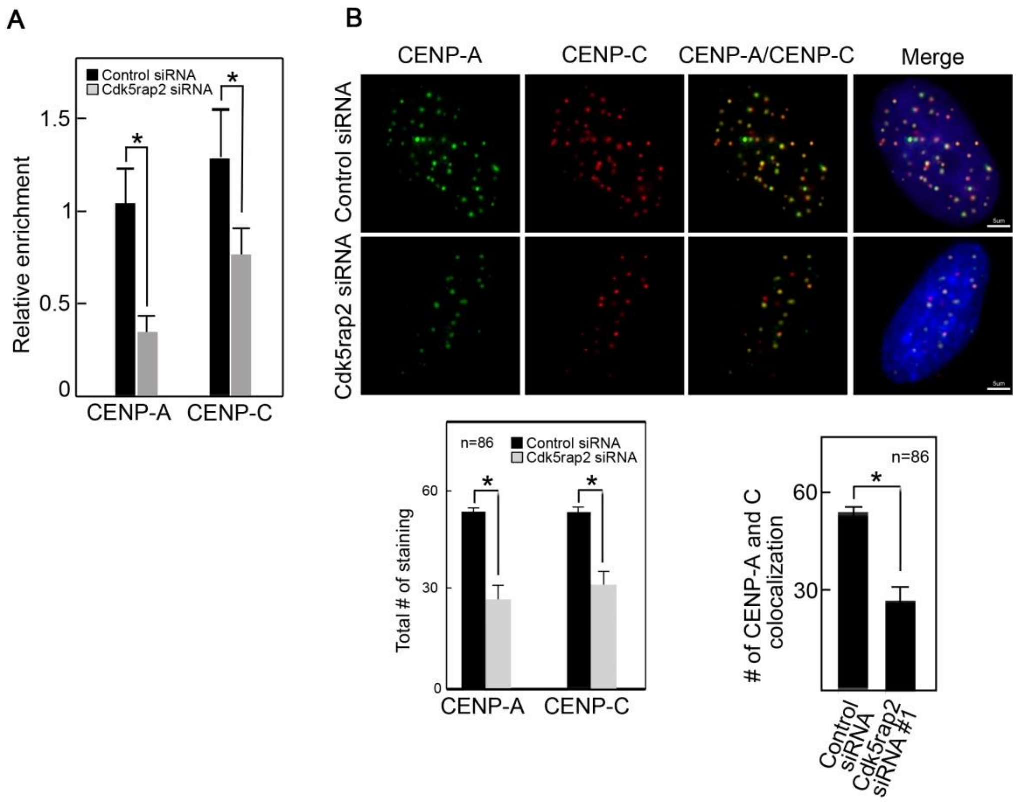

Figure 25. Loss of Cdk5rap2 causes reduced levels of CENP-A and CENP-C at the centromere.

(A) Lysates of SaOS-2 cells transfected with Cdk5rap2 or control siRNA were subjected to ChIP-qPCR as described in Materials and Methods. CENP-A- and CENP-C- cross-linked centromere fragments that were immunoprecipitated using CENP-A and CENP-C antibodies respectively, were analyzed by qPCR, which quantified level of centromere DNA fragments associated with CENP-A and CENP-C. Data represent means ± SD from three independent experiments (n=3). *p=0.0025 for CENP-A. **(B)** SaOS-2 cells transfected with Cdk5rap2 or control siRNA were subjected to immunofluorescence microscopy as described in Materials and Methods. The numbers of CENP-A and CENP-C staining foci and CENP-A/CENP-C co-localization foci in these cells (n=86 for each group) was counted. Data are presented as means ± SD. *p<0.05. Scale bar= 5 μm.

With our finding that Cdk5rap2 serves as a transcription factor for *CENP-A*, it is not surprising that loss of Cdk5rap2 leads to reduced expression of *CENP-A*. However, it is interesting that both CENP-A-deficient cells [308, 309] and Cdk5rap2-depleted cells [173] show defects in chromosome segregation, which were demonstrated by lagging chromosomes. We then sought to examine whether loss of Cdk5rap2 causes other aberrations related to chromosome mis-segregation. By DAPI staining, we found that SaOS-2 cells depleted of Cdk5rap2 have increased formation of micronuclei (Figure 26A) and chromatin bridges (Figure 26B), which are both known to arise from errors in chromosomes segregation. Altogether, our findings further indicate that loss of Cdk5rap2 also causes chromosomal instability**.**

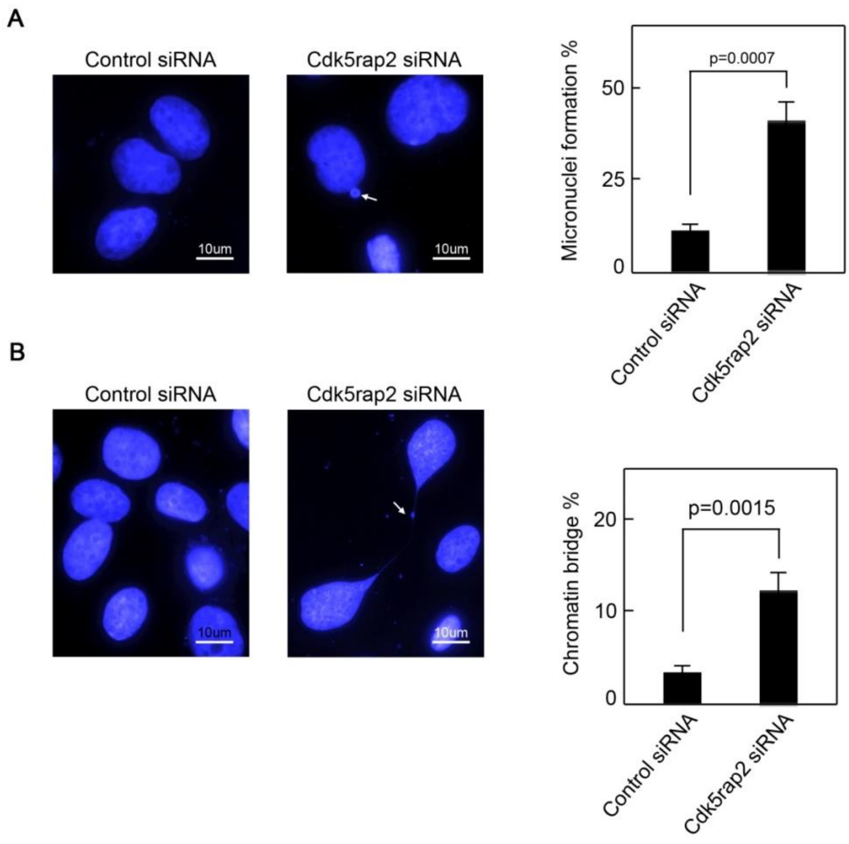

Figure 26. Depletion of Cdk5rap2 induces the formation of micronuclei and chromatin bridges.

(A and B) SaOS-2 cells transfected with control or Cdk5rap2 siRNA #1 were stained with DAPI 72 hrs post-transfection and subjected to microscopic examination. Representative images of transfected cells are shown with arrows directed at a micronucleus (A) and a chromatin bridge (B) in cells depleted of Cdk5rap2. The percentage of cells with micronuclei (B, right panel, n≥400) and chromatin bridges (C, right panel, n≥200) are shown. Data represent means ±SEM from three separate experiments (n=3). *p<0.001.

3.5 Discussion

Cdk5rap2 has been implicated in the regulation of meta-anaphase transition [173] but there is ambiguity on the mechanisms by which it is involved in this process. Here, we determined that as with HeLa cells deficient in Cdk5rap2 [173], SaOS-2 human osteosarcoma cells depleted of Cdk5rap2 exhibit lagging chromosomes. Such phenotype has been observed in cells depleted of CENP-A [308, 309], which acts as an epigenetic marker that defines the centromere. However, the molecular mechanism by which cellular CENP-A level is modulated remains unknown.

Previously, it was shown that loss of Cdk5rap2 corresponds to reduced expression of the spindle checkpoint proteins, BubR1 and Mad2, which act synergistically to inhibit the anaphase-promoting complex [317], and sequester Cdc20, causing an increase in chromatin-associated Cdc20 [173]. It was then found that Cdk5rap2 interacts with the *BubR1* and *Mad2* promoters and regulates their transcription [173]. Since we found that SaOS-2 and BJ-5ta cells depleted of Cdk5rap2 exhibit reduced expression of *CENP-A*, and ectopic expression of Cdk5rap2 in cells depleted of endogenous Cdk5rap2 reverses CENP-A level, we sought to examine the possibility that Cdk5rap2 also regulates the expression of *CENP-A*. Our finding that Cdk5rap2 is a nuclear protein is consistent with the presence of a bipartite nuclear localization-like motif [318] in Cdk5rap2 that is highly conserved among various species

(Supplementary Figure 2A).

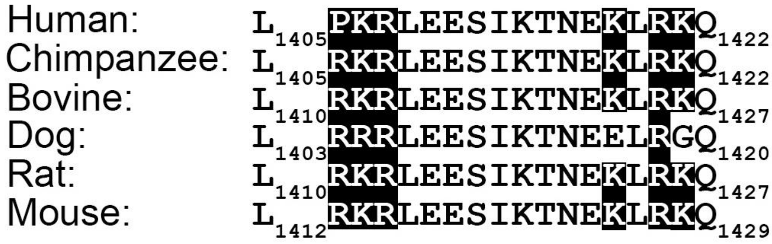

Figure 27. Cdk5rap2 has a highly conserved bipartite nuclear localization-like sequence.

Sequence alignment of the bipartite nuclear localization-like sequence in Cdk5rap2. The basic, functional, residues within this motif are highlighted in black for homology comparison. R, K and H residues were presumed to be functional basic residues. GenBank accession numbers are as follows: human, NP_060719; chimpanzee, NP_001035901; bovine, NP_001179098; dog, XP_855524; rat, NP_775157.2; mouse, NP_666102.

By ChIP and luciferase reporter assays, we provide the first evidence that Cdk5rap2 interacts with the *CENP-A* promoter and upregulates *CENP-A* transcription. By mapping of the Cdk5rap2 binding region in the *CENP-A* promoter, we determined that the length of this region is similar to those in *BuBR1* (345 bps) and *MAD2* (201 bps) promoters [173].

It appears that both the N- and C-terminal regions of Cdk5rap2 are required for complete Cdk5rap2-mediated CENP-A expression as we determined that CENP-A expression is lower in cells overexpressing the N- or C-terminal regions of Cdk5rap2 compared to cells overexpressing full-length Cdk5rap2. Interestingly, by primary sequence analysis of Cdk5rap2, we identified two potentially functional leucine zipper motifs that are highly conserved among various mammalian species (Supplementary Figure 2B). The first leucine zipper motif at the N-terminus consists of four leucine residues from L_{653} to L_{674}, and the second at the C-terminus also contains four leucine residues from L_{1533} to L_{1561} as well as V, which has close structural similarity to L, in human and chimpanzee. Both leucine zipper motifs reside within α-helices, and as with authentic leucine zipper motifs[319], could be involved in dimerization and DNA binding. It is possible that Cdk5rap2 interaction with the CENP-A promoter requires both L_{653}-L_{674} and L_{1533}-L_{1561} as the first leucine zipper motif in Cdk5rap2 is at the N-terminus and the second at the C-terminus, Together with our investigations on the involvement of the putative Cdk5rap2 bipartite nuclear localization motif in the nuclear localization of Cdk5rap2, we are also investigating the involvement of the Cdk5rap2 leucine zipper motifs in DNA binding and subsequent upregulation of CENP-A expression. While we identified a third potential leucine zipper motif from L_{787} to L_{809} (L_{787}LESRPDLLKVVRELLLGQLFL_{809}), we will not study the activity of this motif as the proline residue within the sequence causes a kink in the α-helix, which likely inhibits its functionality.

Upon depletion of Cdk5rap2, we observed reduced enrichment of centromeric CENP-A and CENP-C, which cooperate with each other to induce kinetochore assembly [250, 262]. CENP-A localizes in the centromere through its targeting domain. Centromeric CENP-A interacts with and recruits CENP-C to the centromere where CENP-C recruits kinetochores via its C-terminal domain [320]. CENP-C, which plays a major role in recruiting other centromeric proteins[250, 321], is also recruited by CENP-B to the centromere [322]. This may partly explain our observation that CENP-C level was not reduced as much as CENP-A in Cdk5rap2-depleted cells. Nonetheless, reduced recruitment of CENP-A and CENP-C at the centromere due to loss of Cdk5rap2 can impair centromere organization and function, compromising centromeric chromatin integrity. Thus, it is likely that loss of centromeric chromatin integrity led to the chromosomal instability as manifested by the increased occurrence of lagging chromosomes and the formation of micronuclei and chromatin bridges in Cdk5rap2 knockdown cells.

Our findings indicate that centromeric CENP-A-mediated functions are under the control of Cdk5rap2, and that Cdk5rap2 is critical for the maintenance of centromeric chromatin integrity. Interestingly, loss of function mutations in Cdk5rap2 are associated with primary microcephaly, a rare neurodevelopmental disorder that is characterized by reduced brain size and non-progressive mental retardation [161, 310]. The premise is that small brain size, particularly of the cerebral cortex, results from primary defects in neurogenic mitosis [164]. Since cells depleted of Cdk5rap2 show increased chromosomal instability, it is conceivable that reduced brain size in primary microcephaly results from increased neuronal progenitor cell death due to chromosomal instability.

Reference

1. Shay JW, Wright WE. Hayflick, his limit, and cellular ageing. *Nat Rev Mol Cell Biol.* 2000; 1(1): 72-76.
2. Carrel A, Ebeling AH. Age And Multiplication Of Fibroblasts. *J Exp Med.* 1921; 34(6): 599-623.
3. Hayflick L, Moorhead PS. The serial cultivation of human diploid cell strains. *Exp Cell Res.* 1961; 25: 585-621.
4. Hayflick L. The Limited In Vitro Lifetime Of Human Diploid Cell Strains. *Exp Cell Res.* 1965; 37: 614-636.
5. Ogrodnik M, Salmonowicz H, Jurk D, Passos JF. Expansion and Cell-Cycle Arrest: Common Denominators of Cellular Senescence. *Trends Biochem Sci.* 2019; 44(12): 996-1008.
6. Gorgoulis V, Adams PD, Alimonti A, Bennett DC, Bischof O, Bishop C, Campisi J, Collado M, Evangelou K, Ferbeyre G, Gil J, Hara E, Krizhanovsky V, Jurk D, Maier AB, Narita M, Niedernhofer L, Passos JF, Robbins PD, Schmitt CA, Sedivy J, Vougas K, von Zglinicki T, Zhou D, Serrano M, Demaria M. Cellular Senescence: Defining a Path Forward. *Cell.* 2019; 179(4): 813-827.
7. Burnet FM. Intrinsic mutagenesis: a genetic basis of ageing. *Pathology.* 1974; 6(1): 1-11.
8. Mensa E, Guescini M, Giuliani A, Bacalini MG, Ramini D, Corleone G, Ferracin M, Fulgenzi G, Graciotti L, Prattichizzo F, Sorci L, Battistelli M, Monsurro V, Bonfigli AR, Cardelli M, Recchioni R, Marcheselli F, Latini S, Maggio S, Fanelli M, Amatori

S, Storci G, Ceriello A, Stocchi V, De Luca M, Magnani L, Rippo MR, Procopio AD, Sala C, Budimir I, Bassi C, Negrini M, Garagnani P, Franceschi C, Sabbatinelli J, Bonafe M, Olivieri F. Small extracellular vesicles deliver miR-21 and miR-217 as pro-senescence effectors to endothelial cells. *J Extracell Vesicles.* 2020; 9(1): 1725285.

9. Basatemur GL, Jorgensen HF, Clarke MCH, Bennett MR, Mallat Z. Vascular smooth muscle cells in atherosclerosis. *Nat Rev Cardiol.* 2019; 16(12): 727-744.

10. Kang D, Shin J, Cho Y, Kim HS, Gu YR, Kim H, You KT, Chang MJ, Chang CB, Kang SB, Kim JS, Kim VN, Kim JH. Stress-activated miR-204 governs senescent phenotypes of chondrocytes to promote osteoarthritis development. *Sci Transl Med.* 2019; 11(486).

11. Martin N, Salazar-Cardozo C, Vercamer C, Ott L, Marot G, Slijepcevic P, Abbadie C, Pluquet O. Identification of a gene signature of a pre-transformation process by senescence evasion in normal human epidermal keratinocytes. *Mol Cancer.* 2014; 13: 151.

12. Lopez-Otin C, Blasco MA, Partridge L, Serrano M, Kroemer G. The hallmarks of aging. *Cell.* 2013; 153(6): 1194-1217.

13. Bellei B, Picardo M. Premature cell senescence in human skin: Dual face in chronic acquired pigmentary disorders. *Ageing Res Rev.* 2020; 57: 100981.

14. Campisi J. Senescent cells, tumor suppression, and organismal aging: good citizens, bad neighbors. *Cell.* 2005; 120(4): 513-522.

15. Campisi J. Cellular senescence as a tumor-suppressor mechanism. *Trends Cell Biol.*

2001; 11(11): S27-31.

16. Coppe JP, Desprez PY, Krtolica A, Campisi J. The senescence-associated secretory phenotype: the dark side of tumor suppression. *Annu Rev Pathol.* 2010; 5: 99-118.

17. Mosteiro L, Pantoja C, Alcazar N, Marion RM, Chondronasiou D, Rovira M, Fernandez-Marcos PJ, Munoz-Martin M, Blanco-Aparicio C, Pastor J, Gomez-Lopez G, De Martino A, Blasco MA, Abad M, Serrano M. Tissue damage and senescence provide critical signals for cellular reprogramming in vivo. *Science.* 2016; 354(6315).

18. Calcinotto A, Kohli J, Zagato E, Pellegrini L, Demaria M, Alimonti A. Cellular Senescence: Aging, Cancer, and Injury. *Physiol Rev.* 2019; 99(2): 1047-1078.

19. Kurppa KJ, Liu Y, To C, Zhang T, Fan M, Vajdi A, Knelson EH, Xie Y, Lim K, Cejas P, Portell A, Lizotte PH, Ficarro SB, Li S, Chen T, Haikala HM, Wang H, Bahcall M, Gao Y, Shalhout S, Boettcher S, Shin BH, Thai T, Wilkens MK, Tillgren ML, Mushajiang M, Xu M, Choi J, Bertram AA, Ebert BL, Beroukhim R, Bandopadhayay P, Awad MM, Gokhale PC, Kirschmeier PT, Marto JA, Camargo FD, Haq R, Paweletz CP, Wong KK, Barbie DA, Long HW, Gray NS, Janne PA. Treatment-Induced Tumor Dormancy through YAP-Mediated Transcriptional Reprogramming of the Apoptotic Pathway. *Cancer Cell.* 2020; 37(1): 104-122 e112.

20. Rajarajacholan UK, Riabowol K. Aging with ING: a comparative study of different forms of stress induced premature senescence. *Oncotarget.* 2015; 6(33): 34118-34127.

21. Parry AJ, Hoare M, Bihary D, Hansel-Hertsch R, Smith S, Tomimatsu K, Mannion E, Smith A, D'Santos P, Russell IA, Balasubramanian S, Kimura H, Samarajiwa SA, Narita M. NOTCH-mediated non-cell autonomous regulation of chromatin structure

during senescence. *Nat Commun.* 2018; 9(1): 1840.

22. Zhang Y, Zhang Y, Xiao Y, Zhong C, Xiao F. Expression of Clusterin suppresses Cr(VI)-induced premature senescence through activation of PI3K/AKT pathway. *Ecotoxicol Environ Saf.* 2019; 183: 109465.

23. Freund A, Orjalo AV, Desprez PY, Campisi J. Inflammatory networks during cellular senescence: causes and consequences. *Trends Mol Med.* 2010; 16(5): 238-246.

24. Terzi MY, Izmirli M, Gogebakan B. The cell fate: senescence or quiescence. *Mol Biol Rep.* 2016; 43(11): 1213-1220.

25. Kagawa S, Natsuizaka M, Whelan KA, Facompre N, Naganuma S, Ohashi S, Kinugasa H, Egloff AM, Basu D, Gimotty PA, Klein-Szanto AJ, Bass AJ, Wong KK, Diehl JA, Rustgi AK, Nakagawa H. Cellular senescence checkpoint function determines differential Notch1-dependent oncogenic and tumor-suppressor activities. *Oncogene.* 2015; 34(18): 2347-2359.

26. Nyunoya T, Monick MM, Klingelhutz A, Yarovinsky TO, Cagley JR, Hunninghake GW. Cigarette smoke induces cellular senescence. *Am J Respir Cell Mol Biol.* 2006; 35(6): 681-688.

27. Serrano M, Lin AW, McCurrach ME, Beach D, Lowe SW. Oncogenic ras provokes premature cell senescence associated with accumulation of p53 and p16INK4a. *Cell.* 1997; 88(5): 593-602.

28. Chen Q, Ames BN. Senescence-like growth arrest induced by hydrogen peroxide in human diploid fibroblast F65 cells. *Proc Natl Acad Sci U S A.* 1994; 91(10): 4130-4134.

29. Chan HM, Narita M, Lowe SW, Livingston DM. The p400 E1A-associated protein is a novel component of the p53 --> p21 senescence pathway. *Genes Dev.* 2005; 19(2): 196-201.

30. Michaloglou C, Vredeveld LC, Soengas MS, Denoyelle C, Kuilman T, van der Horst CM, Majoor DM, Shay JW, Mooi WJ, Peeper DS. BRAFE600-associated senescence-like cell cycle arrest of human naevi. *Nature.* 2005; 436(7051): 720-724.

31. Passos JF, Saretzki G, von Zglinicki T. DNA damage in telomeres and mitochondria during cellular senescence: is there a connection? *Nucleic Acids Res.* 2007; 35(22): 7505-7513.

32. Haronikova L, Olivares-Illana V, Wang L, Karakostis K, Chen S, Fahraeus R. The p53 mRNA: an integral part of the cellular stress response. *Nucleic Acids Res.* 2019; 47(7): 3257-3271.

33. Xing R, Li W, Cui J, Zhang J, Kang B, Wang Y, Wang Z, Liu S, Lu Y. Gastrokine 1 induces senescence through p16/Rb pathway activation in gastric cancer cells. *Gut.* 2012; 61(1): 43-52.

34. Douarre C, Mergui X, Sidibe A, Gomez D, Alberti P, Mailliet P, Trentesaux C, Riou JF. DNA damage signaling induced by the G-quadruplex ligand 12459 is modulated by PPM1D/WIP1 phosphatase. *Nucleic Acids Res.* 2013; 41(6): 3588-3599.

35. Kruger A, Stier A, Fischbach A, Burkle A, Hauser K, Mangerich A. Interactions of p53 with poly(ADP-ribose) and DNA induce distinct changes in protein structure as revealed by ATR-FTIR spectroscopy. *Nucleic Acids Res.* 2019; 47(9): 4843-4858.

36. Lossaint G, Besnard E, Fisher D, Piette J, Dulic V. Chk1 is dispensable for G2 arrest

in response to sustained DNA damage when the ATM/p53/p21 pathway is functional. *Oncogene.* 2011; 30(41): 4261-4274.

37. Engeland K. Cell cycle arrest through indirect transcriptional repression by p53: I have a DREAM. *Cell Death Differ.* 2018; 25(1): 114-132.

38. Baker DJ, Wijshake T, Tchkonia T, LeBrasseur NK, Childs BG, van de Sluis B, Kirkland JL, van Deursen JM. Clearance of p16Ink4a-positive senescent cells delays ageing-associated disorders. *Nature.* 2011; 479(7372): 232-236.

39. Xu Y, Li N, Xiang R, Sun P. Emerging roles of the p38 MAPK and PI3K/AKT/mTOR pathways in oncogene-induced senescence. *Trends Biochem Sci.* 2014; 39(6): 268-276.

40. Wong ES, Le Guezennec X, Demidov ON, Marshall NT, Wang ST, Krishnamurthy J, Sharpless NE, Dunn NR, Bulavin DV. p38MAPK controls expression of multiple cell cycle inhibitors and islet proliferation with advancing age. *Dev Cell.* 2009; 17(1): 142-149.

41. Canepa ET, Scassa ME, Ceruti JM, Marazita MC, Carcagno AL, Sirkin PF, Ogara MF. INK4 proteins, a family of mammalian CDK inhibitors with novel biological functions. *IUBMB Life.* 2007; 59(7): 419-426.

42. Lukas J, Parry D, Aagaard L, Mann DJ, Bartkova J, Strauss M, Peters G, Bartek J. Retinoblastoma-protein-dependent cell-cycle inhibition by the tumour suppressor p16. *Nature.* 1995; 375(6531): 503-506.

43. Schafer MJ, White TA, Iijima K, Haak AJ, Ligresti G, Atkinson EJ, Oberg AL, Birch J, Salmonowicz H, Zhu Y, Mazula DL, Brooks RW, Fuhrmann-Stroissnigg H,

Pirtskhalava T, Prakash YS, Tchkonia T, Robbins PD, Aubry MC, Passos JF, Kirkland JL, Tschumperlin DJ, Kita H, LeBrasseur NK. Cellular senescence mediates fibrotic pulmonary disease. *Nat Commun.* 2017; 8: 14532.

44. Narita M, Nunez S, Heard E, Narita M, Lin AW, Hearn SA, Spector DL, Hannon GJ, Lowe SW. Rb-mediated heterochromatin formation and silencing of E2F target genes during cellular senescence. *Cell.* 2003; 113(6): 703-716.

45. Jin B, Wang Y, Wu CL, Liu KY, Chen H, Mao ZB. PIM-1 modulates cellular senescence and links IL-6 signaling to heterochromatin formation. *Aging Cell.* 2014; 13(5): 879-889.

46. Park JW, Kim JJ, Bae YS. CK2 downregulation induces senescence-associated heterochromatic foci formation through activating SUV39h1 and inactivating G9a. *Biochem Biophys Res Commun.* 2018; 505(1): 67-73.

47. Kuilman T, Michaloglou C, Mooi WJ, Peeper DS. The essence of senescence. *Genes Dev.* 2010; 24(22): 2463-2479.

48. Kosar M, Bartkova J, Hubackova S, Hodny Z, Lukas J, Bartek J. Senescence-associated heterochromatin foci are dispensable for cellular senescence, occur in a cell type- and insult-dependent manner and follow expression of p16(ink4a). *Cell Cycle.* 2011; 10(3): 457-468.

49. Zhang P, Kishimoto Y, Grammatikakis I, Gottimukkala K, Cutler RG, Zhang S, Abdelmohsen K, Bohr VA, Misra Sen J, Gorospe M, Mattson MP. Senolytic therapy alleviates Abeta-associated oligodendrocyte progenitor cell senescence and cognitive deficits in an Alzheimer's disease model. *Nat Neurosci.* 2019; 22(5): 719-728.

50. Dimri GP, Lee X, Basile G, Acosta M, Scott G, Roskelley C, Medrano EE, Linskens M, Rubelj I, Pereira-Smith O, et al. A biomarker that identifies senescent human cells in culture and in aging skin in vivo. *Proc Natl Acad Sci U S A.* 1995; 92(20): 9363-9367.

51. Debacq-Chainiaux F, Erusalimsky JD, Campisi J, Toussaint O. Protocols to detect senescence-associated beta-galactosidase (SA-betagal) activity, a biomarker of senescent cells in culture and in vivo. *Nat Protoc.* 2009; 4(12): 1798-1806.

52. Lee BY, Han JA, Im JS, Morrone A, Johung K, Goodwin EC, Kleijer WJ, DiMaio D, Hwang ES. Senescence-associated beta-galactosidase is lysosomal beta-galactosidase. *Aging Cell.* 2006; 5(2): 187-195.

53. Salazar G, Cullen A, Huang J, Zhao Y, Serino A, Hilenski L, Patrushev N, Forouzandeh F, Hwang HS. SQSTM1/p62 and PPARGC1A/PGC-1alpha at the interface of autophagy and vascular senescence. *Autophagy.* 2019: 1-19.

54. Pantsulaia I, Ciszewski WM, Niewiarowska J. Senescent endothelial cells: Potential modulators of immunosenescence and ageing. *Ageing Res Rev.* 2016; 29: 13-25.

55. Hekmatimoghaddam S, Dehghani Firoozabadi A, Zare-Khormizi MR, Pourrajab F. Sirt1 and Parp1 as epigenome safeguards and microRNAs as SASP-associated signals, in cellular senescence and aging. *Ageing Res Rev.* 2017; 40: 120-141.

56. Kuilman T, Michaloglou C, Vredeveld LC, Douma S, van Doorn R, Desmet CJ, Aarden LA, Mooi WJ, Peeper DS. Oncogene-induced senescence relayed by an interleukin-dependent inflammatory network. *Cell.* 2008; 133(6): 1019-1031.

57. Soejima A, Nakabayasi K, Kitamoto K, Nagasawa T, Matsumoto K, Kozaki M. [IgA

nephropathy in a patient with ulcerative colitis]. *Nihon Naika Gakkai Zasshi.* 1988; 77(5): 685-689.

58. van Deursen JM. The role of senescent cells in ageing. *Nature.* 2014; 509(7501): 439-446.

59. Rodier F, Coppe JP, Patil CK, Hoeijmakers WA, Munoz DP, Raza SR, Freund A, Campeau E, Davalos AR, Campisi J. Persistent DNA damage signalling triggers senescence-associated inflammatory cytokine secretion. *Nat Cell Biol.* 2009; 11(8): 973-979.

60. Mrazkova B, Dzijak R, Imrichova T, Kyjacova L, Barath P, Dzubak P, Holub D, Hajduch M, Nahacka Z, Andera L, Holicek P, Vasicova P, Sapega O, Bartek J, Hodny Z. Induction, regulation and roles of neural adhesion molecule L1CAM in cellular senescence. *Aging (Albany NY).* 2018; 10(3): 434-462.

61. Acosta JC, Banito A, Wuestefeld T, Georgilis A, Janich P, Morton JP, Athineos D, Kang TW, Lasitschka F, Andrulis M, Pascual G, Morris KJ, Khan S, Jin H, Dharmalingam G, Snijders AP, Carroll T, Capper D, Pritchard C, Inman GJ, Longerich T, Sansom OJ, Benitah SA, Zender L, Gil J. A complex secretory program orchestrated by the inflammasome controls paracrine senescence. *Nat Cell Biol.* 2013; 15(8): 978-990.

62. Ito Y, Hoare M, Narita M. Spatial and Temporal Control of Senescence. *Trends Cell Biol.* 2017; 27(11): 820-832.

63. Leonard JP, LaCasce AS, Smith MR, Noy A, Chirieac LR, Rodig SJ, Yu JQ, Vallabhajosula S, Schoder H, English P, Neuberg DS, Martin P, Millenson MM, Ely

SA, Courtney R, Shaik N, Wilner KD, Randolph S, Van den Abbeele AD, Chen-Kiang SY, Yap JT, Shapiro GI. Selective CDK4/6 inhibition with tumor responses by PD0332991 in patients with mantle cell lymphoma. *Blood.* 2012; 119(20): 4597-4607.

64. Vizioli MG, Adams PD. Senescence Can Be BETter without the SASP? *Cancer Discov.* 2016; 6(6): 576-578.

65. Ritschka B, Storer M, Mas A, Heinzmann F, Ortells MC, Morton JP, Sansom OJ, Zender L, Keyes WM. The senescence-associated secretory phenotype induces cellular plasticity and tissue regeneration. *Genes Dev.* 2017; 31(2): 172-183.

66. Wong H, Riabowol K. Differential CDK-inhibitor gene expression in aging human diploid fibroblasts. *Exp Gerontol.* 1996; 31(1-2): 311-325.

67. Wang Y, Lim R, Nie G. Elevated circulating HtrA4 in preeclampsia may alter endothelial expression of senescence genes. *Placenta.* 2020; 90: 71-81.

68. Purcell M, Kruger A, Tainsky MA. Gene expression profiling of replicative and induced senescence. *Cell Cycle.* 2014; 13(24): 3927-3937.

69. Wang G, Huang Y, Yang F, Tian X, Wang K, Liu L, Fan Y, Li X, Li L, Shi B, Hao Y, Xia C, Nie Q, Xin Y, Shi Z, Ma L, Xu D, Liu C. High expression of SMYD3 indicates poor survival outcome and promotes tumour progression through an IGF-1R/AKT/E2F-1 positive feedback loop in bladder cancer. *Aging (Albany NY).* 2020; 12(3): 2030-2048.

70. Lessard F, Igelmann S, Trahan C, Huot G, Saint-Germain E, Mignacca L, Del Toro N, Lopes-Paciencia S, Le Calve B, Montero M, Deschenes-Simard X, Bury M, Moiseeva O, Rowell MC, Zorca CE, Zenklusen D, Brakier-Gingras L, Bourdeau V, Oeffinger M,

Ferbeyre G. Senescence-associated ribosome biogenesis defects contributes to cell cycle arrest through the Rb pathway. *Nat Cell Biol.* 2018; 20(7): 789-799.

71. Rodier F, Campisi J. Four faces of cellular senescence. *J Cell Biol.* 2011; 192(4): 547-556.

72. Atadja P, Wong H, Garkavtsev I, Veillette C, Riabowol K. Increased activity of p53 in senescing fibroblasts. *Proc Natl Acad Sci U S A.* 1995; 92(18): 8348-8352.

73. Venkatachalam G, Surana U, Clement MV. Replication stress-induced endogenous DNA damage drives cellular senescence induced by a sub-lethal oxidative stress. *Nucleic Acids Res.* 2017; 45(18): 10564-10582.

74. Rodier F, Munoz DP, Teachenor R, Chu V, Le O, Bhaumik D, Coppe JP, Campeau E, Beausejour CM, Kim SH, Davalos AR, Campisi J. DNA-SCARS: distinct nuclear structures that sustain damage-induced senescence growth arrest and inflammatory cytokine secretion. *J Cell Sci.* 2011; 124(Pt 1): 68-81.

75. Waldera Lupa DM, Kalfalah F, Safferling K, Boukamp P, Poschmann G, Volpi E, Gotz-Rosch C, Bernerd F, Haag L, Huebenthal U, Fritsche E, Boege F, Grabe N, Tigges J, Stuhler K, Krutmann J. Characterization of Skin Aging-Associated Secreted Proteins (SAASP) Produced by Dermal Fibroblasts Isolated from Intrinsically Aged Human Skin. *J Invest Dermatol.* 2015; 135(8): 1954-1968.

76. d'Adda di Fagagna F, Reaper PM, Clay-Farrace L, Fiegler H, Carr P, Von Zglinicki T, Saretzki G, Carter NP, Jackson SP. A DNA damage checkpoint response in telomere-initiated senescence. *Nature.* 2003; 426(6963): 194-198.

77. Maehara K, Takahashi K, Saitoh S. CENP-A reduction induces a p53-dependent

cellular senescence response to protect cells from executing defective mitoses. *Mol Cell Biol.* 2010; 30(9): 2090-2104.

78. Kong X, Feng D, Wang H, Hong F, Bertola A, Wang FS, Gao B. Interleukin-22 induces hepatic stellate cell senescence and restricts liver fibrosis in mice. *Hepatology.* 2012; 56(3): 1150-1159.

79. Rufini A, Tucci P, Celardo I, Melino G. Senescence and aging: the critical roles of p53. *Oncogene.* 2013; 32(43): 5129-5143.

80. Tavana O, Benjamin CL, Puebla-Osorio N, Sang M, Ullrich SE, Ananthaswamy HN, Zhu C. Absence of p53-dependent apoptosis leads to UV radiation hypersensitivity, enhanced immunosuppression and cellular senescence. *Cell Cycle.* 2010; 9(16): 3328-3336.

81. Yosef R, Pilpel N, Tokarsky-Amiel R, Biran A, Ovadya Y, Cohen S, Vadai E, Dassa L, Shahar E, Condiotti R, Ben-Porath I, Krizhanovsky V. Directed elimination of senescent cells by inhibition of BCL-W and BCL-XL. *Nat Commun.* 2016; 7: 11190.

82. Li T, Kon N, Jiang L, Tan M, Ludwig T, Zhao Y, Baer R, Gu W. Tumor suppression in the absence of p53-mediated cell-cycle arrest, apoptosis, and senescence. *Cell.* 2012; 149(6): 1269-1283.

83. Tang JJ, Shen C, Lu YJ. Requirement for pre-existing of p21 to prevent doxorubicin-induced apoptosis through inhibition of caspase-3 activation. *Mol Cell Biochem.* 2006; 291(1-2): 139-144.

84. Zhang Y, Gao Y, Zhang G, Huang S, Dong Z, Kong C, Su D, Du J, Zhu S, Liang Q, Zhang J, Lu J, Huang B. DNMT3a plays a role in switches between

doxorubicin-induced senescence and apoptosis of colorectal cancer cells. *Int J Cancer.* 2011; 128(3): 551-561.

85. Munoz-Espin D, Serrano M. Cellular senescence: from physiology to pathology. *Nat Rev Mol Cell Biol.* 2014; 15(7): 482-496.

86. Van Ly D, Low RRJ, Frolich S, Bartolec TK, Kafer GR, Pickett HA, Gaus K, Cesare AJ. Telomere Loop Dynamics in Chromosome End Protection. *Mol Cell.* 2018; 71(4): 510-525 e516.

87. Blackburn EH, Epel ES, Lin J. Human telomere biology: A contributory and interactive factor in aging, disease risks, and protection. *Science.* 2015; 350(6265): 1193-1198.

88. Victorelli S, Passos JF. Telomeres and Cell Senescence - Size Matters Not. *EBioMedicine.* 2017; 21: 14-20.

89. Harley CB, Futcher AB, Greider CW. Telomeres shorten during ageing of human fibroblasts. *Nature.* 1990; 345(6274): 458-460.

90. d'Adda di Fagagna F. Living on a break: cellular senescence as a DNA-damage response. *Nat Rev Cancer.* 2008; 8(7): 512-522.

91. Zole E, Ranka R. Mitochondria, its DNA and telomeres in ageing and human population. *Biogerontology.* 2018; 19(3-4): 189-208.

92. Liu J, Wang L, Wang Z, Liu JP. Roles of Telomere Biology in Cell Senescence, Replicative and Chronological Ageing. *Cells.* 2019; 8(1).

93. Richter T, von Zglinicki T. A continuous correlation between oxidative stress and telomere shortening in fibroblasts. *Exp Gerontol.* 2007; 42(11): 1039-1042.

94. Blackford AN, Jackson SP. ATM, ATR, and DNA-PK: The Trinity at the Heart of the DNA Damage Response. *Mol Cell.* 2017; 66(6): 801-817.

95. Shay JW, Wright WE. Telomeres and telomerase: three decades of progress. *Nat Rev Genet.* 2019; 20(5): 299-309.

96. Suen H, Brown R, Yang S, Weatherburn C, Ho PJ, Woodland N, Nassif N, Barbaro P, Bryant C, Hart D, Gibson J, Joshua D. Multiple myeloma causes clonal T-cell immunosenescence: identification of potential novel targets for promoting tumour immunity and implications for checkpoint blockade. *Leukemia.* 2016; 30(8): 1716-1724.

97. Brazvan B, Ebrahimi-Kalan A, Velaei K, Mehdipour A, Aliyari Serej Z, Ebrahimi A, Ghorbani M, Cheraghi O, Nozad Charoudeh H. Telomerase activity and telomere on stem progeny senescence. *Biomed Pharmacother.* 2018; 102: 9-17.

98. Liu L. Linking Telomere Regulation to Stem Cell Pluripotency. *Trends Genet.* 2017; 33(1): 16-33.

99. Nault JC, Ningarhari M, Rebouissou S, Zucman-Rossi J. The role of telomeres and telomerase in cirrhosis and liver cancer. *Nat Rev Gastroenterol Hepatol.* 2019; 16(9): 544-558.

100. Le TYL, Pickett HA, Yang A, Ho JWK, Thavapalachandran S, Igoor S, Yang SF, Farraha M, Voges HK, Hudson JE, Dos Remedios CG, Bryan TM, Kizana E, Chong JJH. Enhanced cardiac repair by telomerase reverse transcriptase over-expression in human cardiac mesenchymal stromal cells. *Sci Rep.* 2019; 9(1): 10579.

101. Ivanyi-Nagy R, Ahmed SM, Peter S, Ramani PD, Ong PF, Dreesen O, Droge P. The

RNA interactome of human telomerase RNA reveals a coding-independent role for a histone mRNA in telomere homeostasis. *Elife.* 2018; 7.

102. Gil J, Peters G. Regulation of the INK4b-ARF-INK4a tumour suppressor locus: all for one or one for all. *Nat Rev Mol Cell Biol.* 2006; 7(9): 667-677.

103. Kim WY, Sharpless NE. The regulation of INK4/ARF in cancer and aging. *Cell.* 2006; 127(2): 265-275.

104. Osanai M, Murata M, Nishikiori N, Chiba H, Kojima T, Sawada N. Occludin-mediated premature senescence is a fail-safe mechanism against tumorigenesis in breast carcinoma cells. *Cancer Sci.* 2007; 98(7): 1027-1034.

105. Coppe JP, Patil CK, Rodier F, Sun Y, Munoz DP, Goldstein J, Nelson PS, Desprez PY, Campisi J. Senescence-associated secretory phenotypes reveal cell-nonautonomous functions of oncogenic RAS and the p53 tumor suppressor. *PLoS Biol.* 2008; 6(12): 2853-2868.

106. Gorgoulis VG, Halazonetis TD. Oncogene-induced senescence: the bright and dark side of the response. *Curr Opin Cell Biol.* 2010; 22(6): 816-827.

107. Di Micco R, Fumagalli M, Cicalese A, Piccinin S, Gasparini P, Luise C, Schurra C, Garre M, Nuciforo PG, Bensimon A, Maestro R, Pelicci PG, d'Adda di Fagagna F. Oncogene-induced senescence is a DNA damage response triggered by DNA hyper-replication. *Nature.* 2006; 444(7119): 638-642.

108. Ou HL, Schumacher B. DNA damage responses and p53 in the aging process. *Blood.* 2018; 131(5): 488-495.

109. Wei S, Wei S, Sedivy JM. Expression of catalytically active telomerase does not

prevent premature senescence caused by overexpression of oncogenic Ha-Ras in normal human fibroblasts. *Cancer Res.* 1999; 59(7): 1539-1543.

110. Sinha VC, Qin L, Li Y. A p53/ARF-dependent anticancer barrier activates senescence and blocks tumorigenesis without impacting apoptosis. *Mol Cancer Res.* 2015; 13(2): 231-238.

111. Wei W, Hemmer RM, Sedivy JM. Role of p14(ARF) in replicative and induced senescence of human fibroblasts. *Mol Cell Biol.* 2001; 21(20): 6748-6757.

112. Michaloglou C, Vredeveld LC, Mooi WJ, Peeper DS. BRAF(E600) in benign and malignant human tumours. *Oncogene.* 2008; 27(7): 877-895.

113. Mooi WJ, Peeper DS. Oncogene-induced cell senescence--halting on the road to cancer. *N Engl J Med.* 2006; 355(10): 1037-1046.

114. Wajapeyee N, Serra RW, Zhu X, Mahalingam M, Green MR. Oncogenic BRAF induces senescence and apoptosis through pathways mediated by the secreted protein IGFBP7. *Cell.* 2008; 132(3): 363-374.

115. Acosta JC, O'Loghlen A, Banito A, Guijarro MV, Augert A, Raguz S, Fumagalli M, Da Costa M, Brown C, Popov N, Takatsu Y, Melamed J, d'Adda di Fagagna F, Bernard D, Hernando E, Gil J. Chemokine signaling via the CXCR2 receptor reinforces senescence. *Cell.* 2008; 133(6): 1006-1018.

116. Li R, Jia Z, Trush MA. Defining ROS in Biology and Medicine. *React Oxyg Species (Apex).* 2016; 1(1): 9-21.

117. Macip S, Igarashi M, Fang L, Chen A, Pan ZQ, Lee SW, Aaronson SA. Inhibition of p21-mediated ROS accumulation can rescue p21-induced senescence. *EMBO J.* 2002;

21(9): 2180-2188.

118. Nelson G, Kucheryavenko O, Wordsworth J, von Zglinicki T. The senescent bystander effect is caused by ROS-activated NF-kappaB signalling. *Mech Ageing Dev.* 2018; 170: 30-36.

119. Freeman AK, Monteiro AN. Phosphatases in the cellular response to DNA damage. *Cell Commun Signal.* 2010; 8: 27.

120. Swanepoel B, Nitulescu GM, Olaru OT, Venables L, van de Venter M. Anti-Cancer Activity of a 5-Aminopyrazole Derivative Lead Compound (BC-7) and Potential Synergistic Cytotoxicity with Cisplatin against Human Cervical Cancer Cells. *Int J Mol Sci.* 2019; 20(22).

121. Huck JJ, Zhang M, McDonald A, Bowman D, Hoar KM, Stringer B, Ecsedy J, Manfredi MG, Hyer ML. MLN8054, an inhibitor of Aurora A kinase, induces senescence in human tumor cells both in vitro and in vivo. *Mol Cancer Res.* 2010; 8(3): 373-384.

122. Toledo F, Wahl GM. Regulating the p53 pathway: in vitro hypotheses, in vivo veritas. *Nat Rev Cancer.* 2006; 6(12): 909-923.

123. Kon N, Zhong J, Kobayashi Y, Li M, Szabolcs M, Ludwig T, Canoll PD, Gu W. Roles of HAUSP-mediated p53 regulation in central nervous system development. *Cell Death Differ.* 2011; 18(8): 1366-1375.

124. Sah VP, Attardi LD, Mulligan GJ, Williams BO, Bronson RT, Jacks T. A subset of p53-deficient embryos exhibit exencephaly. *Nat Genet.* 1995; 10(2): 175-180.

125. Floter J, Kaymak I, Schulze A. Regulation of Metabolic Activity by p53. *Metabolites.*

2017; 7(2).

126. Maier B, Gluba W, Bernier B, Turner T, Mohammad K, Guise T, Sutherland A, Thorner M, Scrable H. Modulation of mammalian life span by the short isoform of p53. *Genes Dev.* 2004; 18(3): 306-319.

127. Pollina EA, Brunet A. Epigenetic regulation of aging stem cells. *Oncogene.* 2011; 30(28): 3105-3126.

128. Armata HL, Garlick DS, Sluss HK. The ataxia telangiectasia-mutated target site Ser18 is required for p53-mediated tumor suppression. *Cancer Res.* 2007; 67(24): 11696-11703.

129. Matheu A, Maraver A, Klatt P, Flores I, Garcia-Cao I, Borras C, Flores JM, Vina J, Blasco MA, Serrano M. Delayed ageing through damage protection by the Arf/p53 pathway. *Nature.* 2007; 448(7151): 375-379.

130. Yasaei H, Gilham E, Pickles JC, Roberts TP, O'Donovan M, Newbold RF. Carcinogen-specific mutational and epigenetic alterations in INK4A, INK4B and p53 tumour-suppressor genes drive induced senescence bypass in normal diploid mammalian cells. *Oncogene.* 2013; 32(2): 171-179.

131. Afanasyeva EA, Mestdagh P, Kumps C, Vandesompele J, Ehemann V, Theissen J, Fischer M, Zapatka M, Brors B, Savelyeva L, Sagulenko V, Speleman F, Schwab M, Westermann F. MicroRNA miR-885-5p targets CDK2 and MCM5, activates p53 and inhibits proliferation and survival. *Cell Death Differ.* 2011; 18(6): 974-984.

132. Herbig U, Wei W, Dutriaux A, Jobling WA, Sedivy JM. Real-time imaging of transcriptional activation in live cells reveals rapid up-regulation of the

cyclin-dependent kinase inhibitor gene CDKN1A in replicative cellular senescence. *Aging Cell.* 2003; 2(6): 295-304.

133. Brugarolas J, Chandrasekaran C, Gordon JI, Beach D, Jacks T, Hannon GJ. Radiation-induced cell cycle arrest compromised by p21 deficiency. *Nature.* 1995; 377(6549): 552-557.

134. Vousden KH, Prives C. Blinded by the Light: The Growing Complexity of p53. *Cell.* 2009; 137(3): 413-431.

135. Kaeberlein M, Powers RW, 3rd, Steffen KK, Westman EA, Hu D, Dang N, Kerr EO, Kirkland KT, Fields S, Kennedy BK. Regulation of yeast replicative life span by TOR and Sch9 in response to nutrients. *Science.* 2005; 310(5751): 1193-1196.

136. Pazoki-Toroudi H, Amani H, Ajami M, Nabavi SF, Braidy N, Kasi PD, Nabavi SM. Targeting mTOR signaling by polyphenols: A new therapeutic target for ageing. *Ageing Res Rev.* 2016; 31: 55-66.

137. Budanov AV, Karin M. p53 target genes sestrin1 and sestrin2 connect genotoxic stress and mTOR signaling. *Cell.* 2008; 134(3): 451-460.

138. Feng Z, Hu W, de Stanchina E, Teresky AK, Jin S, Lowe S, Levine AJ. The regulation of AMPK beta1, TSC2, and PTEN expression by p53: stress, cell and tissue specificity, and the role of these gene products in modulating the IGF-1-AKT-mTOR pathways. *Cancer Res.* 2007; 67(7): 3043-3053.

139. Lee JJ, Kim BC, Park MJ, Lee YS, Kim YN, Lee BL, Lee JS. PTEN status switches cell fate between premature senescence and apoptosis in glioma exposed to ionizing radiation. *Cell Death Differ.* 2011; 18(4): 666-677.

140. Munoz-Espin D, Canamero M, Maraver A, Gomez-Lopez G, Contreras J, Murillo-Cuesta S, Rodriguez-Baeza A, Varela-Nieto I, Ruberte J, Collado M, Serrano M. Programmed cell senescence during mammalian embryonic development. *Cell.* 2013; 155(5): 1104-1118.

141. Storer M, Mas A, Robert-Moreno A, Pecoraro M, Ortells MC, Di Giacomo V, Yosef R, Pilpel N, Krizhanovsky V, Sharpe J, Keyes WM. Senescence is a developmental mechanism that contributes to embryonic growth and patterning. *Cell.* 2013; 155(5): 1119-1130.

142. Regulski MJ. Cellular Senescence: What, Why, and How. *Wounds.* 2017; 29(6): 168-174.

143. Flach J, Bakker ST, Mohrin M, Conroy PC, Pietras EM, Reynaud D, Alvarez S, Diolaiti ME, Ugarte F, Forsberg EC, Le Beau MM, Stohr BA, Mendez J, Morrison CG, Passegue E. Replication stress is a potent driver of functional decline in ageing haematopoietic stem cells. *Nature.* 2014; 512(7513): 198-202.

144. Schultz MB, Sinclair DA. When stem cells grow old: phenotypes and mechanisms of stem cell aging. *Development.* 2016; 143(1): 3-14.

145. Cavallucci V, Fidaleo M, Pani G. Neural Stem Cells and Nutrients: Poised Between Quiescence and Exhaustion. *Trends Endocrinol Metab.* 2016; 27(11): 756-769.

146. Segales J, Perdiguero E, Munoz-Canoves P. Regulation of Muscle Stem Cell Functions: A Focus on the p38 MAPK Signaling Pathway. *Front Cell Dev Biol.* 2016; 4: 91.

147. He S, Sharpless NE. Senescence in Health and Disease. *Cell.* 2017; 169(6):

1000-1011.

148. Falandry C, Bonnefoy M, Freyer G, Gilson E. Biology of cancer and aging: a complex association with cellular senescence. *J Clin Oncol.* 2014; 32(24): 2604-2610.

149. Lasry A, Ben-Neriah Y. Senescence-associated inflammatory responses: aging and cancer perspectives. *Trends Immunol.* 2015; 36(4): 217-228.

150. McNairn AJ, Chuang CH, Bloom JC, Wallace MD, Schimenti JC. Female-biased embryonic death from inflammation induced by genomic instability. *Nature.* 2019; 567(7746): 105-108.

151. Boccardi V, Pelini L, Ercolani S, Ruggiero C, Mecocci P. From cellular senescence to Alzheimer's disease: The role of telomere shortening. *Ageing Res Rev.* 2015; 22: 1-8.

152. Wang JZ, Wang ZH. Senescence may mediate conversion of tau phosphorylation-induced apoptotic escape to neurodegeneration. *Exp Gerontol.* 2015; 68: 82-86.

153. Uryga AK, Bennett MR. Ageing induced vascular smooth muscle cell senescence in atherosclerosis. *J Physiol.* 2016; 594(8): 2115-2124.

154. Garrido AM, Bennett M. Assessment and consequences of cell senescence in atherosclerosis. *Curr Opin Lipidol.* 2016; 27(5): 431-438.

155. Jun JI, Lau LF. The matricellular protein CCN1 induces fibroblast senescence and restricts fibrosis in cutaneous wound healing. *Nat Cell Biol.* 2010; 12(7): 676-685.

156. Jun JI, Lau LF. Cellular senescence controls fibrosis in wound healing. *Aging (Albany NY).* 2010; 2(9): 627-631.

157. Liu J, Yang JR, He YN, Cai GY, Zhang JG, Lin LR, Zhan J, Zhang JH, Xiao HS.

Accelerated senescence of renal tubular epithelial cells is associated with disease progression of patients with immunoglobulin A (IgA) nephropathy. *Transl Res.* 2012; 159(6): 454-463.

158. Kraemer N, Issa L, Hauck SC, Mani S, Ninnemann O, Kaindl AM. What's the hype about CDK5RAP2? *Cell Mol Life Sci.* 2011; 68(10): 1719-1736.

159. Ching YP, Qi Z, Wang JH. Cloning of three novel neuronal Cdk5 activator binding proteins. *Gene.* 2000; 242(1-2): 285-294.

160. Wang X, Ching YP, Lam WH, Qi Z, Zhang M, Wang JH. Identification of a common protein association region in the neuronal Cdk5 activator. *J Biol Chem.* 2000; 275(41): 31763-31769.

161. Kim T, Park JS, Lee P, Jin Y, Fu SB, Rosales JL, Lee KY. Novel alternatively spliced variant form of human CDK5RAP2. *Cell Cycle.* 2011; 10(6): 1010-1012.

162. Bond J, Roberts E, Springell K, Lizarraga SB, Scott S, Higgins J, Hampshire DJ, Morrison EE, Leal GF, Silva EO, Costa SM, Baralle D, Raponi M, Karbani G, Rashid Y, Jafri H, Bennett C, Corry P, Walsh CA, Woods CG. A centrosomal mechanism involving CDK5RAP2 and CENPJ controls brain size. *Nat Genet.* 2005; 37(4): 353-355.

163. Zaqout S, Morris-Rosendahl D, Kaindl AM. Autosomal Recessive Primary Microcephaly (MCPH): An Update. *Neuropediatrics.* 2017; 48(3): 135-142.

164. Cox J, Jackson AP, Bond J, Woods CG. What primary microcephaly can tell us about brain growth. *Trends Mol Med.* 2006; 12(8): 358-366.

165. Woods CG. Human microcephaly. *Curr Opin Neurobiol.* 2004; 14(1): 112-117.

166. Park JS, Lee MK, Rosales JL, Lee KY. Primary microcephaly 3 (MCPH3): revisiting two critical mutations. *Cell Cycle.* 2011; 10(8): 1331-1333.

167. Lizarraga SB, Margossian SP, Harris MH, Campagna DR, Han AP, Blevins S, Mudbhary R, Barker JE, Walsh CA, Fleming MD. Cdk5rap2 regulates centrosome function and chromosome segregation in neuronal progenitors. *Development.* 2010; 137(11): 1907-1917.

168. Barr AR, Kilmartin JV, Gergely F. CDK5RAP2 functions in centrosome to spindle pole attachment and DNA damage response. *J Cell Biol.* 2010; 189(1): 23-39.

169. Doxsey S, Zimmerman W, Mikule K. Centrosome control of the cell cycle. *Trends Cell Biol.* 2005; 15(6): 303-311.

170. Barrera JA, Kao LR, Hammer RE, Seemann J, Fuchs JL, Megraw TL. CDK5RAP2 regulates centriole engagement and cohesion in mice. *Dev Cell.* 2010; 18(6): 913-926.

171. Lee S, Rhee K. CEP215 is involved in the dynein-dependent accumulation of pericentriolar matrix proteins for spindle pole formation. *Cell Cycle.* 2010; 9(4): 774-783.

172. Buchman JJ, Tseng HC, Zhou Y, Frank CL, Xie Z, Tsai LH. Cdk5rap2 interacts with pericentrin to maintain the neural progenitor pool in the developing neocortex. *Neuron.* 2010; 66(3): 386-402.

173. Zhang X, Liu D, Lv S, Wang H, Zhong X, Liu B, Wang B, Liao J, Li J, Pfeifer GP, Xu X. CDK5RAP2 is required for spindle checkpoint function. *Cell Cycle.* 2009; 8(8): 1206-1216.

174. Russell JO, Monga SP. Wnt/beta-Catenin Signaling in Liver Development,

Homeostasis, and Pathobiology. *Annu Rev Pathol.* 2018; 13: 351-378.

175. Sharma M, Castro-Piedras I, Simmons GE, Jr., Pruitt K. Dishevelled: A masterful conductor of complex Wnt signals. *Cell Signal.* 2018; 47: 52-64.

176. Aschenbach WG, Ho RC, Sakamoto K, Fujii N, Li Y, Kim YB, Hirshman MF, Goodyear LJ. Regulation of dishevelled and beta-catenin in rat skeletal muscle: an alternative exercise-induced GSK-3beta signaling pathway. *Am J Physiol Endocrinol Metab.* 2006; 291(1): E152-158.

177. Wilkinson MB, Dias C, Magida J, Mazei-Robison M, Lobo M, Kennedy P, Dietz D, Covington H, 3rd, Russo S, Neve R, Ghose S, Tamminga C, Nestler EJ. A novel role of the WNT-dishevelled-GSK3beta signaling cascade in the mouse nucleus accumbens in a social defeat model of depression. *J Neurosci.* 2011; 31(25): 9084-9092.

178. Cervenka I, Valnohova J, Bernatik O, Harnos J, Radsetoulal M, Sedova K, Hanakova K, Potesil D, Sedlackova M, Salasova A, Steinhart Z, Angers S, Schulte G, Hampl A, Zdrahal Z, Bryja V. Dishevelled is a NEK2 kinase substrate controlling dynamics of centrosomal linker proteins. *Proc Natl Acad Sci U S A.* 2016; 113(33): 9304-9309.

179. Faheem M, Naseer MI, Rasool M, Chaudhary AG, Kumosani TA, Ilyas AM, Pushparaj P, Ahmed F, Algahtani HA, Al-Qahtani MH, Saleh Jamal H. Molecular genetics of human primary microcephaly: an overview. *BMC Med Genomics.* 2015; 8 Suppl 1: S4.

180. Yigit G, Brown KE, Kayserili H, Pohl E, Caliebe A, Zahnleiter D, Rosser E, Bogershausen N, Uyguner ZO, Altunoglu U, Nurnberg G, Nurnberg P, Rauch A, Li Y,

Thiel CT, Wollnik B. Mutations in CDK5RAP2 cause Seckel syndrome. *Mol Genet Genomic Med.* 2015; 3(5): 467-480.

181. Chavali PL, Chandrasekaran G, Barr AR, Tatrai P, Taylor C, Papachristou EK, Woods CG, Chavali S, Gergely F. A CEP215-HSET complex links centrosomes with spindle poles and drives centrosome clustering in cancer. *Nat Commun.* 2016; 7: 11005.

182. Nusse R, Varmus HE. Many tumors induced by the mouse mammary tumor virus contain a provirus integrated in the same region of the host genome. *Cell.* 1982; 31(1): 99-109.

183. Rijsewijk F, Schuermann M, Wagenaar E, Parren P, Weigel D, Nusse R. The Drosophila homolog of the mouse mammary oncogene int-1 is identical to the segment polarity gene wingless. *Cell.* 1987; 50(4): 649-657.

184. Monteagudo S, Lories RJ. Cushioning the cartilage: a canonical Wnt restricting matter. *Nat Rev Rheumatol.* 2017; 13(11): 670-681.

185. Perugorria MJ, Olaizola P, Labiano I, Esparza-Baquer A, Marzioni M, Marin JJG, Bujanda L, Banales JM. Wnt-beta-catenin signalling in liver development, health and disease. *Nat Rev Gastroenterol Hepatol.* 2019; 16(2): 121-136.

186. Sinha S. A pedagogical walkthrough of computational modeling and simulation of Wnt signaling pathway using static causal models in MATLAB. *EURASIP J Bioinform Syst Biol.* 2016; 2017(1): 1.

187. Gotzel K, Chemnitzer O, Maurer L, Dietrich A, Eichfeld U, Lyros O, Moulla Y, Niebisch S, Mehdorn M, Jansen-Winkeln B, Vieth M, Hoffmeister A, Gockel I, Thieme R. In-depth characterization of the Wnt-signaling/beta-catenin pathway in an

in vitro model of Barrett's sequence. *BMC Gastroenterol.* 2019; 19(1): 38.

188. Xia YF, Chang J, Yang JF, Ouyang W, Pitt B, Billiar T, Zhang LM. Noncanonical Wnt signaling contributes to ventilatorinduced lung injury through upregulation of WISP1 expression. *Int J Mol Med.* 2019; 43(3): 1217-1228.

189. Jang J, Jung Y, Chae S, Bae T, Kim SM, Shim YJ, Chung SI, Yoon Y. XAV939, a Wnt/beta-catenin pathway modulator, has inhibitory effects on LPS-induced inflammatory response. *Immunopharmacol Immunotoxicol.* 2019; 41(3): 394-402.

190. Yuan G, Yang G, Zheng Y, Zhu X, Chen Z, Zhang Z, Chen Y. The non-canonical BMP and Wnt/beta-catenin signaling pathways orchestrate early tooth development. *Development.* 2015; 142(1): 128-139.

191. Moffat LL, Robinson RE, Bakoulis A, Clark SG. The conserved transmembrane RING finger protein PLR-1 downregulates Wnt signaling by reducing Frizzled, Ror and Ryk cell-surface levels in C. elegans. *Development.* 2014; 141(3): 617-628.

192. He R, Hua K, Zhang S, Wan Y, Gong H, Ma B, Luo R, Zhou R, Jin H. COX-2 mediated crosstalk between Wnt/beta-catenin and the NF-kappaB signaling pathway during inflammatory responses induced by Haemophilus parasuis in PK-15 and NPTr cells. *Dev Comp Immunol.* 2020; 105: 103588.

193. Wan ML, Wang Y, Zeng Z, Deng B, Zhu BS, Cao T, Li YK, Xiao J, Han Q, Wu Q. Colorectal cancer (CRC) as a multifactorial disease and its causal correlations with multiple signaling pathways. *Biosci Rep.* 2020.

194. Liang JJ, Li HR, Chen Y, Zhou Z, Shi YQ, Zhang LL, Xin L, Zhao DB. ZNRF3 Regulates Collagen-Induced Arthritis Through NF-kB and Wnt Pathways.

Inflammation. 2020.

195. Ghasemi F, Shafiee M, Banikazemi Z, Pourhanifeh MH, Khanbabaei H, Shamshirian A, Amiri Moghadam S, ArefNezhad R, Sahebkar A, Avan A, Mirzaei H. Curcumin inhibits NF-kB and Wnt/beta-catenin pathways in cervical cancer cells. *Pathol Res Pract.* 2019; 215(10): 152556.

196. Yang HL, Tsai YC, Korivi M, Chang CT, Hseu YC. Lucidone Promotes the Cutaneous Wound Healing Process via Activation of the PI3K/AKT, Wnt/beta-catenin and NF-kappaB Signaling Pathways. *Biochim Biophys Acta Mol Cell Res.* 2017; 1864(1): 151-168.

197. Liu H, Zheng J, Zheng T, Wang P. Exendin-4 regulates Wnt and NF-kappaB signaling in lipopolysaccharide-induced human periodontal ligament stem cells to promote osteogenic differentiation. *Int Immunopharmacol.* 2019; 75: 105801.

198. Li X, Fan C, Xiao Z, Zhao Y, Zhang H, Sun J, Zhuang Y, Wu X, Shi J, Chen Y, Dai J. A collagen microchannel scaffold carrying paclitaxel-liposomes induces neuronal differentiation of neural stem cells through Wnt/beta-catenin signaling for spinal cord injury repair. *Biomaterials.* 2018; 183: 114-127.

199. Sun SC. The non-canonical NF-kappaB pathway in immunity and inflammation. *Nat Rev Immunol.* 2017; 17(9): 545-558.

200. Ma B, Hottiger MO. Crosstalk between Wnt/beta-Catenin and NF-kappaB Signaling Pathway during Inflammation. *Front Immunol.* 2016; 7: 378.

201. Winston JT, Strack P, Beer-Romero P, Chu CY, Elledge SJ, Harper JW. The SCFbeta-TRCP-ubiquitin ligase complex associates specifically with phosphorylated

destruction motifs in IkappaBalpha and beta-catenin and stimulates IkappaBalpha ubiquitination in vitro. *Genes Dev.* 1999; 13(3): 270-283.

202. Spiegelman VS, Slaga TJ, Pagano M, Minamoto T, Ronai Z, Fuchs SY. Wnt/beta-catenin signaling induces the expression and activity of betaTrCP ubiquitin ligase receptor. *Mol Cell.* 2000; 5(5): 877-882.

203. Wang X, Adhikari N, Li Q, Guan Z, Hall JL. The role of [beta]-transducin repeat-containing protein ([beta]-TrCP) in the regulation of NF-[kappa]B in vascular smooth muscle cells. *Arterioscler Thromb Vasc Biol.* 2004; 24(1): 85-90.

204. Noubissi FK, Elcheva I, Bhatia N, Shakoori A, Ougolkov A, Liu J, Minamoto T, Ross J, Fuchs SY, Spiegelman VS. CRD-BP mediates stabilization of betaTrCP1 and c-myc mRNA in response to beta-catenin signalling. *Nature.* 2006; 441(7095): 898-901.

205. Ougolkov A, Zhang B, Yamashita K, Bilim V, Mai M, Fuchs SY, Minamoto T. Associations among beta-TrCP, an E3 ubiquitin ligase receptor, beta-catenin, and NF-kappaB in colorectal cancer. *J Natl Cancer Inst.* 2004; 96(15): 1161-1170.

206. Jia D, Yang W, Li L, Liu H, Tan Y, Ooi S, Chi L, Filion LG, Figeys D, Wang L. beta-Catenin and NF-kappaB co-activation triggered by TLR3 stimulation facilitates stem cell-like phenotypes in breast cancer. *Cell Death Differ.* 2015; 22(2): 298-310.

207. Bognar MK, Vincendeau M, Erdmann T, Seeholzer T, Grau M, Linnemann JR, Ruland J, Scheel CH, Lenz P, Ott G, Lenz G, Hauck SM, Krappmann D. Oncogenic CARMA1 couples NF-kappaB and beta-catenin signaling in diffuse large B-cell lymphomas. *Oncogene.* 2016; 35(32): 4269-4281.

208. Ma B, Fey M, Hottiger MO. WNT/beta-catenin signaling inhibits CBP-mediated

RelA acetylation and expression of proinflammatory NF-kappaB target genes. *J Cell Sci.* 2015; 128(14): 2430-2436.

209. Choi YS, Hur J, Jeong S. Beta-catenin binds to the downstream region and regulates the expression C-reactive protein gene. *Nucleic Acids Res.* 2007; 35(16): 5511-5519.

210. Yun K, So JS, Jash A, Im SH. Lymphoid enhancer binding factor 1 regulates transcription through gene looping. *J Immunol.* 2009; 183(8): 5129-5137.

211. Jang J, Ha JH, Chung SI, Yoon Y. Beta-catenin regulates NF-kappaB activity and inflammatory cytokine expression in bronchial epithelial cells treated with lipopolysaccharide. *Int J Mol Med.* 2014; 34(2): 632-638.

212. Ma B, Zhong L, van Blitterswijk CA, Post JN, Karperien M. T cell factor 4 is a pro-catabolic and apoptotic factor in human articular chondrocytes by potentiating nuclear factor kappaB signaling. *J Biol Chem.* 2013; 288(24): 17552-17558.

213. Deng J, Miller SA, Wang HY, Xia W, Wen Y, Zhou BP, Li Y, Lin SY, Hung MC. beta-catenin interacts with and inhibits NF-kappa B in human colon and breast cancer. *Cancer Cell.* 2002; 2(4): 323-334.

214. Rodriguez-Pinilla M, Rodriguez-Peralto JL, Hitt R, Sanchez JJ, Sanchez-Verde L, Alameda F, Ballestin C, Sanchez-Cespedes M. beta-Catenin, Nf-kappaB and FAS protein expression are independent events in head and neck cancer: study of their association with clinical parameters. *Cancer Lett.* 2005; 230(1): 141-148.

215. Du Q, Zhang X, Cardinal J, Cao Z, Guo Z, Shao L, Geller DA. Wnt/beta-catenin signaling regulates cytokine-induced human inducible nitric oxide synthase expression by inhibiting nuclear factor-kappaB activation in cancer cells. *Cancer Res.*

2009; 69(9): 3764-3771.

216. Moreau M, Mourah S, Dosquet C. beta-Catenin and NF-kappaB cooperate to regulate the uPA/uPAR system in cancer cells. *Int J Cancer.* 2011; 128(6): 1280-1292.

217. Ma B, van Blitterswijk CA, Karperien M. A Wnt/beta-catenin negative feedback loop inhibits interleukin-1-induced matrix metalloproteinase expression in human articular chondrocytes. *Arthritis Rheum.* 2012; 64(8): 2589-2600.

218. Die L, Yan P, Jun Jiang Z, Min Hua T, Cai W, Xing L. Glycogen synthase kinase-3 beta inhibitor suppresses Porphyromonas gingivalis lipopolysaccharide-induced CD40 expression by inhibiting nuclear factor-kappa B activation in mouse osteoblasts. *Mol Immunol.* 2012; 52(1): 38-49.

219. Jiang R, Chen D, Hou J, Tan Z, Wang Y, Huang X, Wang X, Sun B. Survival and inflammation promotion effect of PTPRO in fulminant hepatitis is associated with NF-kappaB activation. *J Immunol.* 2014; 193(10): 5161-5170.

220. Duan Y, Liao AP, Kuppireddi S, Ye Z, Ciancio MJ, Sun J. beta-Catenin activity negatively regulates bacteria-induced inflammation. *Lab Invest.* 2007; 87(6): 613-624.

221. Sun J, Hobert ME, Duan Y, Rao AS, He TC, Chang EB, Madara JL. Crosstalk between NF-kappaB and beta-catenin pathways in bacterial-colonized intestinal epithelial cells. *Am J Physiol Gastrointest Liver Physiol.* 2005; 289(1): G129-137.

222. Ke B, Shen XD, Kamo N, Ji H, Yue S, Gao F, Busuttil RW, Kupiec-Weglinski JW. beta-catenin regulates innate and adaptive immunity in mouse liver ischemia-reperfusion injury. *Hepatology.* 2013; 57(3): 1203-1214.

223. Buss H, Dorrie A, Schmitz ML, Frank R, Livingstone M, Resch K, Kracht M.

Phosphorylation of serine 468 by GSK-3beta negatively regulates basal p65 NF-kappaB activity. *J Biol Chem.* 2004; 279(48): 49571-49574.

224. Martin M, Rehani K, Jope RS, Michalek SM. Toll-like receptor-mediated cytokine production is differentially regulated by glycogen synthase kinase 3. *Nat Immunol.* 2005; 6(8): 777-784.

225. Nalapareddy K, Nattamai KJ, Kumar RS, Karns R, Wikenheiser-Brokamp KA, Sampson LL, Mahe MM, Sundaram N, Yacyshyn MB, Yacyshyn B, Helmrath MA, Zheng Y, Geiger H. Canonical Wnt Signaling Ameliorates Aging of Intestinal Stem Cells. *Cell Rep.* 2017; 18(11): 2608-2621.

226. Cho CH, Yoo KH, Oliveros A, Paulson S, Hussaini SMQ, van Deursen JM, Jang MH. sFRP3 inhibition improves age-related cellular changes in BubR1 progeroid mice. *Aging Cell.* 2019; 18(2): e12899.

227. Varecza Z, Kvell K, Talaber G, Miskei G, Csongei V, Bartis D, Anderson G, Jenkinson EJ, Pongracz JE. Multiple suppression pathways of canonical Wnt signalling control thymic epithelial senescence. *Mech Ageing Dev.* 2011; 132(5): 249-256.

228. Ye X, Zerlanko B, Kennedy A, Banumathy G, Zhang R, Adams PD. Downregulation of Wnt signaling is a trigger for formation of facultative heterochromatin and onset of cell senescence in primary human cells. *Mol Cell.* 2007; 27(2): 183-196.

229. Delmas V, Beermann F, Martinozzi S, Carreira S, Ackermann J, Kumasaka M, Denat L, Goodall J, Luciani F, Viros A, Demirkan N, Bastian BC, Goding CR, Larue L. Beta-catenin induces immortalization of melanocytes by suppressing p16INK4a

expression and cooperates with N-Ras in melanoma development. *Genes Dev.* 2007; 21(22): 2923-2935.

230. Emelyanov A, Bulavin DV. Wip1 phosphatase in breast cancer. *Oncogene.* 2015; 34(34): 4429-4438.

231. Yi W, Hu X, Chen Z, Liu L, Tian Y, Chen H, Cong YS, Yang F, Zhang L, Rudolph KL, Zhang Z, Zhao Y, Ju Z. Phosphatase Wip1 controls antigen-independent B-cell development in a p53-dependent manner. *Blood.* 2015; 126(5): 620-628.

232. Shi Y, Nikulenkov F, Zawacka-Pankau J, Li H, Gabdoulline R, Xu J, Eriksson S, Hedstrom E, Issaeva N, Kel A, Arner ES, Selivanova G. ROS-dependent activation of JNK converts p53 into an efficient inhibitor of oncogenes leading to robust apoptosis. *Cell Death Differ.* 2014; 21(4): 612-623.

233. Zhu Y, Demidov ON, Goh AM, Virshup DM, Lane DP, Bulavin DV. Phosphatase WIP1 regulates adult neurogenesis and WNT signaling during aging. *J Clin Invest.* 2014; 124(7): 3263-3273.

234. Goloudina AR, Kochetkova EY, Pospelova TV, Demidov ON. Wip1 phosphatase: between p53 and MAPK kinases pathways. *Oncotarget.* 2016; 7(21): 31563-31571.

235. Yoda A, Toyoshima K, Watanabe Y, Onishi N, Hazaka Y, Tsukuda Y, Tsukada J, Kondo T, Tanaka Y, Minami Y. Arsenic trioxide augments Chk2/p53-mediated apoptosis by inhibiting oncogenic Wip1 phosphatase. *J Biol Chem.* 2008; 283(27): 18969-18979.

236. Lowe JM, Cha H, Yang Q, Fornace AJ, Jr. Nuclear factor-kappaB (NF-kappaB) is a novel positive transcriptional regulator of the oncogenic Wip1 phosphatase. *J Biol*

Chem. 2010; 285(8): 5249-5257.

237. Zhu YH, Zhang CW, Lu L, Demidov ON, Sun L, Yang L, Bulavin DV, Xiao ZC. Wip1 regulates the generation of new neural cells in the adult olfactory bulb through p53-dependent cell cycle control. *Stem Cells.* 2009; 27(6): 1433-1442.

238. Choi J, Nannenga B, Demidov ON, Bulavin DV, Cooney A, Brayton C, Zhang Y, Mbawuike IN, Bradley A, Appella E, Donehower LA. Mice deficient for the wild-type p53-induced phosphatase gene (Wip1) exhibit defects in reproductive organs, immune function, and cell cycle control. *Mol Cell Biol.* 2002; 22(4): 1094-1105.

239. Takekawa M, Adachi M, Nakahata A, Nakayama I, Itoh F, Tsukuda H, Taya Y, Imai K. p53-inducible wip1 phosphatase mediates a negative feedback regulation of p38 MAPK-p53 signaling in response to UV radiation. *EMBO J.* 2000; 19(23): 6517-6526.

240. Lee JS, Lee MO, Moon BH, Shim SH, Fornace AJ, Jr., Cha HJ. Senescent growth arrest in mesenchymal stem cells is bypassed by Wip1-mediated downregulation of intrinsic stress signaling pathways. *Stem Cells.* 2009; 27(8): 1963-1975.

241. Schalch T, Steiner FA. Structure of centromere chromatin: from nucleosome to chromosomal architecture. *Chromosoma.* 2017; 126(4): 443-455.

242. Westhorpe FG, Straight AF. The centromere: epigenetic control of chromosome segregation during mitosis. *Cold Spring Harb Perspect Biol.* 2014; 7(1): a015818.

243. Cheeseman IM, Desai A. Molecular architecture of the kinetochore-microtubule interface. *Nat Rev Mol Cell Biol.* 2008; 9(1): 33-46.

244. Hara M, Fukagawa T. Dynamics of kinetochore structure and its regulations during mitotic progression. *Cell Mol Life Sci.* 2020.

245. Thiriet C, Hayes JJ. Histone dynamics during transcription: exchange of H2A/H2B dimers and H3/H4 tetramers during pol II elongation. *Results Probl Cell Differ.* 2006; 41: 77-90.

246. Sharma AB, Dimitrov S, Hamiche A, Van Dyck E. Centromeric and ectopic assembly of CENP-A chromatin in health and cancer: old marks and new tracks. *Nucleic Acids Res.* 2019; 47(3): 1051-1069.

247. Srivastava S, Zasadzinska E, Foltz DR. Posttranslational mechanisms controlling centromere function and assembly. *Curr Opin Cell Biol.* 2018; 52: 126-135.

248. Tachiwana H, Kagawa W, Shiga T, Osakabe A, Miya Y, Saito K, Hayashi-Takanaka Y, Oda T, Sato M, Park SY, Kimura H, Kurumizaka H. Crystal structure of the human centromeric nucleosome containing CENP-A. *Nature.* 2011; 476(7359): 232-235.

249. Black BE, Foltz DR, Chakravarthy S, Luger K, Woods VL, Jr., Cleveland DW. Structural determinants for generating centromeric chromatin. *Nature.* 2004; 430(6999): 578-582.

250. Carroll CW, Milks KJ, Straight AF. Dual recognition of CENP-A nucleosomes is required for centromere assembly. *J Cell Biol.* 2010; 189(7): 1143-1155.

251. Fachinetti D, Folco HD, Nechemia-Arbely Y, Valente LP, Nguyen K, Wong AJ, Zhu Q, Holland AJ, Desai A, Jansen LE, Cleveland DW. A two-step mechanism for epigenetic specification of centromere identity and function. *Nat Cell Biol.* 2013; 15(9): 1056-1066.

252. Bergmann JH, Rodriguez MG, Martins NM, Kimura H, Kelly DA, Masumoto H, Larionov V, Jansen LE, Earnshaw WC. Epigenetic engineering shows H3K4me2 is required for HJURP targeting and CENP-A assembly on a synthetic human kinetochore. *EMBO J.* 2011; 30(2): 328-340.

253. Bade D, Pauleau AL, Wendler A, Erhardt S. The E3 ligase CUL3/RDX controls centromere maintenance by ubiquitylating and stabilizing CENP-A in a CAL1-dependent manner. *Dev Cell.* 2014; 28(5): 508-519.

254. Nakano M, Cardinale S, Noskov VN, Gassmann R, Vagnarelli P, Kandels-Lewis S, Larionov V, Earnshaw WC, Masumoto H. Inactivation of a human kinetochore by specific targeting of chromatin modifiers. *Dev Cell.* 2008; 14(4): 507-522.

255. Jansen LE, Black BE, Foltz DR, Cleveland DW. Propagation of centromeric chromatin requires exit from mitosis. *J Cell Biol.* 2007; 176(6): 795-805.

256. Silva MC, Bodor DL, Stellfox ME, Martins NM, Hochegger H, Foltz DR, Jansen LE. Cdk activity couples epigenetic centromere inheritance to cell cycle progression. *Dev Cell.* 2012; 22(1): 52-63.

257. Erhardt S, Mellone BG, Betts CM, Zhang W, Karpen GH, Straight AF. Genome-wide analysis reveals a cell cycle-dependent mechanism controlling centromere propagation. *J Cell Biol.* 2008; 183(5): 805-818.

258. Dunleavy EM, Roche D, Tagami H, Lacoste N, Ray-Gallet D, Nakamura Y, Daigo Y, Nakatani Y, Almouzni-Pettinotti G. HJURP is a cell-cycle-dependent maintenance and deposition factor of CENP-A at centromeres. *Cell.* 2009; 137(3): 485-497.

259. Foltz DR, Jansen LE, Bailey AO, Yates JR, 3rd, Bassett EA, Wood S, Black BE,

Cleveland DW. Centromere-specific assembly of CENP-a nucleosomes is mediated by HJURP. *Cell.* 2009; 137(3): 472-484.

260. Barnhart MC, Kuich PH, Stellfox ME, Ward JA, Bassett EA, Black BE, Foltz DR. HJURP is a CENP-A chromatin assembly factor sufficient to form a functional de novo kinetochore. *J Cell Biol.* 2011; 194(2): 229-243.

261. Carroll CW, Silva MC, Godek KM, Jansen LE, Straight AF. Centromere assembly requires the direct recognition of CENP-A nucleosomes by CENP-N. *Nat Cell Biol.* 2009; 11(7): 896-902.

262. Guse A, Carroll CW, Moree B, Fuller CJ, Straight AF. In vitro centromere and kinetochore assembly on defined chromatin templates. *Nature.* 2011; 477(7364): 354-358.

263. Heun P, Erhardt S, Blower MD, Weiss S, Skora AD, Karpen GH. Mislocalization of the Drosophila centromere-specific histone CID promotes formation of functional ectopic kinetochores. *Dev Cell.* 2006; 10(3): 303-315.

264. Navarro-Mendoza MI, Perez-Arques C, Panchal S, Nicolas FE, Mondo SJ, Ganguly P, Pangilinan J, Grigoriev IV, Heitman J, Sanyal K, Garre V. Early Diverging Fungus Mucor circinelloides Lacks Centromeric Histone CENP-A and Displays a Mosaic of Point and Regional Centromeres. *Curr Biol.* 2019; 29(22): 3791-3802 e3796.

265. Jia Y, Fong KW, Choi YK, See SS, Qi RZ. Dynamic recruitment of CDK5RAP2 to centrosomes requires its association with dynein. *PLoS One.* 2013; 8(7): e68523.

266. Graser S, Stierhof YD, Nigg EA. Cep68 and Cep215 (Cdk5rap2) are required for centrosome cohesion. *J Cell Sci.* 2007; 120(Pt 24): 4321-4331.

267. Kim S, Rhee K. Importance of the CEP215-pericentrin interaction for centrosome maturation during mitosis. *PLoS One.* 2014; 9(1): e87016.

268. Hanafusa H, Kedashiro S, Tezuka M, Funatsu M, Usami S, Toyoshima F, Matsumoto K. PLK1-dependent activation of LRRK1 regulates spindle orientation by phosphorylating CDK5RAP2. *Nat Cell Biol.* 2015; 17(8): 1024-1035.

269. Rosales JL, Rattner JB, Lee KY. The primary microcephaly 3 (MCPH3) interacting protein, p35 and its catalytic subunit, Cdk5, are centrosomal proteins. *Cell Cycle.* 2010; 9(3): 618-620.

270. Nasser H, Vera L, Elmaleh-Berges M, Steindl K, Letard P, Teissier N, Ernault A, Guimiot F, Afenjar A, Moutard ML, Heron D, Alembik Y, Momtchilova M, Milani P, Kubis N, Pouvreau N, Zollino M, Guilmin Crepon S, Kaguelidou F, Gressens P, Verloes A, Rauch A, El Ghouzzi V, Drunat S, Passemard S. CDK5RAP2 primary microcephaly is associated with hypothalamic, retinal and cochlear developmental defects. *J Med Genet.* 2020.

271. Lancaster MA, Renner M, Martin CA, Wenzel D, Bicknell LS, Hurles ME, Homfray T, Penninger JM, Jackson AP, Knoblich JA. Cerebral organoids model human brain development and microcephaly. *Nature.* 2013; 501(7467): 373-379.

272. Cai B, Ma W, Bi C, Yang F, Zhang L, Han Z, Huang Q, Ding F, Li Y, Yan G, Pan Z, Yang B, Lu Y. Long noncoding RNA H19 mediates melatonin inhibition of premature senescence of c-kit(+) cardiac progenitor cells by promoting miR-675. *J Pineal Res.* 2016; 61(1): 82-95.

273. Lee JS, Mo Y, Gan H, Burgess RJ, Baker DJ, van Deursen JM, Zhang Z. Pak2 kinase

promotes cellular senescence and organismal aging. *Proc Natl Acad Sci U S A.* 2019; 116(27): 13311-13319.

274. De Meyer T, Nawrot T, Bekaert S, De Buyzere ML, Rietzschel ER, Andres V. Telomere Length as Cardiovascular Aging Biomarker: JACC Review Topic of the Week. *J Am Coll Cardiol.* 2018; 72(7): 805-813.

275. Zhu H, Blake S, Kusuma FK, Pearson RB, Kang J, Chan KT. Oncogene-Induced Senescence: from Biology to Therapy. *Mech Ageing Dev.* 2020: 111229.

276. Gu Y, Han J, Jiang C, Zhang Y. Biomarkers, oxidative stress and autophagy in skin aging. *Ageing Res Rev.* 2020; 59: 101036.

277. Bartkova J, Rezaei N, Liontos M, Karakaidos P, Kletsas D, Issaeva N, Vassiliou LV, Kolettas E, Niforou K, Zoumpourlis VC, Takaoka M, Nakagawa H, Tort F, Fugger K, Johansson F, Sehested M, Andersen CL, Dyrskjot L, Orntoft T, Lukas J, Kittas C, Helleday T, Halazonetis TD, Bartek J, Gorgoulis VG. Oncogene-induced senescence is part of the tumorigenesis barrier imposed by DNA damage checkpoints. *Nature.* 2006; 444(7119): 633-637.

278. Le Guezennec X, Bulavin DV. WIP1 phosphatase at the crossroads of cancer and aging. *Trends Biochem Sci.* 2010; 35(2): 109-114.

279. Salminen A, Kaarniranta K. Control of p53 and NF-kappaB signaling by WIP1 and MIF: role in cellular senescence and organismal aging. *Cell Signal.* 2011; 23(5): 747-752.

280. Stewart DJ. Wnt signaling pathway in non-small cell lung cancer. *J Natl Cancer Inst.* 2014; 106(1): djt356.

281. Georgakilas AG, Martin OA, Bonner WM. p21: A Two-Faced Genome Guardian. *Trends Mol Med.* 2017; 23(4): 310-319.

282. Sakai H, Fujigaki H, Mazur SJ, Appella E. Wild-type p53-induced phosphatase 1 (Wip1) forestalls cellular premature senescence at physiological oxygen levels by regulating DNA damage response signaling during DNA replication. *Cell Cycle.* 2014; 13(6): 1015-1029.

283. Chen Z, Yi W, Morita Y, Wang H, Cong Y, Liu JP, Xiao Z, Rudolph KL, Cheng T, Ju Z. Wip1 deficiency impairs haematopoietic stem cell function via p53 and mTORC1 pathways. *Nat Commun.* 2015; 6: 6808.

284. Tang Y, Liu L, Sheng M, Xiong K, Huang L, Gao Q, Wei J, Wu T, Yang S, Liu H, Mu Y, Li K. Wip1 knockout inhibits the proliferation and enhances the migration of bone marrow mesenchymal stem cells. *Exp Cell Res.* 2015; 334(2): 310-322.

285. Yoshino Y, Ishioka C. Inhibition of glycogen synthase kinase-3 beta induces apoptosis and mitotic catastrophe by disrupting centrosome regulation in cancer cells. *Sci Rep.* 2015; 5: 13249.

286. Blankesteijn WM, van de Schans VA, ter Horst P, Smits JF. The Wnt/frizzled/GSK-3 beta pathway: a novel therapeutic target for cardiac hypertrophy. *Trends Pharmacol Sci.* 2008; 29(4): 175-180.

287. Demidov ON, Timofeev O, Lwin HN, Kek C, Appella E, Bulavin DV. Wip1 phosphatase regulates p53-dependent apoptosis of stem cells and tumorigenesis in the mouse intestine. *Cell Stem Cell.* 2007; 1(2): 180-190.

288. Xiong AS, Yao QH, Peng RH, Duan H, Li X, Fan HQ, Cheng ZM, Li Y. PCR-based

accurate synthesis of long DNA sequences. *Nat Protoc.* 2006; 1(2): 791-797.

289. Le Roux I, Konge J, Le Cam L, Flamant P, Tajbakhsh S. Numb is required to prevent p53-dependent senescence following skeletal muscle injury. *Nat Commun.* 2015; 6: 8528.

290. Seong HA, Ha H. Murine protein serine-threonine kinase 38 activates p53 function through Ser15 phosphorylation. *J Biol Chem.* 2012; 287(25): 20797-20810.

291. Mattson MP, Camandola S. NF-kappaB in neuronal plasticity and neurodegenerative disorders. *J Clin Invest.* 2001; 107(3): 247-254.

292. Feng Y, Xia Y, Yu G, Shu X, Ge H, Zeng K, Wang J, Wang X. Cleavage of GSK-3beta by calpain counteracts the inhibitory effect of Ser9 phosphorylation on GSK-3beta activity induced by H(2)O(2). *J Neurochem.* 2013; 126(2): 234-242.

293. Shimizu I, Minamino T. Cellular senescence in cardiac diseases. *J Cardiol.* 2019; 74(4): 313-319.

294. Tang X, Zheng D, Hu P, Zeng Z, Li M, Tucker L, Monahan R, Resnick MB, Liu M, Ramratnam B. Glycogen synthase kinase 3 beta inhibits microRNA-183-96-182 cluster via the beta-Catenin/TCF/LEF-1 pathway in gastric cancer cells. *Nucleic Acids Res.* 2014; 42(5): 2988-2998.

295. Wang Z, Wu T, Shi L, Zhang L, Zheng W, Qu JY, Niu R, Qi RZ. Conserved motif of CDK5RAP2 mediates its localization to centrosomes and the Golgi complex. *J Biol Chem.* 2010; 285(29): 22658-22665.

296. Leonard MK, Hill NT, Bubulya PA, Kadakia MP. The PTEN-Akt pathway impacts the integrity and composition of mitotic centrosomes. *Cell Cycle.* 2013; 12(9):

1406-1415.

297. Santaguida S, Amon A. Short- and long-term effects of chromosome mis-segregation and aneuploidy. *Nat Rev Mol Cell Biol.* 2015; 16(8): 473-485.

298. Kamenz J, Hauf S. Time To Split Up: Dynamics of Chromosome Separation. *Trends Cell Biol.* 2017; 27(1): 42-54.

299. Perea-Resa C, Blower MD. Centromere Biology: Transcription Goes on Stage. *Mol Cell Biol.* 2018; 38(18).

300. Aldrup-Macdonald ME, Sullivan BA. The past, present, and future of human centromere genomics. *Genes (Basel).* 2014; 5(1): 33-50.

301. Karpen GH, Allshire RC. The case for epigenetic effects on centromere identity and function. *Trends Genet.* 1997; 13(12): 489-496.

302. Sullivan BA, Blower MD, Karpen GH. Determining centromere identity: cyclical stories and forking paths. *Nat Rev Genet.* 2001; 2(8): 584-596.

303. Fukagawa T, Earnshaw WC. The centromere: chromatin foundation for the kinetochore machinery. *Dev Cell.* 2014; 30(5): 496-508.

304. Blower MD, Sullivan BA, Karpen GH. Conserved organization of centromeric chromatin in flies and humans. *Dev Cell.* 2002; 2(3): 319-330.

305. Bodor DL, Mata JF, Sergeev M, David AF, Salimian KJ, Panchenko T, Cleveland DW, Black BE, Shah JV, Jansen LE. The quantitative architecture of centromeric chromatin. *Elife.* 2014; 3: e02137.

306. Lacoste N, Woolfe A, Tachiwana H, Garea AV, Barth T, Cantaloube S, Kurumizaka H, Imhof A, Almouzni G. Mislocalization of the centromeric histone variant

CenH3/CENP-A in human cells depends on the chaperone DAXX. *Mol Cell.* 2014; 53(4): 631-644.

307. Kato H, Jiang J, Zhou BR, Rozendaal M, Feng H, Ghirlando R, Xiao TS, Straight AF, Bai Y. A conserved mechanism for centromeric nucleosome recognition by centromere protein CENP-C. *Science.* 2013; 340(6136): 1110-1113.

308. Regnier V, Vagnarelli P, Fukagawa T, Zerjal T, Burns E, Trouche D, Earnshaw W, Brown W. CENP-A is required for accurate chromosome segregation and sustained kinetochore association of BubR1. *Mol Cell Biol.* 2005; 25(10): 3967-3981.

309. Sathyan KM, Fachinetti D, Foltz DR. alpha-amino trimethylation of CENP-A by NRMT is required for full recruitment of the centromere. *Nat Commun.* 2017; 8: 14678.

310. Park JS, Lee MK, Kang S, Jin Y, Fu S, Rosales JL, Lee KY. Species-Specific Expression of Full-Length and Alternatively Spliced Variant Forms of CDK5RAP2. *PLoS One.* 2015; 10(11): e0142577.

311. Revenkova E, Eijpe M, Heyting C, Gross B, Jessberger R. Novel meiosis-specific isoform of mammalian SMC1. *Mol Cell Biol.* 2001; 21(20): 6984-6998.

312. Evans PD, Vallender EJ, Lahn BT. Molecular evolution of the brain size regulator genes CDK5RAP2 and CENPJ. *Gene.* 2006; 375: 75-79.

313. Hirano T. SMC proteins and chromosome mechanics: from bacteria to humans. *Philos Trans R Soc Lond B Biol Sci.* 2005; 360(1455): 507-514.

314. Fong KW, Hau SY, Kho YS, Jia Y, He L, Qi RZ. Interaction of CDK5RAP2 with EB1 to track growing microtubule tips and to regulate microtubule dynamics. *Mol Biol*

Cell. 2009; 20(16): 3660-3670.

315. Fong KW, Choi YK, Rattner JB, Qi RZ. CDK5RAP2 is a pericentriolar protein that functions in centrosomal attachment of the gamma-tubulin ring complex. *Mol Biol Cell.* 2008; 19(1): 115-125.

316. Lawo S, Hasegan M, Gupta GD, Pelletier L. Subdiffraction imaging of centrosomes reveals higher-order organizational features of pericentriolar material. *Nat Cell Biol.* 2012; 14(11): 1148-1158.

317. Fang G. Checkpoint protein BubR1 acts synergistically with Mad2 to inhibit anaphase-promoting complex. *Mol Biol Cell.* 2002; 13(3): 755-766.

318. Nguyen Ba AN, Pogoutse A, Provart N, Moses AM. NLStradamus: a simple Hidden Markov Model for nuclear localization signal prediction. *BMC Bioinformatics.* 2009; 10: 202.

319. Landschulz WH, Johnson PF, McKnight SL. The leucine zipper: a hypothetical structure common to a new class of DNA binding proteins. *Science.* 1988; 240(4860): 1759-1764.

320. Trazzi S, Perini G, Bernardoni R, Zoli M, Reese JC, Musacchio A, Della Valle G. The C-terminal domain of CENP-C displays multiple and critical functions for mammalian centromere formation. *PLoS One.* 2009; 4(6): e5832.

321. Shono N, Ohzeki J, Otake K, Martins NM, Nagase T, Kimura H, Larionov V, Earnshaw WC, Masumoto H. CENP-C and CENP-I are key connecting factors for kinetochore and CENP-A assembly. *J Cell Sci.* 2015; 128(24): 4572-4587.

322. Suzuki N, Nakano M, Nozaki N, Egashira S, Okazaki T, Masumoto H. CENP-B

interacts with CENP-C domains containing Mif2 regions responsible for centromere localization. *J Biol Chem.* 2004; 279(7): 5934-5946.